

**Probing the Splicing and Enzymatic function of fission
yeast Prp16 – A DEAD box RNA helicase**

A thesis

Submitted for the degree of

Doctor of Philosophy

In the Faculty of Science

By

Amit Kumar Sharma



Department of Microbiology and Cell Biology

INDIAN INSTITUTE OF SCIENCE

BANGALORE - 560 012, INDIA

July 2019

Acknowledgement

I express my heartfelt gratitude to my PhD supervisor Prof. Usha Vijayraghavan for giving me an opportunity to work in her lab. I would like to thank her for her constant supervision and guidance throughout my doctoral study. I will always be indebted to her for all her efforts she has put for the improvement of my scientific skills.

I thank the past and present Chairperson of the department Prof. V Nagaraja and Prof. Umesh Varshney and Prof. Usha Vijayraghavan for maintaining excellent infrastructure and scientific environment in the Department.

I thank my pre-viva committee: Prof. Arun Kumar, Prof. Raghavan Varadarajan, Prof. Saumitra Das and Prof. Umesh Varshney.

I would like to thank the office of International relation for all the help extended to me.

I would like to thank all the laboratories of the department and its members.

I would like to thank all the faculties of the department for their suggestions for my work and I would also like to thank office staff of the department for all their help.

It will always be grateful to my seniors in the lab for their help and guidance and teaching me all techniques specially Drisya. I thank all my past and present lab members for keeping the atmosphere of the lab very lively. I would thank all the project trainees and project assistants for their help in my work.

I thank all my friends in IISc for helping me and my stay in IISc pleasant.

Words will not suffice for me thank my parents and my brother for all the unconditional love and support.

CONTENTS

CHAPTER I : Review of Literature

**CHAPTER II : Probing the functional conservation of Prp16 and
its role in splicing in fission yeast**

CHAPTER III : Biochemical characterization of SpPrp16

**CHAPTER IV : Understanding the role of SpPrp16 in splice-site
recognition**

CHAPTER V : Summary and Conclusions

REFERENCES

LIST OF ABBREVIATIONS

APPENDICES

PUBLICATION

Chapter I

Review of Literature

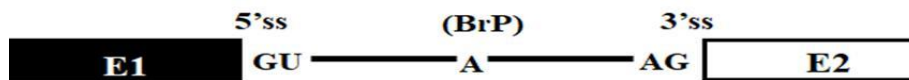
I.1 Introduction

The functional continuity of the eukaryotic genes is interrupted by stretches of non-coding DNA sequence called introns (term coined by Gilbert.,1978). The process by which these intervening sequences are removed is called splicing and it is one of the important levels at which a gene can be regulated. In splicing there is precise recognition and removal of introns. General architecture of pre-mRNA introns includes 5' splice-site which begins with GU, branch point adenosine, located at 18 to 40 nucleotides upstream from the 3' end of an intron and a 3' splice-site with AG conserved at its end. Introns also have polypyrimidine tract YNYRAY, where Y indicates a pyrimidine, N denotes any nucleotide, R denotes any purine and A denotes adenine (**Figure I.1A**). Mutations in these conserved sequences or changes in the length between the 3' splice-site and branch point affects splicing efficiency and accuracy. Regardless of the organisms, all nuclear pre-mRNA introns are removed from nascent transcript via two consecutive transesterification (phosphodiester transfer) reaction steps. In the first transesterification step, the 2' hydroxyl group of branch point adenosine of the intron forms a bond with the phosphorus atom at 5' splice-site ligating 5' end of the intron to the branch point adenosine forming lariat intermediate. In the second transesterification step, 3' hydroxyl group of 5' exon attacks the phosphorus group at 3' splice-site which finally results in ligation of exons releasing intron in the form of lariat (**Figure I.1B**). These transesterification reactions are catalyzed by a large ribonucleoprotein complex, the spliceosome, which consists of five uridine rich small nuclear RNAs (snRNAs) U1, U2, U4, U5 and U6 in the form of small nuclear ribonucleoprotein particles (snRNPs) and above 100 protein factors most of which have essential functions during identification, positioning of splice-sites in the catalytic center and in aiding catalysis (Moore et al., 1993; Will and Lührmann, 2011). *In vitro* studies with mammalian and budding yeast cell free extracts and mini pre-mRNAs show the spliceosome is a highly dynamic structure, components of which are assembled by sequential binding of the snRNPs and protein factors.

Intron Architecture across Species

Fungi have shorter and lesser number of introns per gene. Despite their short size the content of information is highly conserved in the 5' splice-site, branch site, and 3' splice-site regions of their introns when compared to the exonic regions flanking the introns (Kupfer et al., 2004;

A.



B.

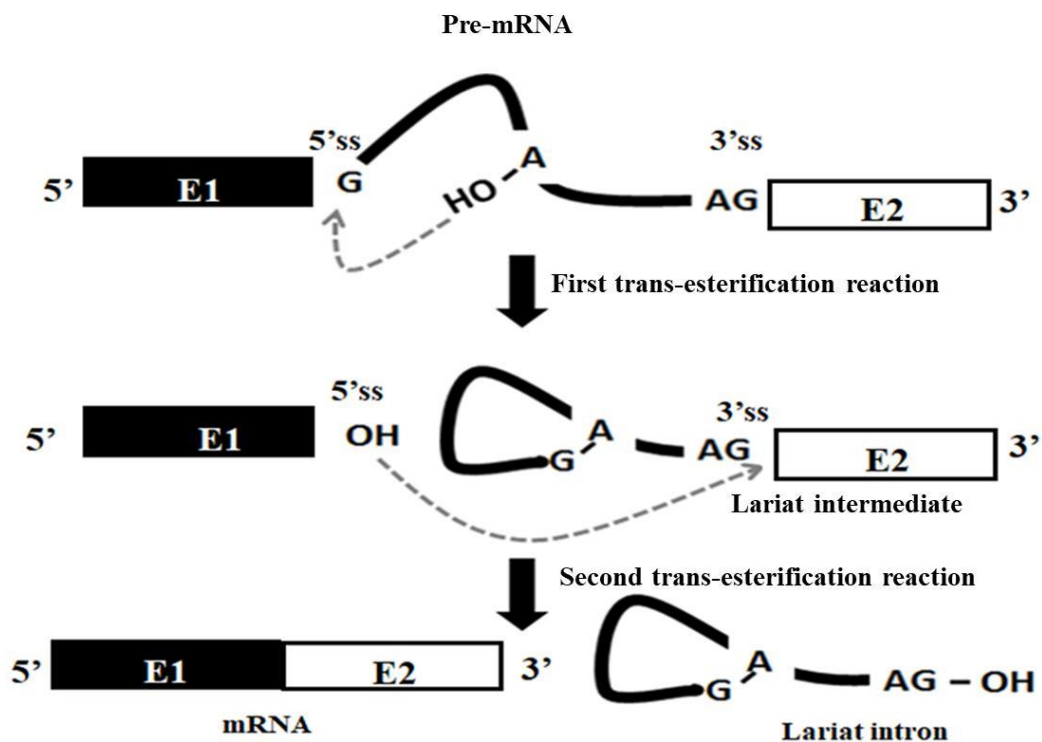


Figure I.1: A. General architecture of nuclear pre-mRNA introns. Conserved splice-site residues of the intron are shown - 5' splice-site, branch site and 3' splice-site. B. Schematic representation of SN2 type transesterification reactions of pre-mRNA splicing. The pre-mRNA splicing reaction involves two catalysis steps. The first step is cleavage of the 5' splice-site and the formation of lariat intermediate via a 2'-5' phosphodiester linkage. The second step is cleavage of the 3' splice-site and ligation of the two exons.

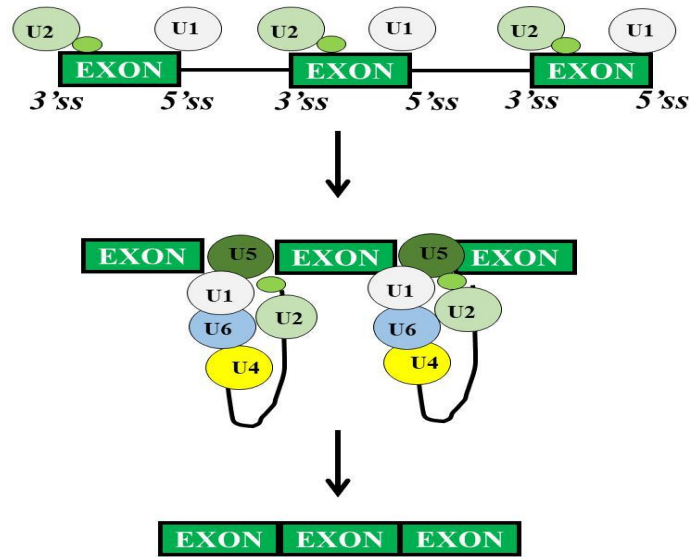
Collins and Penny, 2006). Among the fungi, in budding yeast the introns are relatively longer with its mean length being 270 nts. Splice-site consensus sequences like the 5'ss, branch site consensus and 3'ss are highly conserved in budding yeast while in fission yeast and other higher eukaryotes they are more degenerate (Kuhn and Käufer, 2003). *S. pombe* introns have an unconventional positioning of polypyrimidine tract which is present between 5'ss and branch site (Reed and Maniatis, 1985). The introns of *C. elegans* surprisingly lack polypyrimidine tract in their introns. Plant introns are relatively short with their AU intronic content being a major feature which determines the efficiency of splicing (Sakharkar et al., 2004; Goodall and Filipowicz, 1989).

Intron and Exon definition model for splice-site recognition

Successful recognition of the correct splice-sites and distinction between exon and intron with nucleotide precision by the spliceosome has been one of the major challenges in RNA splicing among the huge variety of pre-mRNA molecules. Vertebrate genes have short exons (~170 nts) interrupted by longer introns (~5kb) (Zhang, 1998; Sakharkar et al., 2005). Interestingly, when the lengths of exons were increased to >300 nts, the spliceosome formation was inhibited, demonstrating the influence of exon and intron size on splicing. In the transcripts with small exons and long introns, the spliceosome tends to assemble across an exon, as juxtaposition of small exon units here is easier compared to long introns (Fox-Walsh et al, 2005; Roberson et al., 1990). Hence, 'exon definition' model was proposed. All five snRNPs are reported to be present in exon defined spliceosomal complexes (Schneider et al., 2010). It was observed that the binding of U1 snRNP at 5'ss *in vitro* enhances the splicing efficiency and recognition of 3'ss, upstream of the exon (Fox-Walsh et al., 2005).

In lower eukaryotes such as *Drosophila* and *C. elegans* where introns are smaller and exons longer, spliceosomal assembly takes place across an intron for pairing of splice-sites. Therefore, the 'intron definition' model is predominant here. This was supported by the observation from *in vitro* experiments in yeast (intron length < 100 nts) and *Drosophila* (nearly half of total introns in genome is <100 nts) where increase of the intron length resulted in retention of intron (Goguel and Rosbash, 1993; Hawkins, 1988; Talerico and Berget, 1994; Guo et al., 1993). Splicing in *S. pombe* follow 'intron definition' model as mutating splice-sites resulted in intron retention as opposed to exon skipping seen in vertebrates. Also, cryptic 5'ss junctions in fission transcript were found to be present within the introns as opposed to what is observed in metazoans (Romfo et al., 2000) (**Figure I.2**).

A.



B.

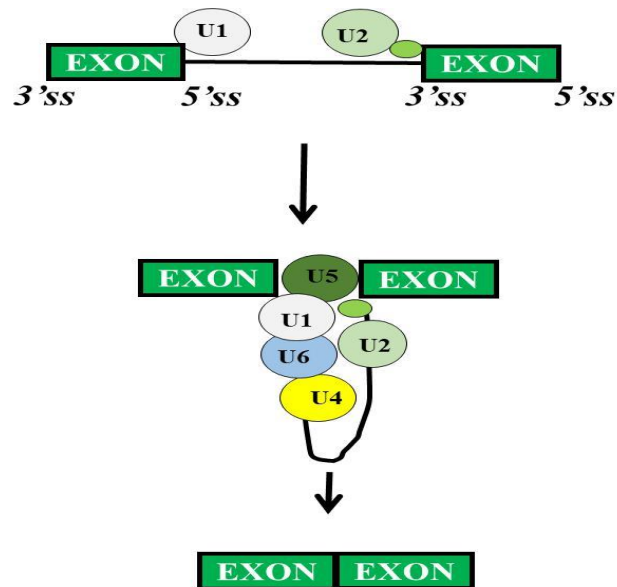


Figure I.2: Diagrammatic depiction of exon and intron definition models of splicing. **A.** Exon definition takes place by the binding of U1 to 5' splice-site downstream of the exon and U2AF large and small subunits to the polypyrimidine tract and 3' splice-site found upstream of that exon. Therefore, the basal splicing machinery binding forms a cross exon recognition complex flanking the same exon. **B.** Intron definition takes place by binding of U1 to the upstream 5' splice-site and U2AF large and small subunits to the downstream polypyrimidine tract and 3' splice-site respectively of the same intron (adapted from Ast G, 2004).

***S. pombe* as model to study splicing**

S. pombe has long been being used as model organism for studying eukaryotic cells. It is the sixth model organism with a fully sequenced genome (Wood et al., 2002) and with many tools for functional genetics and genomics. Recently, 161 natural isolates of fission yeast have been analysed for their genetic and phenotypic variation adding to our knowledge about this model (Jeffares et al., 2015). The early demonstration of the precise splicing of the mammalian viral SV40 T-antigen intron in *S. pombe* showed that splicing machinery in fission yeast can recognise and splice introns from higher eukaryotes suggesting that the splicing components which include snRNA and splicing factors are more similar to mammals. As depicted from evolutionary distance (**Figure I.3**) (Sipiczki, 2000) many features of *S. cerevisiae* introns and splicing factors are different from other fungi members and higher eukaryotes. *S. pombe* has 4824 predicted genes, 43% of which have introns, and many have multiple introns per gene (Smith and Valcárcel, 2000; Wood et al., 2002). It is in contrast with *S. cerevisiae* where only ~5% of genes have introns. While introns in *S. pombe* vary in length from 29 to 819 nucleotides, the average length is only ~85 nts hence, the genome has largely small introns. Intronic features like 5' splice-site, branch point sequence (CURAY) and the 3' splice-site are more degenerate in *S. pombe* than in *S. cerevisiae*. *S. pombe* introns have additional *cis* regulatory elements. Examples being exonic splice enhancers (ESEs) and intronic splice enhancers (ISEs) or exonic splice silencers (ESS) and intronic splice silencers (ISS) which offer additional mechanisms of splicing and gene regulation similar to that of higher eukaryotes (Webb et al., 2005, Schwartz et al., 2008). Many introns in *S. pombe* genes have unusual positioning of the polypyrimidine tract between 5' splice-site and branch point site and is often the case for other fungal introns. *S. pombe*, also has many unique features for alternative splicing (a mechanism which increases the proteomic diversity in multicellular eukaryotes) which resemble the mammalian system (**Figure I.4**). *S. pombe* genome encoding members of serine/arginine-rich (SR) family of splicing regulators and several SR-like proteins are implicated in the regulation of alternative splicing (Lützelberger et al., 1999). Therefore, these features make *S. pombe* a suitable model to investigate the mechanism of splice-site recognition and spliceosome assembly that could be representative of other fungal introns.

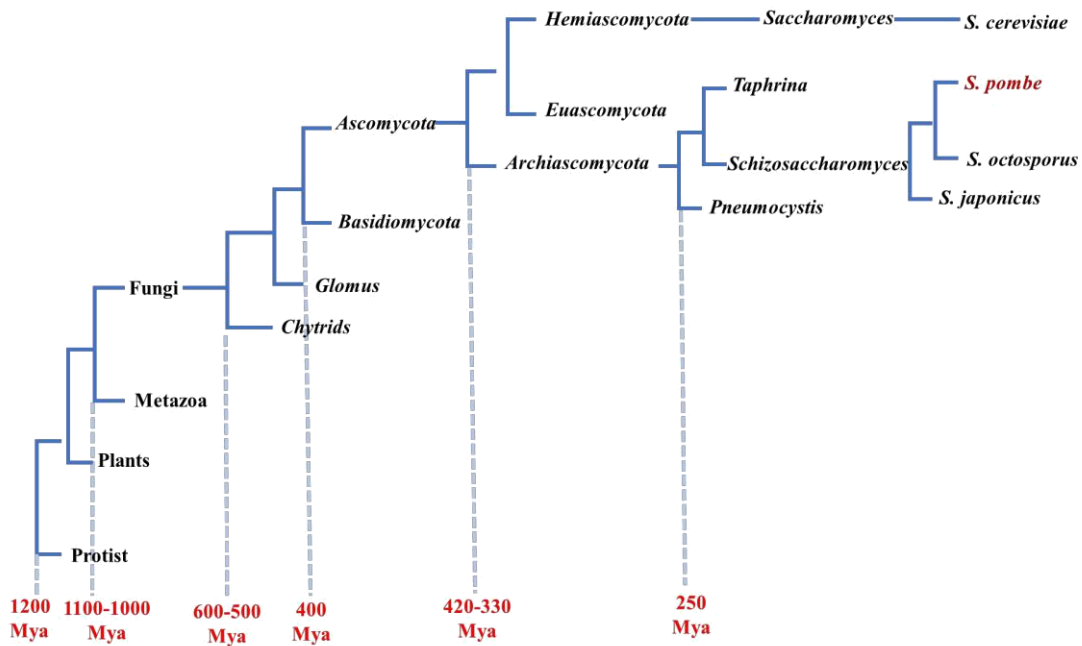


Figure I.3: Phylogeny of yeasts. Time in million years (Adapted from Sipiczki, 2000)

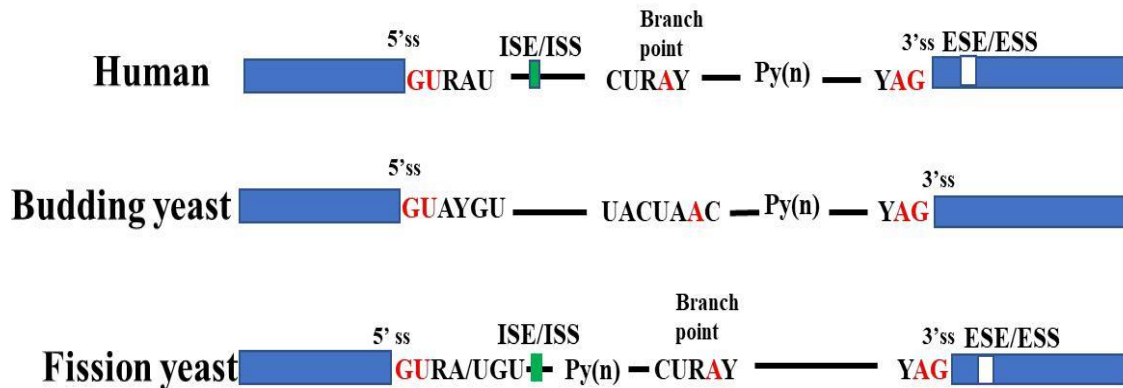


Figure I.4: Diagrammatic illustration of the exon-intron architecture of humans, *S. cerevisiae* (budding yeast) and *S. pombe* (fission yeast) highlighting the *cis* intronic features. The invariant residues in the consensus elements have been highlighted in red. 5'ss - 5' splice-site; 3'ss - 3' splice-site; BrP - Branch sequence; Py(n) - polypyrimidine tract; ISE - intronic splicing enhancers; ISS - Intronic Splicing Silencer; ESE - Exonic Splicing Enhancer; ESS - Exonic Splicing Silencer.

Small nuclear ribonucleoproteins

Spliceosomal complex consists of five snRNAs namely U1, U2, U4, U5 and U6 which associate with proteins to form snRNPs (Jurica and Moore, 2003; Wahl et al., 2009). Minor spliceosome (U12-dependent spliceosome) present in human contains U11, U12, U4-atac, U5 and U6-atac (Steitz et al., 2008). The snRNAs in mammals are encoded by multiple genes, whereas in budding yeast and fission yeast they are encoded by single gene in single copy number. Several studies have revealed that the snRNA crucial for splicing are closely related between fission yeast and budding yeast (Brennwald, 1988; Tani and Ohshima, 1989; Porter et al., 1990; Dandekar et al., 1989).

Spliceosomal Assembly

Spliceosome assembly is a sequential binding of the snRNAs (U1, U2, U4, U5 and U6), in the form of small nuclear ribonucleoprotein particles (snRNPs) along with numerous non-snRNP proteins onto the pre-mRNA (Jurica and Moore., 2003; Wahl et al., 2009) (**Figure I.5**). The snRNPs play a critical role in splice junction recognition which enable the two transesterification splicing reactions (Valadkhan S, 2005). Non-snRNP proteins of DExD/H ATPases family facilitate several structural and compositional changes within the spliceosome in the course of assembly, catalysis and disassembly by mediating the stabilization and disruption of RNA-RNA, RNA-protein and protein-protein interactions. DExD/H box containing helicases also ensure splicing fidelity by kinetic proofreading of intronic elements and thus are indispensable for the generation of a functional transcriptome (Staley and Guthrie, 1998). Spliceosome assembly is initiated by the precise recognition and base pairing of 5' end of U1 snRNP with the 5'ss in the exon-intron junction in an ATP dependent manner (Mount et al., 1983; Krämer et al., 1984). This is followed by the association of the SF1/BBP protein with branchpoint sequence followed by the binding of U2 auxiliary factor large subunit, U2AF65 to the 3'ss and U2AF35 to the polypyrimidine tract resulting in E complex. There is cooperative binding interaction between SF1/BBP at the branch site with U2AF65 through the C-terminal RRM motif of U2AF65. Now the SF1 is displaced by ATP dependent U2 snRNA base pairing with the branch site in the intron forming the B/A complex. This base pairing U2 snRNA and BS is stabilized by SF3a and SF3b heteromeric components of the U2 snRNP (Gozani et al., 1996). After the formation of the B/A complex, the U4/U6 and U5 snRNPs recruit as a preassembled U4/U6•U5 tri-snRNP

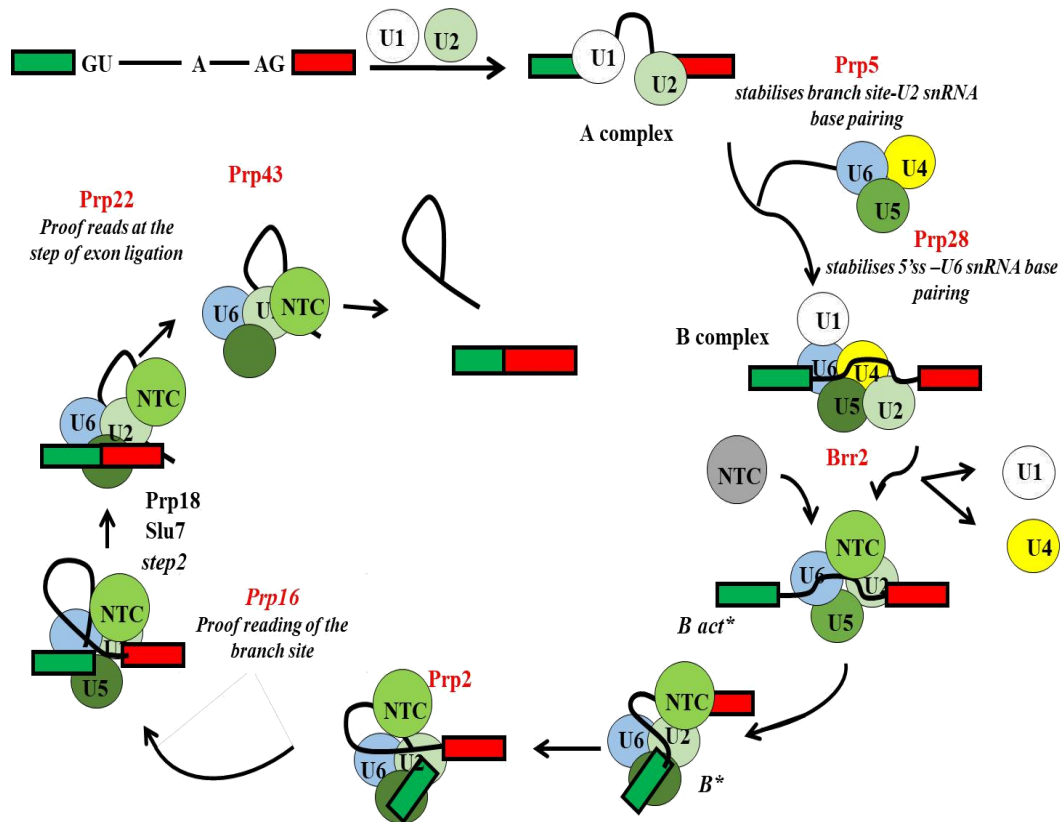


Figure I.5: Diagrammatic representation of stepwise assembly pathway of spliceosomal machinery in *S. cerevisiae*. The pathway has four stages: assembly, activation, catalysis and disassembly. Names of the ordered complexes are indicated.

to the complex, forming the B complex. The U1 snRNA binding to the 5'ss and the binding of U2 snRNA to the branch site is also stabilized by proteins of DExH/DExD ATPase family. This catalytically inactive complex undergoes compositional and conformational rearrangements to become active, marked by dissociation of U1-5'ss and U4-U6 snRNAs by DExD/DExH helicases Prp28 and Brr2 respectively (Cheng and Abelson, 1987; Lamond et al., 1988; Staley and Guthrie, 1998; Raghunathan and Guthrie, 1998; Lagerbauer et al., 1998). This is followed by base pairing between U6 and 5'ss and between U6 and U2 (Madhani and Guthrie, 1994). The Prp19-complex (NTC) then associates with the spliceosome resulting in a catalytically active spliceosome - the B* complex (Chan et al., 2003). The U2-U6 base-paired structure, called helix I, was proposed to contribute to the spliceosome active site. DExH ATPase Prp2 which is required during the first step associates along with Spp2p cofactor (Roy et al., 1995) which functions in releasing the SF3a and SF3b complex from the catalytic complex. These events facilitate the binding of non-snRNP protein factors Cwc25 and Yju2 that assist the first catalytic step (Lardelli et al., 2010; Warkocki et al., 2009; Yeh et al., 2011). The product of first splicing reactions are exon with a free 3'OH and intron lariat intron-3'exon (lariat intermediate). After the first step of catalysis Prp16, a DExH box RNA helicase further remodels the spliceosome by destabilising the U2-U6 helix I and dislodges the first step splicing factors (Mefford and Staley, 2009; Tseng et al., 2011). Subsequently, the binding of second step splicing factors like Slu7, Prp18 takes place. This facilitates the second step of splicing by 3'ss recognition and selection further leading to exon-exon ligation and excision of lariat intron (Frank and Guthrie, 1992; Horowitz and Abelson, 1993; Schwer and Gross, 1998). mRNA is now released in the form of an mRNP and spliceosomal dissociation is initiated with the help of DExH box ATPase Prp22. These complexes are further dissociated by the concerted action of Prp43 along with other factors like Ntr1 and Ntr2 and the disassembled spliceosomal components then undergo recycling for further rounds of splicing (**Figure I.5**).

S. pombe from the perspective of splicing of primary transcripts is similar to higher eukaryotes more importantly to humans which makes it an apt model to understand the complex networking of splicing in highly evolved eukaryotes. However, cell free extracts which is competent for splicing to analyse splicing *in vitro* has not been obtained in *S. pombe*. Large-scale purification of endogenous U2•U5•U6 complex from *S. pombe* revealed to be containing excised introns in abundance, indicative of the complex being an intron lariat spliceosome (ILS) complex showing that spliceosomal disassembly is slow in *S. pombe*. Prp43 and Brr2 play role in disassembling of the spliceosomal complex and their level were found to be sub stoichiometric which could be the reason for ILS complex accumulation in

logarithmically dividing *S. pombe* cells and failure of obtaining extracts competent for splicing (Chen et al., 2014). Similar to the initial identification of factors responsible for splicing in budding yeast (Vijayraghavan et al., 1989) identification of fission yeast splicing factors also began by genetic screening for conditional mutants which exhibited splicing defects (Potashkin and Frendewey, 1989). However, more extensive studies of fission yeast splicing factor and understanding their role in the specific phases of splicing began with genetic and proteomic approaches. Few of the well-studied factors in *S. pombe* splicing include SpPrp2/U2AF⁵⁹ which binds to polypyrimidine tract downstream of branchpoint sequence (Potashkin et al., 1993; Zamore et al., 1992). SpPrp4 which phosphorylates SpPrp1 plays role in the activation of spliceosome (Bottner et al., 2005). SpCwf10 a GTPase (homolog of budding yeast Snu114) and a core component of U5 snRNP, SpSlu7 and SpPrp18 show unexpected early precatalytic splicing roles. The DEAH/D box RNA helicases which are key remodellers of the spliceosomes are less studied and poorly understood in *S. pombe*.

DExD/H Box Helicases: Driving Forces of the Spliceosome

Rearrangement of RNA-RNP structures is accomplished with the help of protein factors in the spliceosome. Prime factors belong to DExD or DExH family of proteins. DExD/H-type ATP dependent helicases were discovered and characterised by yeast genetic and biochemical studies. Eight DExD/H-box proteins - Sub2/UAP56, Prp5, Prp28, Brr2, Prp2, Prp16, Prp22, and Prp43 are conserved in *S. cerevisiae* and humans. Each of these helicases act at specific steps of splicing.

Prp28

Prp28 functions in destabilising the interaction of U1 snRNA with 5'ss in exchange for U6 snRNA, thus forming U6/5'ss association which is required for 5'ss selection. This function was uncovered in screening for *leu13* residue mutants of U1C protein (stabilizes the binding of U1 snRNA with 5'ss) that could genetically suppress cold sensitive *prp28-102* mutant. The Zn finger domain of U1C protein stabilises the binding of U1 snRNA with 5'ss (Will et al., 1996; Tang et al., 1999) (reviewed by Schwer, 2001). Prp28 stabilizes and proofreads the U6/5'ss (Yang et al., 2013). Similar to the functions of budding yeast Prp28, hprp28 performs the ATP dependent helicase function to destabilise the U1/5'ss interaction as hPrp28p was observed to cross link with 5'ss (Ismaili et al., 2001; Teigelkamp et al., 1997).

Prp5

It is one of the early required DEAD-box proteins, which assist in formation of the pre-spliceosome (Ruby et al., 1993). *In vitro*, Prp5p enhances deoxyoligo-directed RNase H cleavage of U2 snRNP (Wiest et al., 1996) and the ATPase activity of the Prp5 is stimulated by U2 snRNA (O'Day et al., 1996). U2 alternates between two conformations involving stem-loop II in its 5' end region, but only one conformation Stem-loop IIA is the active forms of U2 snRNA and this activation of U2 snRNA is facilitated by Prp5 which displaces the Cus2 from U2 snRNP (Perriman et al., 2003).

Sub2

Sub2 is a DExD/H-box protein known to be involved in early in spliceosomal assembly. In the initial phase of spliceosome assembly Mud2 a yeast homolog of U2AF binds to the 3' splice-site and branch point binding protein binds to branch site of the intron. Sub2 functions in dislodging these two factors which facilitates the binding of U2 snRNP in the spliceosome (Kistler and Guthrie, 2001).

Brr2

Brr2 first identified in the screening for cold sensitive mutants showing splicing defects is a DEIH-box containing protein which belongs to Ski2 like subfamily with two consecutive helicase modules, where both the modules have Ski2 like helicase (H) domain and a Sec63 domain, intervened by winged helix (WH) domain (Noble and Guthrie, 1996; Bleichert and Beserga, 2007; Santos et al., 2012). Brr2p is conserved across species and its N-terminal helicase module (H1-Sec63-1) performs catalytic functions (Kim et al., 1999). The human homolog of Brr2 has been known to unwind yeast U4/U6 duplexes *in vitro* (Laggerbauer et al., 1998). It is also implicated in disassembly of spliceosome. The N-terminal region of Brr2 is essential for stable association with the tri-snRNP and its stability and retention of U5 and U6 snRNAs during spliceosome activation. The C-terminal region of the Prp8 protein which consists of RNase H-like and Jab1/MPN-like domains can enhance or suppress the Brr2 functions (Reviewed in Absmeier et al., 2016). Prp16 has been shown to directly interact with Sec63-2 domain of Brr2p, this association regulates the RNA binding and the RNA stimulated ATP hydrolysis by Prp16 at catalytic core (Cordin et al., 2014).

Prp2

Prp2 acts as a molecular motor like other DExH ATPases family members and function in the activation of the precatalytic spliceosome for the transesterification reaction. Prp2p functions

in the final ATP-dependent step necessary for 5' splice-site cleavage (Kim et al., 1992; Wlodaver and Staley, 2014). A G-patch cofactor Spp2p interacts with Prp2 for association with spliceosome, further resulting in its activation. Further dissociation requires ATPase activity of Prp2 (Roy et al., 1995; Silverman et al., 2004; Fabrizio et al., 2009). Prp2 binds to the region of pre-mRNA which is downstream to branch site, mediated by another splicing factor Brr2 which facilitate first step of splicing (Teigelkamp et al., 1994). Prp2 has been studied to destabilise the association of the U2 snRNP complex SF3, RES complex, and the NTC-related factors Cwc24 and Cwc27 from the spliceosome (Bessonov et al., 2008; Fabrizio et al., 2009; Warkocki et al., 2009; Lardelli et al., 2010; Agafonov et al., 2011; Ohrt et al., 2012). This destabilisation of early acting factors by Prp2 facilitate binding of Cwc25p and Yju2p, required for first step catalysis (Liu et al., 2007; Chiu et al., 2009; Ohrt et al., 2012). It has been studied to facilitate destabilisation of U2/U6 helix I, this helix is responsible for conformational rearrangement of 5' splice-site, branch site and metal ion positioning in the catalytic core and functions as fidelity factor by proofreading formation of the catalytic core (Mefford and Staley, 2009; Sun and Maley, 1995; Semlow and Staley, 2012; Wlodaver and Staley, 2014).

Prp16

Prp16 was discovered as *prp16-1* mutant in the screening for mutants which suppressed the branch site mutation where invariant A was replaced by C (Couto et al., 1987). PRP16-immunodepleted extract showed defect in second step of splicing showing its requirement for the second transesterification reaction. Prp16 utilises ATP hydrolysis to promote conformational rearrangement in the spliceosome hence protection of the 3' splice-site against RNase H cleavage (Schwer and Guthrie, 1992). An *in vivo* analysis revealed that Prp16 discards aberrant branched substrates, hence, helps in proofreading of branch site and in concerted action with Prp43, it assists in proofreading of 5'ss (Burgess and Guthrie, 1993; Koodathingal et al., 2010). The non-conserved N-terminal domain is responsible for association of Prp16 to the spliceosome, which is also, mediated by another splicing factor Brr2 as revealed by two-hybrid assays (Wang et al., 1998; Van Nues and Beggs, 2001). Prp16 triggers the ejection of Cwc25 and Yju2 by its translocation along the RNA or by structural rearrangement which destabilizes and displaces these proteins (Tseng et al., 2011; Lardelli et al., 2010). Prp16 facilitates disruption of another U2-U6 helix I - a RNA-RNA interaction to promote catalytic second step reaction along with *cwc2* which is a NTC component (Hogg et al., 2014).

Prp22

Prp22 belongs to DExD/H box family of ATP-dependent RNA helicases. It functions in the release of mRNA from the spliceosomes at the expense of ATP (Wagner et al., 1998). Upon immunodepleting Prp22 from the splicing extracts accumulation of first step products were seen, implicating its function in second step of catalysis. The distance between branchpoint and the 3'ss determines the essentiality of Prp22 for the second step of catalysis. It was shown that Prp22 is required for second step of catalysis only when the distance between the branchpoint and the 3' splice-site is >21 nucleotides. Prp22 in concert with Slu7 and Prp18 functions in positioning of 3' and 5' splice-sites for catalysis (Schwer and Gross, 1998).

Prp43

Prp43 was discovered in screening by PCR on genomic DNA of *S. cerevisiae* using degenerate primers corresponding to highly conserved sequence typical of DEAH box helicases and known to play a role in spliceosomal disassembly (Arenas et al., 1997). Ntr1 acts as a cofactor and binds to Prp43 which helps in its association to the spliceosome. It also functions to activate Prp43 for its enzymatic function, which results in the dissociation of lariat intron RNA and spliceosomal disassembly, the terminal step of splicing (Tsai et al., 2005; Tanaka, 2007). Lariat-intron RNA after release from the splicing complex is cleaved by Dbr1, a branch-specific phosphodiesterase, and the linearized intron undergoes degradation (Ruskin and Green, 1985; Martin et al., 2002). Any failure in the disassembly of spliceosome affects recycling of the spliceosomal components for further rounds of splicing. Suboptimal splicing substrates with aberrant splice-sites, undergo discard pathway mediated by Prp43 (Koodathingal et al., 2010).

Second step Splicing Factors

The major components of the spliceosome which facilitate the second step of splicing are Prp16, Prp17, Prp18, Slu7, Prp8 and Prp22. These factors exhibit physical and genetic interactions among themselves and with U2, U5 and U6 snRNPs (Frank et al., 1992; Jones et al., 1995; Seshadri et al., 1996; Zhang and Schwer, 1997; Ben-Yehuda et al., 2000). Prp16 (described in previous section) and Prp17 act at initial stage which is ATP dependent, this is followed by ATP independent action of Slu7 and Prp18. Prp16, Prp8, Slu7 and Prp22 (described in previous section) are shown to be directly interacting with 3'ss region (McPheeters and Muhlenkamp, 2003; Umen and Guthrie, 1995).

Prp17

First identified in the screening for temperature sensitive mutants for defects in pre-mRNA splicing, Prp17 participates in the second step of the splicing reaction. Although not essential for splicing, intermediates accumulate even at the permissive temperature in *prp17* mutants (Vijayraghavan et al., 1989). Mutations in N-terminal regions of Prp17 have shown synthetic lethality with Prp16 and Prp18 mutants as well as with mutations in U5 snRNA, highlighting that its N-terminal region is critical for its interactions with Prp16, Prp18 and U5 snRNA (Seshadri et al., 1996). Human homologs of Prp17 has been cloned based on sequence similarity and have been shown to play role in the second catalytic step of pre-mRNA splicing in humans. Chimeric Prp17 with N-terminal region from yeast and C-terminal region from human fully complements *prp17 allele*, which shows Prp17 is functionally conserved across species (Horowitz & Krainer, 1997; Ben-Yehuda et al., 1998; Lindsey & Garcia-Blanco, 1998; Zhou & Reed, 1998). Splicing-sensitive DNA microarray data from our laboratory show Prp17 play a role in splicing of introns with length more than 200 nts and its role is superfluous when spacing between their branchpoint nucleotide and 3' splice-site is less (13 nts or less) (Sapra et al., 2004).

Prp18

Prp18 is a non-essential gene in *S. cerevisiae*, initially identified as a temperature sensitive allele *prp18-1* showed splicing defect in second step of catalysis (Vijayraghavan et al., 1989) The globular and functional C-terminal domain of Prp18 is composed of five α -helices and plays important role in stabilizing the exons and the spliceosomal interaction. It is known to interact with Slu7 and U5 snRNP (Jiang et al., 2000; Crotti et al., 2007). Rescue of Splicing defect in hPrp18-depleted HeLa cell extracts by yeast Prp18, showed that functional regions of the proteins is conserved across species and it is required for the second catalytic step. Human Prp18 differ from yeast Prp18 in having weak association with the snRNAs (Horowitz and Krainer, 1996). Slu7 and Prp18 were suggested to show coordinated function in the spliceosome as the requirement of Prp18 could be eluded when Slu7 was over expressed. The two-hybrid assay showed the existence of direct physical interaction between Slu7 and Prp18 (Zhang and Schwer, 1997). However, studies from our lab report that the fission yeast homologues of Slu7 and Prp18 do not show direct interaction and also SpPrp18 interaction with U5 snRNA is not observed (Piyush Khandelia, IISc Thesis). Also, contrary to the observation in budding yeast where Prp18 functions in the second step, fission yeast Prp18 like SpSlu7 has been reported to have an early splicing role and genetic interaction with early acting splicing factors of spliceosome (Vijaykrishna et al., 2016; Melangath et al., 2017)

Slu7

Slu7 (synthetic lethal with U5) a cysteine-rich zinc knuckle motif containing protein was first identified in the screening for alleles which showed lethal interaction with mutant U5 and were conditional lethal with wild type U5 (Frank et al., 1994; Frank and Guthrie, 1992). Slu7 is required for the second step of splicing and is required for 3'ss in introns with longer BrP to 3'ss distance (Frank and Guthrie, 1992), whereas intron with short BrP to 3'ss distance are independent of Slu7 suggesting its role in alternative-splicing regulation. It has been reported that there is interaction among Slu7, Prp18, Prp16, and U5 snRNA and are required for the completion of the second step of splicing (Frank et al., 1992). Through immunoprecipitation studies the hierarchy of recruitment of second step factors to the spliceosome was shown as Slu7>Prp18>Prp22 (James et al., 2002). Studies from our lab show that in *S. pombe* it is an essential splicing factor and in contrast to its human and budding yeast counterpart it has been reported to play role before any catalysis step. It showed salt-stable association with U5 snRNP and showed lethal genetic interaction with *spprp1* which is an early acting splicing factor (Banerjee et al., 2013).

Prp8

Through pull down experiments followed by mass spectrometry it has been identified that Prp8p is a component of the U5 snRNP and U5•U4/U6 tri-snRNP (Lossky et al., 1987; Teigelkamp et al., 1997; Gottschalk et al., 1999; Stevens and Abelson, 1999). Through cross linking experiments Prp8p was shown to be binding to the conserved GU residues at 5'ss, (Reyes et al., 1996, 1998) and the branchpoint (McPheeters and Muhlenkamp, 2003) and the 3'ss (Teigelkamp et al., 1995) in the pre-mRNA. Prp8 is also shown to be interacting with U5 snRNA (Dix et al., 1998) and U6 snRNAs (Vidal et al., 1999), all of which are considered to be in the catalytic centre of the spliceosome. Prp8 is implicated in the formation of U5•U4/U6 tri-snRNP complex and their incorporation into the spliceosome. It also interacts with Snu114 which regulates Brr2 function hence regulating the unwinding of U4/U6 di-snRNP. Hence, it is crucial for early spliceosomal assembly (Laggerbauer et al., 1998; Raghunathan and Guthrie, 1998; Small et al., 2006). In addition to its interaction with the pre-mRNA substrate, Prp8p is found to be associated with spliceosomes containing the reaction intermediates (products of the first *trans*-esterification reaction) or the excised intron (Teigelkamp et al., 1995).

I.2 Scope of Study

In splicing, the precise recognition and removal of introns is essential as they interrupt functional continuity of eukaryotic genes. Regardless of organisms, all nuclear pre-mRNA introns are removed from nascent transcript via two consecutive transesterification (phosphodiester transfer) reaction steps, catalysed by a large ribonucleoprotein complex, the spliceosome, which consists of five uridine rich small nuclear RNAs (snRNAs) and above 100 protein factors most of which have essential functions during identification, positioning of splice-sites in the catalytic center and in aiding catalysis (Moore et al., 1993; Will and Lührmann, 2011). *In vitro* studies with mammalian and budding yeast cell-free extracts and mini-pre-mRNAs show the spliceosome is a highly dynamic structure, components of which are assembled by sequential binding of the snRNPs and protein factors. As mentioned earlier spliceosome assembly is a dynamic process where sequential formation and disruption of RNA-RNA interactions is essential to formation of the catalytic centre and spliceosome disassembly. These rearrangements of the spliceosome machinery are important for intronic *cis* element recognition and formation of catalytic site. Prime factors belong to DExD or DExH families of proteins which facilitate these ordered re-arrangements. Prp16 is a DExD box helicase well characterised in *S. cerevisiae* as an essential factor for spliceosome conformational change that remodels the spliceosome catalytic centre after the first catalytic step. Prp16 recognizes the branch nucleotide at the branch consensus intronic element and the intron-exon 3'ss and aid in formation of catalytic centre for the second step reaction. Prp16 also acts to proofread the branch-site and reject aberrant lariat intron-3'exon intermediates from participating in second step reaction. The fission yeast genome with multiple short introns, degenerate intronic consensus elements and unconventionally positioned polypyrimidine tract is a useful alternative model to study splicing mechanisms that occur by intron definition relevant to many fungal, plant, worm and other eukaryotic genomes with similar intronic features. Prior studies from our laboratory on functions for some predicted fission yeast homologs of budding yeast second step splicing factors (Slu7 and Prp18) suggest that in fission yeast, these factors likely associate and have roles in early precatalytic spliceosome before the first catalytic step.

To study if the C-terminal enzymatic region of SpPrp16 is functionally conserved, we expressed chimeric Prp16 protein and full length in the budding yeast strain *scprp16-2* temperature sensitive recessive mutant. The N-terminal from budding yeast was translationally fused to the C-terminal of SpPrp16. These recombinant plasmids were used

transform *scprp16-2* mutant and transformants were scored for ability to rescue temperature sensitivity. Clones that express only the full-length fission yeast SpPrp16 were tested for complementation of *scprp16-2* strain. To functionally characterise the *S. pombe* essential gene *spprp16+*, further studies were carried out using two missense mutants *spprp16G515A* and *spprp16F528S* previously created in lab (Drisya V., IISc Thesis; Vijayakumari et al., 2019). As budding yeast ScPrp16 functions are largely during second step splicing, we examined fission yeast RNA transcriptome in *spprp16F528S* and found two predicted cellular introns *alp41 I5(intron 5)* and *gms2 I2 (intron2)* to evaluate if fission yeast Prp16 is required for second step of splicing. Their splicing status was analysed by semi-quantitative RT-PCR and by in-depth primer extension assays which also score for accumulation of lariat intermediate species if there is defect in second step of splicing.

The conserved G373 residue in *ScPRP16* corresponds to G515 residue in fission yeast *spprp16+*. The budding yeast *scprp16G373S* mutant can suppress mutations in the *ACT1* intron branch nucleotide (Burgess et al., 1990; Burgess and Guthrie, 1993). Hence, we created the analogous mutation in fission yeast protein. To analyse SpPrp16 interactions with branch point nucleotide the branch point mutation was made in *tjIID+ E1-II-E2eGFP (exon1-intron1-exon2eGFP)* mini-gene and its splicing was studied in *spprp16+ dbr1Δ* and *spprp16G515A dbr1Δ* double mutant (strains generated by Drisya V., IISc). Additionally, in this study to expand the repertoire of fission yeast mutants for future functional studies two other mutants were created. These residues were chosen based on mutants studied in its *S. cerevisiae* homolog ScPrp16 where such conditional alleles have been reported and splicing of one cellular transcript was tested. The *spprp16F528S*, a slow growing mutant, had a functional helicase domain *in vitro* while *spprp16G515A* was a poor helicase *in vitro* (Drisya V., IISc Thesis) Using the same bacterial purified helicase domain proteins, in parallel, this study probed their ATPase activities. The RNA binding of SpPrp16+ and SpPrp16G515A mutant was examined. Prior data in the laboratory by collaborator Drisya V. IISc and others have determined the global splicing profile in *spprp16+* and *spprp16F528S* strains by deep sequencing which confirm a critical and global role for SpPrp16 in fission yeast. Further, these work from lab collaborators showed the intronic 5'ss consensus, particularly minor variations in the frequency of specific nucleotides at its +4 to +6 positions could discriminate SpPrp16 dependent vs. independent splicing. Further, since the U6 snRNA-5'ss and U2 snRNA-branch site base pairing interactions play a critical role in the formation of catalytic centre for the first transesterification reaction and its conformational change for the second splicing reaction, these interactions were re-examined. Based on leads from these in-depth bio-informatic studies in the laboratory, in my study a SpPrp16 dependent intron *Seb1+ II*

(*intron1*) was chosen for experimental studies particularly to study the effects of mutation at its 5'ss. For these studies plasmid expressed mini-transcript with wild type intron features was analysed for splicing and was compared with mutants at the 5'ss. Particularly, the test was designed to ask if the weakening of 5'ss and U6 snRNA can render a Prp16 dependent intron to an independent intron. In the complementary study we chose to strengthen the 5'ss-U6 snRNA interaction for the candidate intron *new13 II* which splice independently of SpPrp16. The splicing analysis of the wild type and mutant mini transcripts were then done in *spprp16+* and *spprp16F528S* mutant strains. Another mini-transcript with the *tif313 I2* was analysed to investigate the cumulative effects of interaction between 5'ss-U6 snRNA and BS-U2 snRNA in contributing to SpPrp16 dependence for splicing. Investigations utilizing these mini-transcripts in fission yeast Prp16 mutants will throw light on the interplay of splice-site-U snRNA strength and conformational transitions facilitated by splicing helicase Prp16 in the short introns of fission yeast.

Chapter II

Probing the functional conservation of Prp16 and its role in splicing in fission yeast

II.1 Introduction

Nuclear pre-mRNA splicing occurs in a ribonucleoprotein complex called spliceosome where two transesterification reactions typical of splicing take place. Spliceosome consists of five uridine rich small nuclear RNAs (snRNAs), in the form of small nuclear ribonucleoprotein particles (snRNPs) and above 100 protein factors. Most of these factors have essential functions during identification, positioning of splice-sites in the catalytic centre and in aiding catalysis (Moore et al., 1993; Will and Lührmann, 2011). Spliceosomal DExD/H box containing RNA helicases (Prp28, Prp5, Brr2, Prp2, Prp16, Prp22 and Prp43) have been studied for their role in driving transitions in the catalytic core in the spliceosome during splicing. These proteins harness energy from ATP hydrolysis for the catalysis and help in dynamic spliceosomal remodelling. The roles for these factors have been studied predominantly in budding yeast using genetic and biochemical approaches and by *in vitro* reactions using mammalian cell extracts.

Prp16 is a DExD box helicase well characterised in *S. cerevisiae* as an essential factor, a mutant which was identified as a suppressor of branch point mutation TACTAAC to TACTACC of the model mini transcript of actin (*act1 E1-II-E2*) (Couto et al., 1987). *In vitro* splicing assays elucidated its role in second step of splicing, showed its RNA-dependent ATPase activity, role in conformational rearrangement around the 3' splice-site in spliceosome after the first catalytic step (Wang et al., 1998; Schwer and Guthrie, 1992; Sapra et al., 2004). A role for Prp16 in kinetic proofreading and recognition of 3' splice-site is also known (Burgess and Guthrie, 1993; reviewed by Horowitz 2011; Villa and Guthrie, 2005; Koodathingal et al, 2010).

The fission yeast genome with multiple short introns, more degenerate intronic features like 5' splice-site, branch point sequence and the 3' splice-site and unconventionally positioned polypyrimidine tract makes it an alternative model to study BrP recognition and splicing mechanisms. Here, functional studies on *spprp16+* were carried out using two mutants generated in the lab (Drisy V., IISc Thesis) and two additional mutants were generated for *in vivo* studies in *S. pombe*.

II.2 Materials and Methods

Generation of chimeric Prp16 construct

C-terminal helicase domain of *spprp16+* 3.2 kb cDNA (430 amino acid) cloned in the bacterial cloning vector pBSKS (pBSKS SpPrp16 C-terminal) was available (Drisya V., IISc Thesis). N-terminal non-conserved budding yeast specific domain of 894bp (298 amino acid) was amplified from *ycp50Scprp16* plasmid and cloned in pBSKS. The C-terminal SpPrp16 was excised as a ClaI fragment from its pBSKS clone (pBSKS SpPrp16 C-terminal) and assembled as a translational fusion by taking the ClaI linearized pBSKS ScPrp16 N-terminal clone. In the recombinant clone pBSKS N+C chimeric Prp16, the translational fusion junction was confirmed by sequencing. This fusion would allow the expression of chimeric protein after it is cloned into yeast shuttle vector under suitable yeast promoter. The chimeric cDNA was excised as SalI fragment and ligated into SalI site in budding yeast pG1 shuttle vector for expression from the constitutive GPD promoter.

Generation of Chimeric construct with F528S mutation for Expression in *S. cerevisiae*.

The mutagenic primers were designed to introduce the F528S mutation in the C-terminal SpPrp16 domain of the chimera. Inverse PCR was carried out using the Chimeric construct pG1GPD (N-term. ScPrp16 + C-term. SpPrp16) as a template. The inverse PCR product obtained was run on gel to check the product. The PCR product was then treated with DpnI (NEB) to digest away the template plasmid. The DpnI treated PCR product was ethanol precipitated with 3M sodium acetate. The samples were spun at 12000 rpm and washed with 70% alcohol for 3 minutes at 12000 rpm. The pellet was resuspended in 10 µl H₂O. *E. coli* DH5 alpha was transformed with this product in parallel with the DpnI treated test PCR product. The bacterial colonies from this mutagenesis experiment were taken up for screening and confirm the occurrence of mutations by sequencing. Plasmids were isolated from around 10 transformants and two each were sequenced. Mutations at desired residues were confirmed by sequencing in the plasmid pG1Prp16 (N+C) chiF528S.

Yeast transformation

S. pombe cells were grown in EMM complete or selective medium to an OD (695 nm) of ~0.8 to 1.2. The culture was then pelleted at 3500 rpm to collect 10 OD cells. The pellet was washed with 1 ml sterile MQ H₂O and resuspended in 0.1M lithium acetate (pH-4.9). Following incubation for 90 minutes at 30°C ~4µg (in 10µl of H₂O) DNA to be transformed and 290 µl of PEG were added and incubated for 1 hour at 30°C. Heat shock treatment was done at 43°C for 15 minutes followed by incubation at room temperature for 10 minutes. The sample was then centrifuged at 3500 rpm for 3 minutes and the pellet was washed with 1 ml of sterile MQ H₂O. The washed pellet was resuspended in 100µl of water and plated on the required drop out media.

II.3 Results

Sequence homology between two yeast models

ATP dependent DExD/H box RNA helicases contain several conserved motifs. Prp16 is a DEAH box RNA helicase and in budding yeast its C-terminal domain is known for catalytic functions. This domain in its orthologs too harbors six signatory conserved motifs that could function for ATP binding, ATP hydrolysis and RNA unwinding. The two-model unicellular fungal species - fission yeast and budding yeast diverged 370 million years ago (Sipiczki, 2000) yet the C-terminal domain of Prp16 is highly conserved across species. *S. pombe* Prp16 (SpPrp16) is an essential splicing factor (Kim et al., 2010, Vijayakumari et al., 2019). Prp16 of *S. pombe* shows 37.6% identity at the level of amino acids with Prp16 of *S. cerevisiae*, a model organism in which its role in splicing mechanism has been extensively studied. The C-terminal region Prp16 between the two yeasts shows 53.5% identity and 70.9% similarity while the N-terminal domain which is known to function in spliceosomal recruitment in budding yeast shows 14.6% identity and 29.9% similarity with fission yeast N-terminal domain at the level of amino acids which reflects the N-terminal domain is non-conserved (Figure II.1).

A.

N-terminal region



B.

C-terminal region



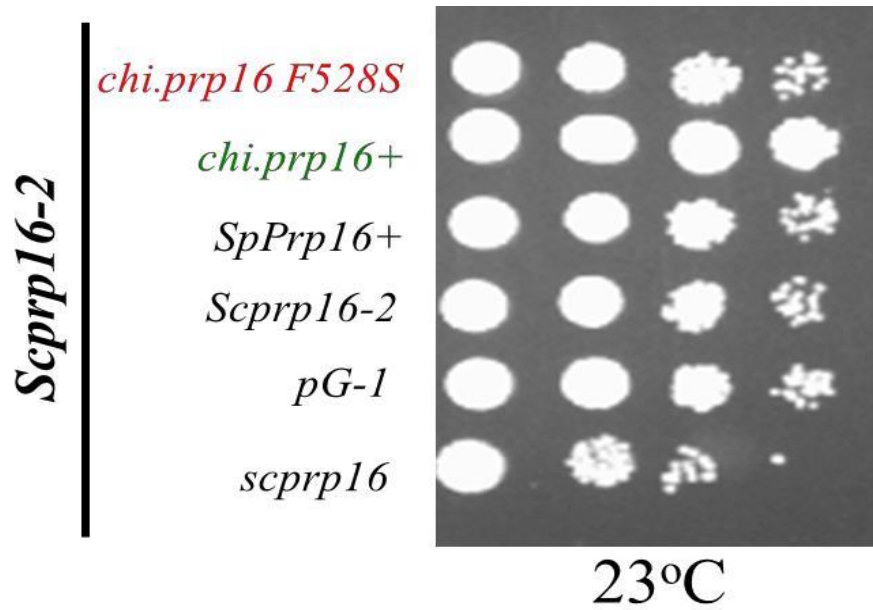
Figure II.1: Sequence alignment of Prp16 of *S. cerevisiae* and *S. pombe*. **A.** N-terminal region - 298 amino acid of *S. cerevisiae* aligned to 430 amino acid of *S. pombe* (29.9% Similarity) **B.** C-terminal region - 773 amino acid of *S. cerevisiae* aligned to 733 amino acid of *S. pombe* (70.9% similarity).

Genetic complementation of a *temperature-sensitive* budding yeast mutant

PRP16 in *S. cerevisiae* is recruited during assembly of spliceosome primarily via its non-conserved N-terminal domain of 298 amino acids (Wang et al., 1998) and C-terminal region performs the enzymatic functions. To study if the C-terminal region of SpPrp16 is functionally conserved between these yeasts, we generated constructs to express chimeric Prp16 protein in the budding yeast strain *scprp16-2* temperature sensitive recessive mutant. As a control, the full-length budding yeast PRP16 was also tested for complementation of the temperature sensitive phenotype. N-terminal 298 amino acids from budding yeast ScPrp16 which is non-conserved was translationally fused to the C-terminal 430 amino acids of SpPrp16 wild-type. The translation fusion was also made with 430 amino acid with SpPrp16F528S mutation, a conditional allele of SpPrp16 generated in the lab (Drisy V., IISc Thesis). This fission yeast mutant shows slow growth phenotype at all temperatures and a majority of *S. pombe* introns are inefficiently spliced (Vijayakumari et al., 2019).

The recombinant DNA fusion was first made in bacterial vector pBSKS and sequenced to validate the reading frame for translational fusion. The chimeric DNA and full length ScPrp16 were cloned in yeast pG-1 vector under GPD promoter with TRP selection marker. The recombinant chimeric clones with F528S mutation in the *S. pombe* C-terminal domain in were generated by inverse PCR on the pG-1GPDPrp16 chimeric clones using mutagenic primer for replacement of phenylalanine at 528 position to serine. The mutation was confirmed by sequencing the candidate mutant clones. The chimeric recombinant plasmids were used to transform *scprp16-2* a temperature sensitive mutant and the transformants were scored for their ability to rescue temperature sensitive growth phenotype on minimal synthetic defined agar media. The chimeric recombinant Prp16 protein where N-terminal domain from ScPrp16 and C-terminal domain from SpPrp16 are wild-type, fully rescued the temperature sensitive growth defect of *scprp16-2* and growth kinetics was comparable to cells transformed with the budding yeast plasmid Ycp50 with the native full-length budding yeast Prp16. On the other hand, *scprp16-2* cells with plasmid expressing the chimeric protein having C-terminal SpPrp16F528S mutation and also the transformants with plasmids for full-length fission yeast SpPrp16 in pG-1 vector expressed from GPD promoter failed to rescue growth of *scprp16-2* at 37°C (**Figure II.2**). These observations reaffirm the functional conservation of the C-terminal domain of Prp16 and show that N-terminal domain of budding yeast ScPrp16 is required for spliceosomal association. These data also show that the helicase and ATPase activities of fission yeast SpPrp16 is able to carry out 3'ss and Branch point recognition of budding yeast introns.

A.



B.

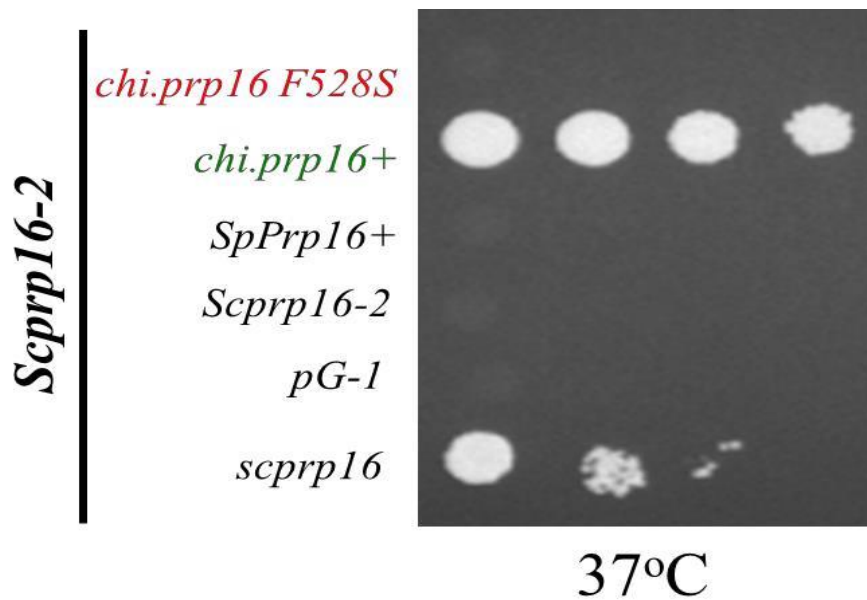
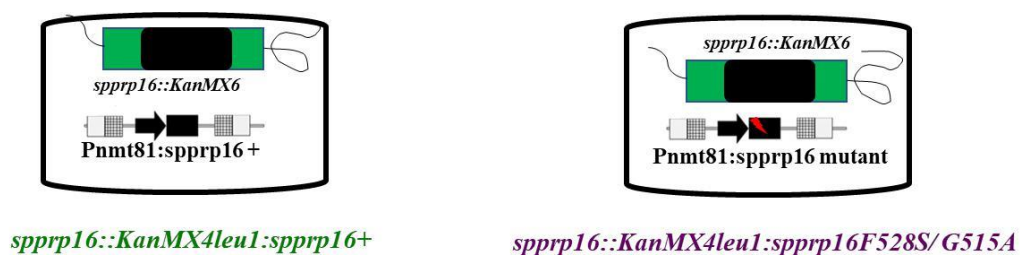
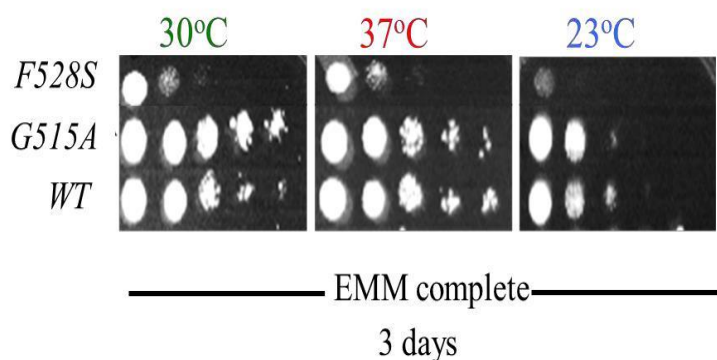


Figure II.2: Assay for complementation of the temperature sensitive budding yeast mutant *scprp16-2* by wild-type (ScPrp16 N-term - SpPrp16 C-term) or mutant (ScPrp16 N-term - SpPrp16F528S C-term) chimeric constructs and full length SpPrp16. The *ScPRP16*⁺ served as the positive control and pG-1 vector alone served as negative control. Growth phenotype was assessed at **A.** *scprp16-2* permissive temperature 23°C and **B.** *scprp16-2* non-permissive temperature 37°C.

A.



B.



C.

Introns of varying features were analysed for its *in vivo* splicing in the Prp16 mutants:

Intron	Length (nts)	5'SS sequence	Branch site sequence	3'SS sequence	Splicing Status in F528S mutant	Splicing Status in G515A mutant
<i>tfl1d</i> ⁺ I1	255	GTAAGT	CTAAT	TAG	Pre-mRNA accumulation	unaffected
<i>mdm35</i> ⁺ I1	62	GTAGAG	CTAAA	CAG	Pre-mRNA accumulation	unaffected
<i>nda3</i> ⁺ I4	51	GTAAGC	CTAAC	AAG	Pre-mRNA accumulation	unaffected

Figure II.3: A. Schematic representation of the genotype of *sprpr16+* and *sprpr16F528S/G515A* mutant integrant strains (Strains generated by Drisya V., IISc Thesis) B. Growth kinetics of the *sprpr16::KanMX4leu1:sprpr16+* and *sprpr16::KanMX4leu1:sprpr16F528S/G515A* strains at 30°C, 23°C and 37°C C. List of candidate introns with diverse *cis* features examined in the wild type and mutant strains with their splicing phenotype (Summary of data from collaborator Drisya V., IISc Thesis).

Generation of site-directed mutants at residues D712 and T643 in the DEAH motif containing domain of SpPrp16

For functional studies of essential gene *spprp16*, the mutagenesis and characterisation of random amino acid replacement at G515 and F528 residues of fission yeast SpPrp16 homologous to *S. cerevisiae* G373 and Y386 residues respectively were carried out in the laboratory (Drisy V., IISc Thesis) (**Figure II.3A and B**). In *S. cerevisiae* Y386D mutation does not map to conserved walker motifs. This mutant shows defective ATP hydrolysis along with defective splicing with precursor and lariat accumulation. The mutant *prp16-101* (G373S) in motif I has relaxed branch site fidelity but is splicing proficient and showed reduced *in vitro* ATPase activity (Burgess et al., 1990). Here, generation of additional mutants were taken up at T643 and D712 residue of *spprp16+* to create additional alleles for genetic and biochemical studies. Both T643 and D712 residues lie in DEAH box motif within helicase domain. The T501I mutant in the *S. cerevisiae* PRP16 (corresponding to T643 residue in *S. pombe*) had reduced *in vitro* ATPase activity but efficient *in vitro* splicing functions. Interestingly, in this budding yeast mutant, the mutation in invariant Br residue A were suppressed and this mutation was isolated as a suppressor of branch point nucleotide mutation (Burgess and Guthrie, 1993). Mutations in the D575N (asparagine) residue of budding yeast ScPrp16 (corresponding to D712 residue in *S. pombe*) confer temperature sensitive growth and arrest splicing with accumulated pre-mRNA and lariat species (Vijayraghavan et al., 1989). This indicates poor progression in both first and second step splicing transitions that lead to catalysis. For creating similar replacements in fission yeast *spprp16+*, we used WT type ORF in a fission yeast integration vector pJK148 as the template for the mutagenesis. The mutagenesis was done by inverse PCR using degenerate mutagenic primers where the residue was mutated such that the products will represent a pool of mutations that can introduce all other 19 amino acids (T643X and D712X). The inverse PCR product obtained was treated with DpnI to digest away the template plasmid with the wild type *spprp16+* gene. In parallel, input template DNA alone was treated with an equivalent concentration of DpnI as control. An equimolar concentration of DpnI treated PCR and DpnI treated template were used to transform *E. Coli* DH5 alpha cells. In the inverse PCR reactions done to mutagenize T643 residue, we obtained 65 colonies. In control transformation of DpnI treated input vector DNA, we found zero colony as expected.

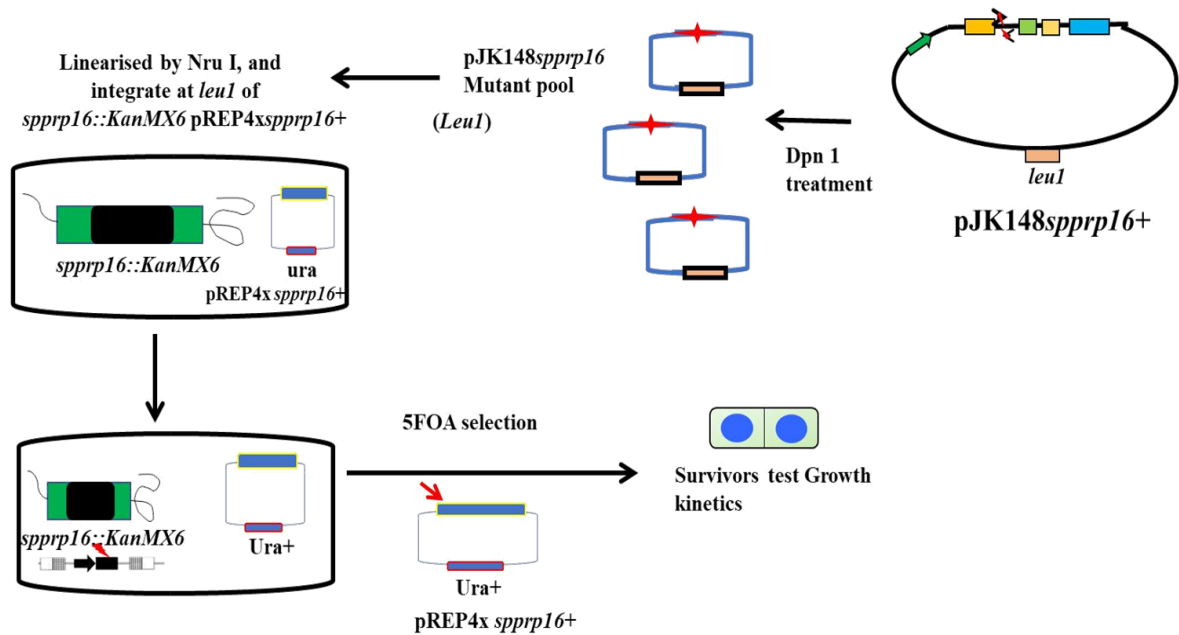


Figure II.4: Diagrammatic representation of the generation of mutants in *SpPrp16*. The residues chosen for mutagenesis were T643 and D712 and the site directed mutagenesis was done using mutagenic degenerate primers on the template *pREP81x spprp16+*. *spprp16::KanMX6 pREP4x spprp16+* was transformed with the DpnI treated PCR product and the transformants were selected on EMM L⁻. The transformants were made to evict the *spprp16+* Ura marked plasmid by patching on FOA. Those colonies which evicted the wt plasmid were colony purified and analysed for growth with respect to the *spprp16+* strain by dilution spotting.

For reactions where D712 mutagenesis was being done 72 colonies were obtained from the transformation using test inverse PCR product, while again as expected, no colony was obtained in DpnI treated template control. The bacterial colonies from each of these mutagenesis experiments were taken up for screening to confirm the occurrence of mutations. Plasmids were isolated from around 10 transformants in each case (i.e., pJK148 *spprp16T643K* and pJK148 *spprp16D712X*) and two each were sequenced. One of the plasmids had mutant ORF of T643K (pJK148 *spprp16T643K*) while the other plasmid turned out to be wild type *spprp16+*. This pJK148 *spprp16T643K* plasmid was linearised with NruI and taken for integration into the *S. pombe* genome at the *leu1* locus. This was done in a haploid strain constructed in the lab (Drisy V., IISc Thesis) where the endogenous *spprp16+* gene was disrupted with KanMX cassette which was kept viable by a plasmid expressing the wild type gene (pREP4x *spprp16+* which is *ura4+* marked). The transformants (*leu+* and *ura+*) obtained on EMM L⁻ U⁻ after integration of plasmid pJK148 *spprp16T643K* were purified. 6 single colonies were subsequently patched on to EMM L⁻ + 5FOA media to force evict the pREP4x *spprp16+* (*ura4+*) plasmid with the functional SpPrp16+. The survivors would yield integrants with a mutant *spprp16* allele at the *leu1* locus. Seven *leu+* *ura-* positive colonies on the 5FOA plate were colony purified and retested on EMM U⁻ to ascertain their uracil auxotrophy. Two of these confirmed colonies *spprp16::KanMX4leu1:spprp16T643K* were taken for further studies (**Figure II.4**) The inverse PCR amplicon pool for pJK148 *spprp16D712X* representing all possible amino acid substitution were NruI linearized and subsequent procedure for integration colony purification was followed as described for pJK148 *spprp16T643K*. Sequencing of PCR amplicon from genomic DNA derived from one *spprp16::KanMX4leu1:spprp16D712R* colony revealed D712R mutation.

Growth kinetics and analysis of splicing status of cellular transcripts in the mutants

The growth kinetics of strains with *spprp16T643K* and *spprp16D712R* mutant alleles were compared to a strain where the wild type allele was integrated at the *leu1* locus. These growth assays were performed at different temperatures – 23°C, 30°C and 37°C, by serial dilution on selective EMM agar media. We found that the *spprp16T643K* and *spprp16D712R* mutants showed growth comparable to wild type at all the temperatures (**Figure. II.5A**).

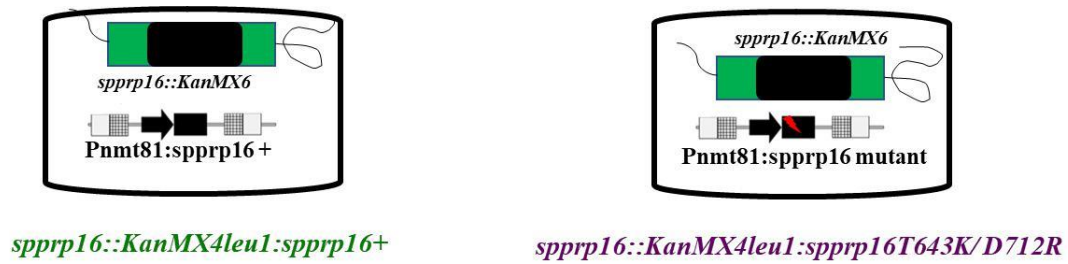
Next, we investigated the splicing efficiency of the 171nts intron 1 in the cellular *tif313+* transcript in both the strains. In parallel *tif313 II* splicing was also tested in *spprp16G515A*

and *spprp16F528S* mutants previously generated strains (Vijayakumari et al., 2019). Strains with the *spprp16T643K*, *spprp16D712R*, *spprp16F528S*, *spprp16G515A* mutant and *spprp16+* allele were grown in EMM L⁻ media at 30°C for 40 hours. These cells were harvested, and total RNA was extracted. The splicing was analyzed by semi-quantitative RT-PCR where we scored for the levels of pre-mRNA and mRNA. Efficient splicing of pre-mRNA converts it to mRNA whereas splicing defect leads to accumulation of pre-mRNA. From the DNase I treated RNA of SpPrp16+, *spprp16T643K*, *spprp16D712R*, *spprp16F528S* and *spprp16G515A* mutant strain cDNA synthesis was done using a reverse primer corresponding to exon 2 which is immediately downstream of intron 1. The tracer amount of α^{32} dATP was added in PCR reaction to radio label the PCR product for ease of visualisation of products separated on 8% native PAGE. Normalised signal intensities for mRNA and pre-mRNA in each RNA samples were analysed. These experiments revealed that *tif313 II* was poorly spliced in *spprp16T643K* mutant at levels comparable to *spprp16F528S* mutant (Drisya V., IISc Thesis). No detectable splicing defect was observed for *spprp16D712R* and this was comparable to the phenotype shown by *spprp16G515A* mutant (Drisya V., IISc Thesis) (**Figure II.5B**). The analysis of splicing status for more candidate cellular transcripts needs to be carried out to evaluate if the *spprp16T643K* mutant has other transcripts dependent on SpPrp16 functions.

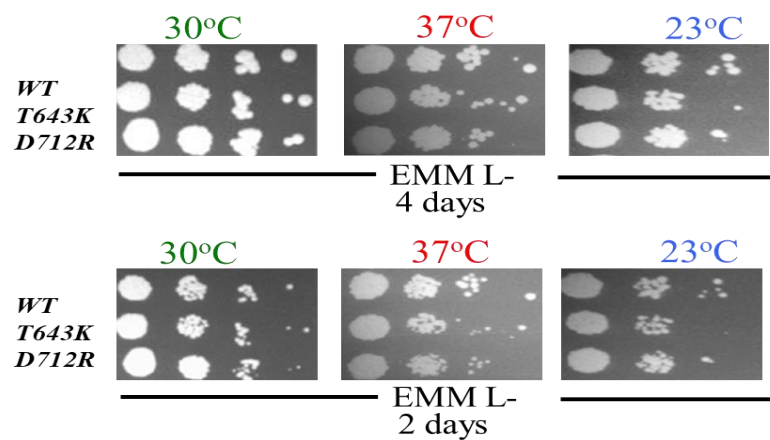
Examining the contribution of SpPrp16 in second step of splicing

ScPrp16 plays a major role in the spliceosomal rearrangement after the first catalytic step to recognise intron-exon 3'ss and facilitate second step of catalysis. This is evident from the accumulation of lariat intermediate species, a hallmark for second step splicing defect seen for several *scprp16* mutants studied (Burgess and Guthrie, 1993; Couto et al., 1987; Vijayraghavan et al., 1989; Madhani and Guthrie, 1994). My collaborator (Drisya V, IISc) in lab previously examined the role of SpPrp16 in fission yeast cellular splicing using two conditional alleles *spprp16G515A* and *spprp16F528S*. *spprp16G515A* mutant, with normal growth kinetics, was splicing proficient for several candidate introns in cellular transcript. In contrast, splicing arrest before the first step of catalysis was observed for candidate introns tested in the *spprp16F528S* mutant (Vijayakumari et al., 2019). However, the corresponding mutant for *spprp16F528S* in *S. cerevisiae* (*prp16-1*,) showed high levels of lariat intron-3'exon and precursor mRNA and thus *scprp16-1* allele is defective for both the steps of splicing (Couto et al., 1987). Therefore, whole genome transcriptome sequencing data from *spprp16F528S* strain was re-examined to check for any fission yeast transcript intron where

A.



B.



C.

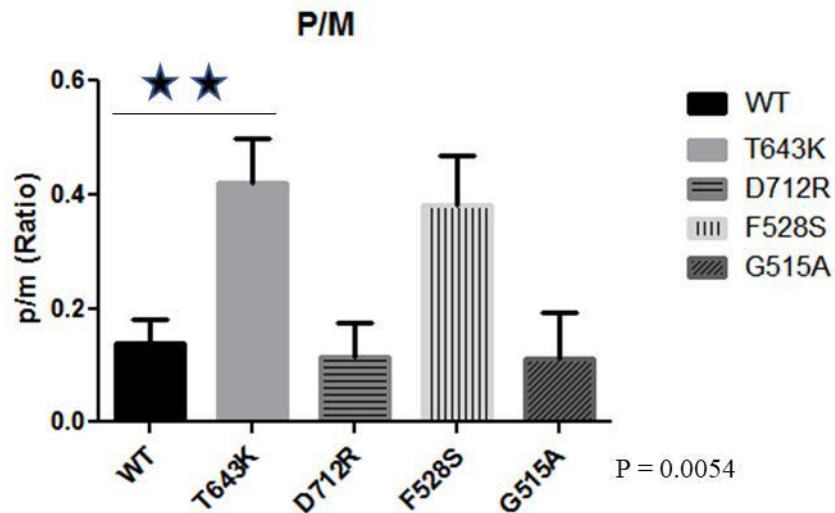
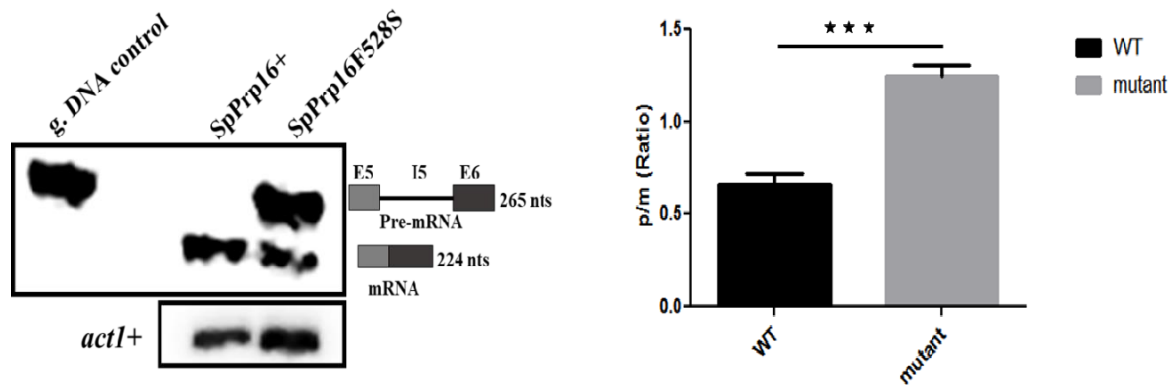


Figure. II.5: A. Schematic representation of the genotype of wild type and T643K and D712R mutant integrant strains. B. Growth kinetics of the *spprp16::KanMX4leu1:spprp16+* and *spprp16::KanMX4leu1:spprp16T643K/D712R* strains by serial dilution spotting. C. Analysis of the splicing of cellular *tif313+ I2* in Prp16 wild type and indicated mutant strains by RT-PCR.

A.



B.

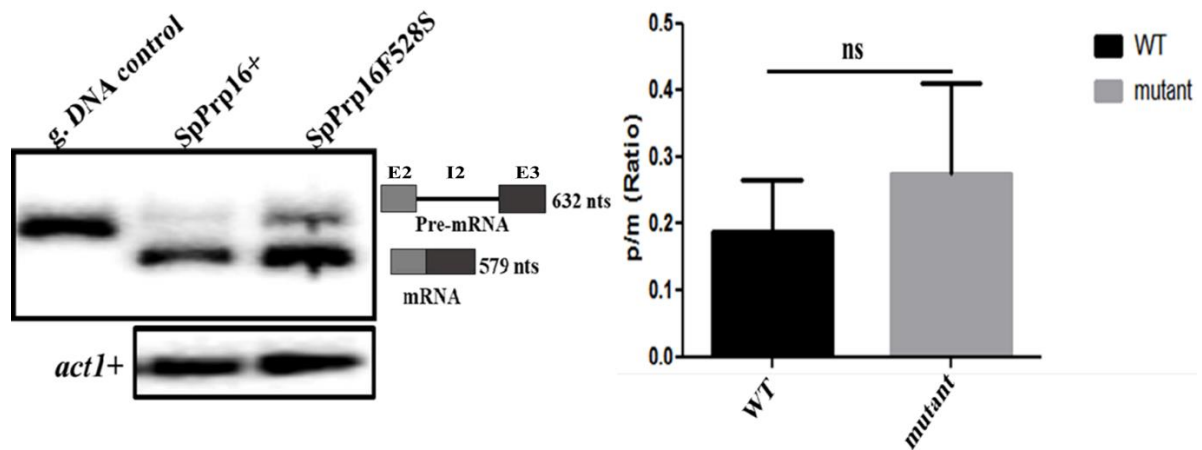


Figure II.6: Splicing analysis of cellular transcript predicted to be showing second step splicing defect. Semi-quantitative RT-PCR of **A.** *alp41 I5* in *spprp16* wild type and *spprp16F528S* mutant strain **B.** *gms2 I2* in *spprp16* wild type and *spprp16F528S* mutant strain.

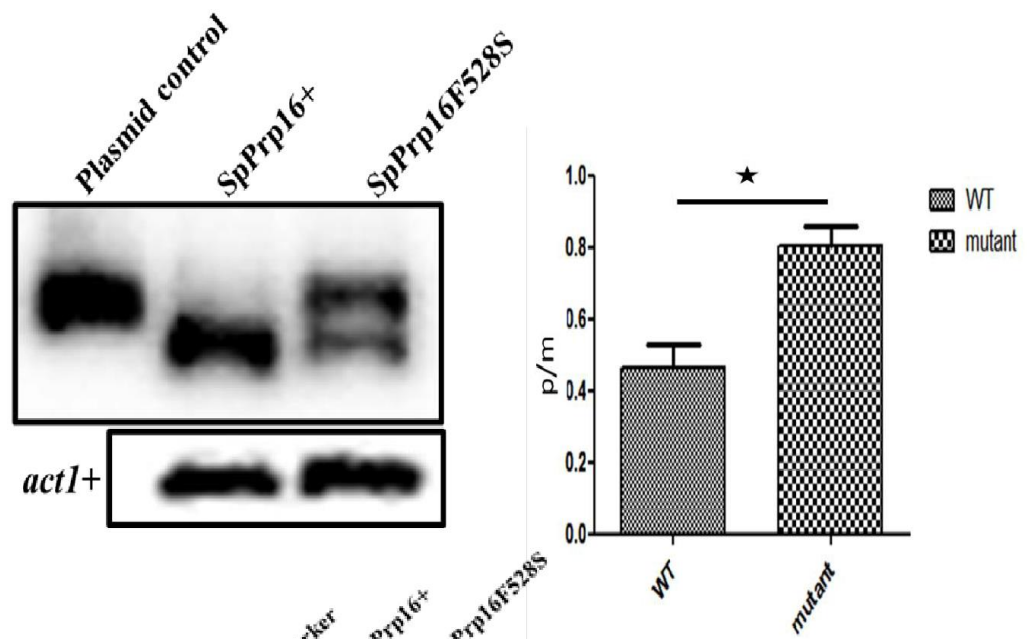
Prp16 is required for second step splicing reaction. Thus, we now scrutinized for NGS reads or transcripts where for specific introns there was decreased mRNA read intensities but for this corresponding intron it was not accompanied with significant increase in pre-mRNA or spliced junction read counts. The reads in the *spprp16F528S* mutant were compared to that in wild type cells. The 42 nucleotide *alp41 I5* and 43 nucleotide *gms2 I2* were potential candidates for further evaluation. The splicing status for these introns were first analysed in their cellular context. Semi-quantitative RT-PCR showed that both *alp41 I5* and *gms2 I2* cellular transcripts were efficiently spliced in wildtype *spprp16+* strain, while precursor accumulation was seen with corresponding mRNA decrease (**Figure II.6**). We also tested for the splicing of *alp41+ I5* when expressed as mini transcript. Hence, we generated the mini-gene construct pDblet *alp41+ E1-E6* that expresses *alp41 E1* to *E6* transcript from the *tbp1* promoter. *spprp16+* and *spprp16F528S* cells were transformed with this mini-gene plasmid and its splicing kinetics was analysed by RT-PCR. To further detect any accumulation of lariat intron E6, primer extension was carried out. Similar to splicing status observed for *alp41+ I5* in cellular transcript, both these assays showed *alp41 I5* was not efficiently spliced in *spprp16F528S* cells. Further, here too we do not detect lariat intermediate RNA species in primer extension assay. This inefficient splicing is caused by arrest before any catalysis which is evident by precursor accumulation (**Figure II.7**). Hence, we conclude that low read counts for spliced mRNA and failure to detect pre-mRNA in the NGS dataset could be an artefact of RNA sequencing or an indirect outcome of splicing that alters the stability of this mRNA in the *spprp16F528S* mutant.

SpPrp16 interactions with substrate Branch point sequence

Prp16 in *S. cerevisiae* is known to play a proofreading function at the branch site as many *scprp16* mutants which show compromised ATPase activity were shown to suppress the splicing defects of mutants at the branch consensus of *ACT1* intron (Tseng et al., 2011, Burgess and Guthrie, 1993, Couto et al., 1987). In *S. cerevisiae* for the *ACT1* transcript with intronic BrP A259 to C mutation, there was arrest at or prior to the first step of catalysis (Vijayraghavan et al., 1989; Query and Konarska, 2004). As previously mentioned other studies also point to BrP recognition by ScPrp16. We aimed to check the interaction of fission yeast SpPrp16 with BrP residue in mini-gene transcript *tflID E1-II-E2eGFP* with wild-type branch residue A (A441) or a mini-transcript with invariant branch residue A

substituted with a C or G which were available in lab (Drisy V., IISc Thesis) in fission yeast strains *spprp16+*, *spprp16F528S* and *spprp16G515A* that were also mutant for lariat debranchase (*dbr1*). Lack of any *dbr1* activity in strains with splicing factor mutants that are defective for second step of splicing would stabilise the lariat intermediate species by impeding their turnover. However, the *spprp16F528S dbr1Δ* (generated by Drisy V. IISc) showed synthetic lethality but the *spprp16G515A dbr1Δ* double mutant was viable with growth comparable to parent strains *spdbr1Δ* null. The *spprp16G515A dbr1Δ* at 37°C showed synthetic sickness (Drisy V., IISc Thesis). Therefore, we examined splicing for mini-transcript with Br-A or Br-C in the *spprp16G515A dbr1Δ* and *spprp16+ dbr1Δ* all grown at 30°C and 37°C. Primer extension assays were done to assess levels of cDNAs representing the pre-mRNA, mRNA and lariat intron-3' exon species. Here, we observed the mini-transcripts with Br-A and Br-C was adequately spliced in *spprp16+ dbr1Δ*. While the mini-transcript with Br-A was adequately spliced in *spprp16G515A*, its splicing was affected where the BrP was C evident by pre-mRNA accumulation and decrease in mRNA. At 37°C, the non-permissive temperature with sick growth, the Br-C containing transcript showed splicing defect both in *spprp16+ dbr1Δ* and *spprp16G515A dbr1Δ* mutant. Here too, precursor accumulation was seen with decrease in mRNA compared to the splicing of mini-gene with Br-A, in *spprp16+ dbr1Δ* and *spprp16G515A dbr1Δ* cells and in both strains accumulation of lariat intermediate was not observed (**Figure II.8**). Thus, we note an additive effect on combining Br-C *cis* mutant in substrate with *spprp16G515A* splicing factor mutant with no arrest before any catalysis. This contrasts with the ability of budding yeast *scprp16-1* to suppress the first step splicing defects of the Br-C substrates. This observation helps us infer that Branch site recognition and its interaction with SpPrp16 is different between the two yeasts.

A.



B.

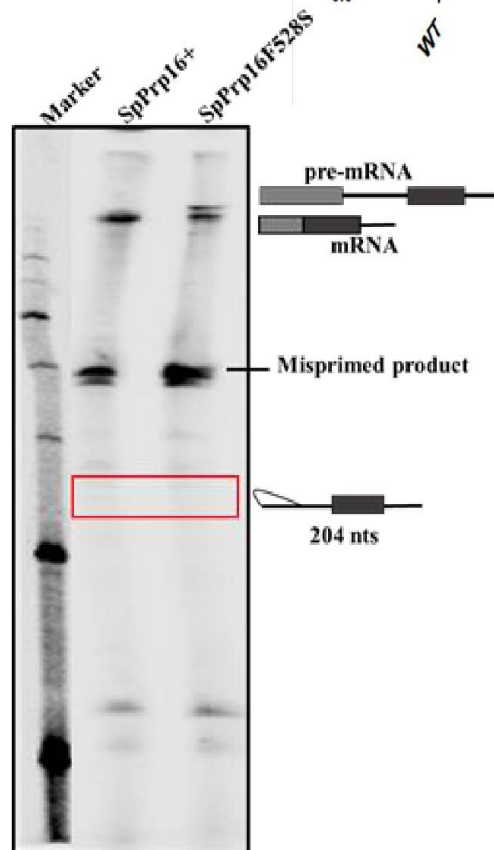


Figure II.7: *In vivo* splicing analysis of *alp41* E1-E6 mini-gene transcript by **A.** Semi-quantitative RT-PCR in *spprp16* wild type and *spprp16F528S* mutant strain **B.** by primer extension assay in *spprp16* wild type and *spprp16F528S* mutant strain.

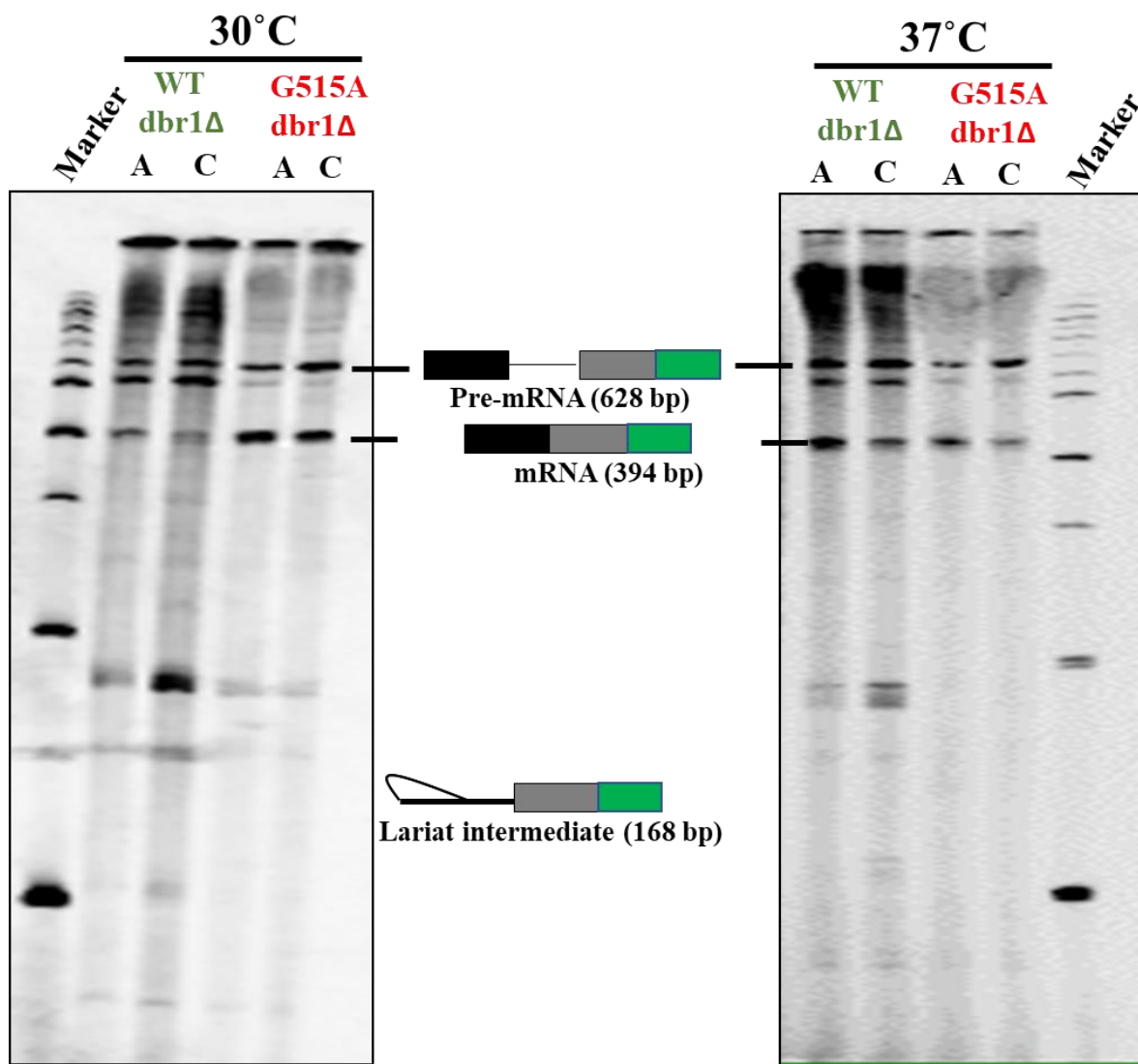


Figure II.8: Primer extension to analyse splicing of *tFIID* mini-gene transcripts wild type and branch site mutant in *spprp16+ dbr1Δ* and *spprp16G515A dbr1Δ* strain at 30°C and 37°C. GFPRP-1 was used for primer extension which corresponds to eGFP translationally fused to mini-transcript.

II.4 Discussion

Here, we show the chimeric Prp16 protein with the N-terminal and C-terminal domain from the two different yeasts, rescue the temperature sensitivity of budding yeast *scprp16-2* which reaffirm the functional conservation of the Prp16 however the failure of full length SpPrp16 to complement the *scprp16-2* mutant help us infer that the non-conserved ScPrp16 N-terminal domain is critical for its spliceosomal associations.

In this study, we show that splicing consequences of substrates with variant branch residues differ between budding and fission yeasts. The *spprp16G515A dbr1Δ* double mutant is unable to suppress the branch point mutation in the *tfIIId II* mini transcript where invariant A is substituted to C which is in contrast with the ability of corresponding budding yeast *scprp16-1* mutant to suppress the splicing defects of the Br-C substrates. The first transesterification reaction begins when Cwc25 binds to the branch site. After this reaction, Prp16 hydrolyzes ATP and translocates along the precursor RNA to release Cwc25 and Yju2 from the branch site to facilitate binding of second step factors. However, in mutant Br-C substrates the association of Cwc25 with weaker branch site slows down the first step (Tseng et al., 2011; Chiu et al., 2009). Here, Prp16 at the expense of ATP brings conformational change which can result in dissociation of Cwc25 before first step catalysis. Prp16 mutants with compromised ATP hydrolysis suppress the first step arrest of Br-C substrates due to the delayed conformational remodelling triggered by Prp16. This allows longer association of Cwc25 and Br-C which promotes 5'ss cleavage in Br-C substrates. Based on these studies, it was proposed that the first step catalysis and conformational change by Prp16 are in kinetic competition. Also, the association of Cwc25 with mutant Br-C substrates is stabilized by wild-type ScPrp16 to favour first step catalysis (Tseng et al., 2011; Burgess and Guthrie, 1993). The inability of the *spprp16G515A dbr1Δ* to suppress the first step arrest of the Br-C mutant could be possibly because the SpPrp16G515A mutant protein may be failing to stabilize Br-C-Cwf25 interaction in the activated spliceosome, which is reported for *S. cerevisiae* Prp16.

Our lab has reported the role of fission yeast Prp16 before first step of splicing by both *in vivo* splicing assays and genetic interaction studies (Vijayakumari et al., 2019). In this study also we saw the two transcripts *alp41 I5* and *gms2 I2* though predicted to be showing second step arrest from NGS data for *spprp16F528S* mutant (Drisya V., IISc Thesis) upon

examination for splicing by RT-PCR and primer extension experiment showed arrest at first step evident by the accumulation of precursor-RNA.

Chapter III

Biochemical characterization of SpPrp16

III.1 Introduction

The spliceosome which facilitates the two catalytic reactions of splicing is comprised of five snRNPs and numerous non-snRNP proteins. The snRNPs primarily function in identification of splice-sites and binding to these specific sequences on the pre-mRNA substrate and position the nucleotides to facilitate splicing (Valadkhan S, 2005). The non-snRNP proteins like DExD/H box containing ATP dependent RNA helicase play essential role in stabilization and disruption of RNA-RNA, RNA-protein and protein-protein interactions which facilitate structural and compositional changes during assembly, catalysis and disassembly in the spliceosomal machinery. Extensive genetic analyses and biochemical *in vitro* splicing assays in budding yeast and mammals has deciphered eight ATP dependent DExD/H box RNA helicases: Prp28, Prp5, Brr2, Prp2, UAP56/Sub2, Prp16, Prp22 and Prp43. Prp28 aids in stabilising 5'ss-U6 snRNA base pairing by functioning in destabilisation of U1/5'ss helix, also known to have proofreading function for 5'ss (Yang et al., 2013). Prp5 stabilises branch site-U2 snRNA base pairing and proofreads the branch site (Xu and Query, 2007). Brr2 helps in U4/U6 unwinding and positioning of 3' splice-site. Prp2 plays role in destabilization of early splicing factors and promotes binding of Cwc25 and Yju2 for 5' splice-site cleavage (Chiu et al., 2009; Ohrt et al., 2012). Based on *in vitro* assays ScPrp16 has been suggested to destabilize the U2-U6 helix I in the spliceosome active site and data suggest that this occurs between the first and second step of splicing allowing progression to the second step along with cwc2 which is a NTC component (Hogg et al., 2014). Prp22 plays proofreading function at second step of exon ligation. Prp43 promotes spliceosomal disassembly after a splicing cycle is completed (Arenas et al., 1997).

Study of enzymatic properties by *in vitro* biochemical (Helicase and ATP hydrolysis) assays of the above ATP dependent RNA helicases have enabled us to understand their functions in splicing. Prp16 has been extensively studied biochemically in *S. cerevisiae* as a DEAH-box RNA helicase particularly for its ATP-dependent RNA unwinding activity. Prior studies done by collaborator in laboratory created two missense *spprp16F528S* and *spprp16G515A* mutants in this essential fission yeast *spprp16+* gene (Drisya V., IISc Thesis). These two mutants of SpPrp16 generated in the helicase domain were used to decipher the enzymatic property by *in vitro* biochemical assays.

III.2 Materials and Methods

ATPase assay

The ATPase assays were carried out with 20, 40, 80,160 nM of the MBP tagged WT helicase domain of SpPrp16 and SpPrp16F528S and SpPrp16G515A mutant proteins. Reactions were incubated at 30°C for 30 minute in reaction buffer containing 40 mM HEPESKOH (pH 7.9), 100 mM KOAc, 0.5 mM MgCl₂, 1.0 mM ATP, 5 nM protein and trace amounts of [γ P³²] ATP (0.001 μ l of 3500 μ ci/mM) (γ P³²ATP from BARC). The reaction was stopped using 0.05 M EDTA. 1 μ l reaction sample of reaction sample was taken from all the reaction setup with different concentration of protein and separation of product (inorganic phosphate) from substrate ATP was carried out on PEI–cellulose thin layer chromatography plate (MERCK). The buffer for the TLC was 0.5 M LiCl, 0.5 M formic acid and run for 45 minutes. The results were quantified using a phosphor imager. The same protein samples (SpPrp16+, SpPrp16F528S, SpPrp16G515A) were also tested for helicase assay by our collaborator (Drisy V., IISc Thesis; Vijayakumari et al., 2019).

RNA EMSA

Chemically synthesized ssRNA of 47 nucleotides was 5' end labelled by setting up a 20 μ l reaction with 1 μ l of cold ssRNA, 25 μ ci of gamma γ P³²ATP with polynucleotide kinase (NEB) incubated at 37°C for 45 minutes and purified by G-25 sephadex column and use in RNA binding assays. A 20 μ l reaction was setup using labelled ssRNA incubated at 30°C for 30 minutes in presence of the specified amount of WT and mutant proteins in the helicase buffer (40 mM HEPES-KOH (pH-7.9), 50 mM potassium acetate, 1mM DTT, 0.05 mg/ml BSA, 3mM MgCl₂) without ATP. The reactions were loaded on a 10% native PAGE and electrophoresed in 0.5X TBE running buffer at 100 volts. The results were acquired using Phosphor imager.

III.3 Results

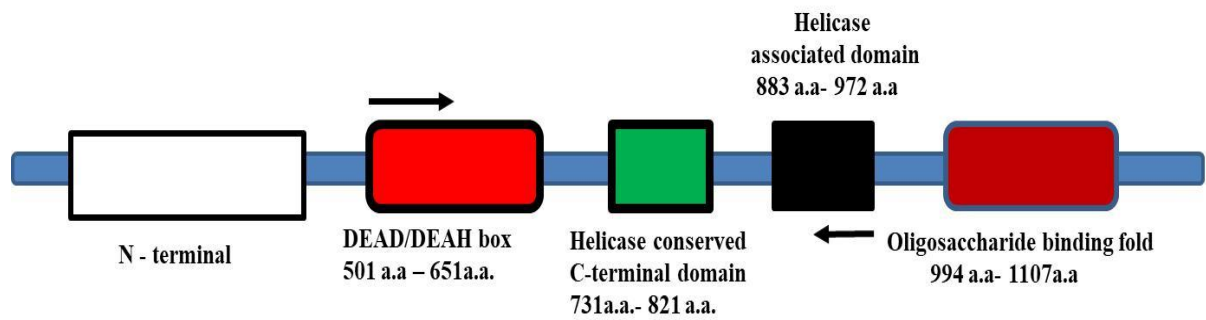
Purification of bacterially expressed helicase domain of SpPrp16 wild type and mutant proteins for biochemical study

Prior studies done by collaborator in laboratory (Drisya V., IISc thesis) created two mis-sense *spprp16F528S* and *spprp16G515A* mutants in this essential fission yeast *spprp16+* gene, characterized their growth phenotype, their effects on genome-wide splicing and their *in vitro* dsRNA helicase activities (Vijayakumari et al., 2019). To co-relate the different growth phenotypes, splicing and enzymatic functions in the helicase domain, the lab collaborator had generated plasmids for overexpression in bacteria of SpPrp16+, SpPrp16F528S and SpPrp16G515A helicase domain. The helicase domain (amino acid 501-862) from wild-type SpPrp16, SpPrp16F528S and SpPrp16G515A mutants were cloned in-translational fusion to the MBP tag in the bacterial expression vector pMALC2X (Drisya V., IISc Thesis). C41 *E. coli* competent cells were transformed with these plasmids and transformants were used for protein expression induced with IPTG and purified by using amylose resin and stored. Independent batches of proteins were raised and preparation with similar purity were used (Figure III.1).

Correlating unwinding activity of SpPrp16G515A/F528S mutants with their ATP hydrolysing ability

The purified MBP tagged SpPrp16 helicase domain with the F528S mutation was tested for helicase activity on dsRNA duplexes and compared to the MBP tagged wild-type protein (Drisya V., IISc thesis). The activities were surprisingly found to be equivalent *in vitro*, whereas MBP tagged SpPrp16G515A helicase protein showed compromised helicase activity (Fig. III.2) (Drisya V., IISc thesis). Here, the ATPase activity was measured for same MBP tagged SpPrp16+, SpPrp16F528S and SpPrp16G515A helicase domain protein preparations in order to discern if the poor RNA unwinding by the SpPrp16G515A helicase protein can be attributed to its ATPase activity. We tested the effects on release of terminal P³² from γ P³² ATP on incubation with increasing protein concentration (20, 40, 80 and 160 nM) of wildtype, SpPrp16F528S and SpPrp16G515A. The percentage ATP hydrolysis was plotted

A.



B.

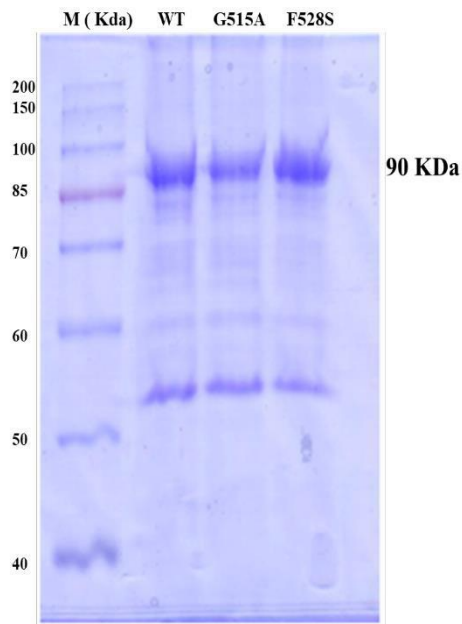


Figure III.1: **A.** Schematic of SpPrp16 domain architecture. Arrow marks indicate primer positions used by collaborator (Drisya V. IISc) to amplify the helicase domain (501–862 amino acids) of SpPrp16 wild type and mutant proteins. **B.** The SpPrp16 WT, SpPrp16F528S and SpPrp16G515A mutant helicase proteins fused to MBP tag (90.3 KDa) was run on 8% SDS PAGE and visualised by Coomassie blue staining.

against concentration of protein for respective protein. The protein concentration dependent increase in Pi released from $\gamma\text{p}^{32}\text{ATP}$ occurred in reaction carried out for 30 minutes at 30°C *in vitro* for wild-type and also the SpPrp16F528S helicase protein. Thus, these proteins are ATPase proficient *in vitro*. However, ATP hydrolysis by MBP-SpPrp16G515A helicase was poor as is evident from slower enzyme kinetics for released Pi compared to the Prp16 wild-type or the SpPrp16F528S protein (**Figure III. 3A**). ATP hydrolysis was also tested in time dependent manner using fixed amount of each of the three helicase proteins (10 nM concentration). The reactions were arrested at the mentioned time intervals ranging from 0 to 50 minutes using EDTA. The percentage ATP hydrolysis was calculated and plotted against time of incubation. The time dependent increase in Pi released from $\gamma\text{p}^{32}\text{ATP}$ occurred on incubation with either 10 nM wild-type or 10 nM SpPrp16F528S helicase protein reaching saturation by 50 minutes confirming their ATPase proficiency. However, ATP hydrolysis by SpPrp16G515A protein showed slower enzyme kinetics than either the wild-type or the SpPrp16F528S protein. As expected, for the control reaction done with purified MBP protein (10 nM) tag alone, only background signal was observed (**Figure III. 3B**). These experiments revealed that SpPrp16F528S with impaired *in vivo* splicing, poor growth but proficient in helicase activity (Drisya V., IISc thesis) also showed proficient ATPase activity comparable to WT helicase.

Investigations into the stimulatory role of RNA in ATP hydrolysis function of SpPrp16

Budding yeast ScPRP16 and other DExD/H-box protein with ATP hydrolysing activity are reported to be stimulated in the presence of RNA (Schwer and Guthrie, 1991; Hamann et al., 2019). Hence, we tested if there was stimulatory role of RNA in ATP hydrolysis activity of SpPrp16. Varying concentration (0 to 1200 nM) of dsRNA oligo was supplemented to reactions with 10 nM of the Prp16 wild type helicase domain and trace level of $\gamma\text{p}^{32}\text{ATP}$ as substrate in the ATPase assay at 30°C for 30 minutes. The release of Pi occurred on incubation with wild type helicase protein. Whereas, the negative control reaction setup with 0 and 1200 nM of dsRNA oligo without protein showed no ATP hydrolysis, only background signal was observed (**Figure III.4**). This observation show that presence of RNA plays a stimulatory for ATP hydrolysis for SpPrp16.



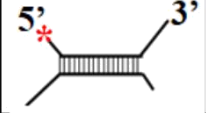
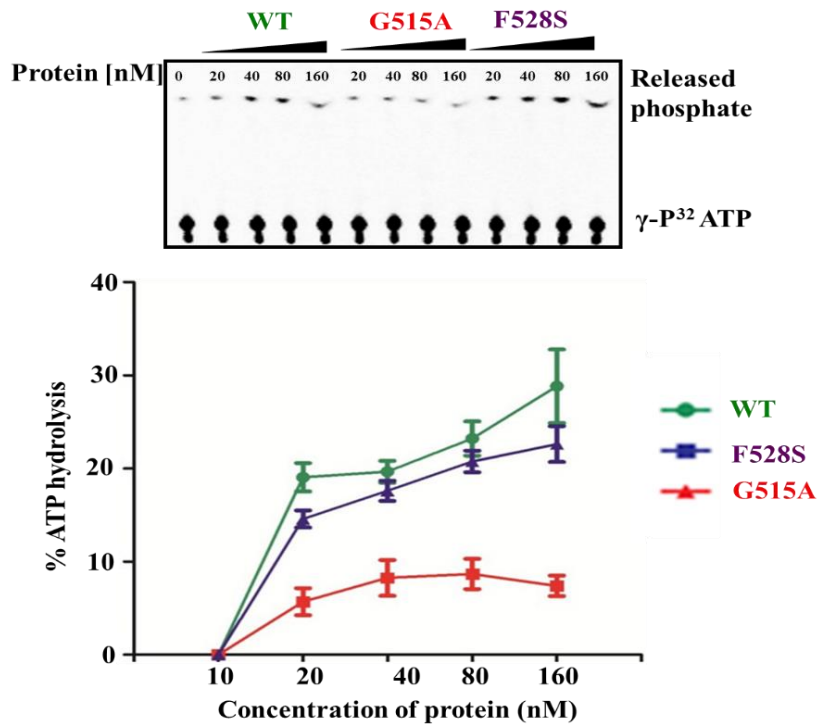
	A	B	C	D
1	RNA Duplex	SpPrp16 WT helicase domain	SpPrp16G515A helicase domain	SpPrp16F528S helicase domain
2		*****	*	*****
3		*	*	*
4		*****	*	*****

Figure III 2: SpPrp16 shows 3'-5' helicase activity. Summary of the evaluation of helicase activity of SpPrp16 WT, SpPrp16F528S and SpPrp16G515A mutant helicase protein. Column A represents dsRNA oligos with different overhangs (5'+ 3' overhang, 5' overhang and 3' overhang) with their 5' end labelled denoted by red *. Stars (*) in column B, C and D represent the efficiency in helicase activity of SpPrp16 WT, SpPrp16F528S and SpPrp16G515A mutant helicase protein respectively (Drisy V., IISc Thesis; Dr. Rakesh Kumar, IISc., Vijayakumari et al., 2019).

A.



B.

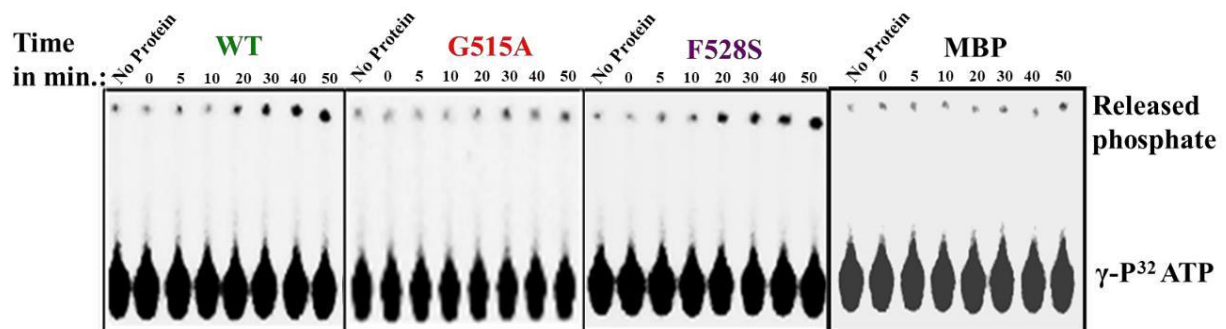


Figure III 3: Biochemical characterization of Spprp16 WT, SpPrp16G515A and SpPrp16F528S helicase domain. **A.** ATP hydrolysis by Spprp16 WT, SpPrp16G515A and SpPrp16F528S helicase protein upon incubating different concentration of each protein (20, 40, 80 and 160 nM) with 1 mM ATP and tracer amounts of $\gamma\text{P}^{32}\text{ATP}$ at 30°C for 30 minutes. **B.** ATP hydrolysis by SpPrp16 WT, SpPrp16G515A and SpPrp16F528S helicase protein upon incubating 10 nM of each protein with 1mM ATP and tracer amounts of $\gamma\text{P}^{32}\text{ATP}$ at 30°C for the different time points (5, 10, 20, 30, 40 and 50 minutes) contrast, SpPrp16G515A mutant which was splicing proficient with normal growth kinetics had poor helicase activity and also showed poor ATP hydrolysis. These data show that the poor RNA unwinding activity by SpPrp16G515A mutant protein could be mainly due to its distinguishably weaker *in vitro* ATPase activity that is not observed *in vivo* in the *spprp16G515A* mutant strain.

Correlating unwinding activity of SpPrp16+ and SpPrp16G515A mutant with their RNA binding ability.

Since, SpPrp16G515A protein had showed reduced *in vitro* dsRNA helicase and compromised ATPase activity, we were intrigued to examine if these poor enzymatic functions may relate to its ability to bind RNA substrate. Therefore, we took up the test of RNA binding by the wild-type and G515A MBP fusion helicase proteins to check complex formation by electro-mobility shift assays. The substrate was chemically synthesized ssRNA of 47 nucleotides which was 5' end labelled and taken for binding reactions at 30°C for 30 minutes. The MBP tagged Prp16 wild type and G515A mutant helicase proteins were taken at the range of 100 nM to 800 nM with fixed amount of labelled RNA (10 nM). The wild-type helicase protein formed RNA-protein complexes that increased with higher protein concentrations. However, SpPrp16G515A protein exhibited poor RNA binding over a wide range of protein concentrations (**Figure III.5**) As a control, MBP tag alone was used in same varying concentration with 10 nM labelled RNA. The poor unwinding and ATP hydrolysis could be the outcome of its poor RNA binding ability.

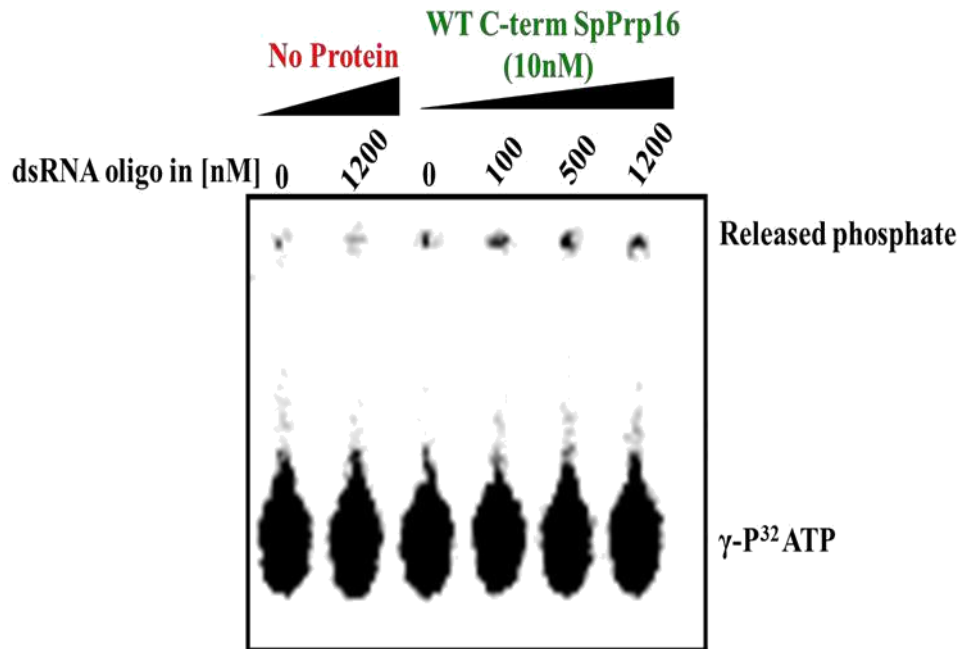


Figure III 4: dsRNA stimulates ATPase activity of SpPrp16. ATP hydrolysis by SpPrp16 WT helicase protein (10 nM) upon incubating with dsRNA oligo at different concentration (100, 500 and 1200nM) with 1mM ATP and tracer amounts of $\gamma\text{P}^{32}\text{ATP}$ at 30°C for 30 minutes.

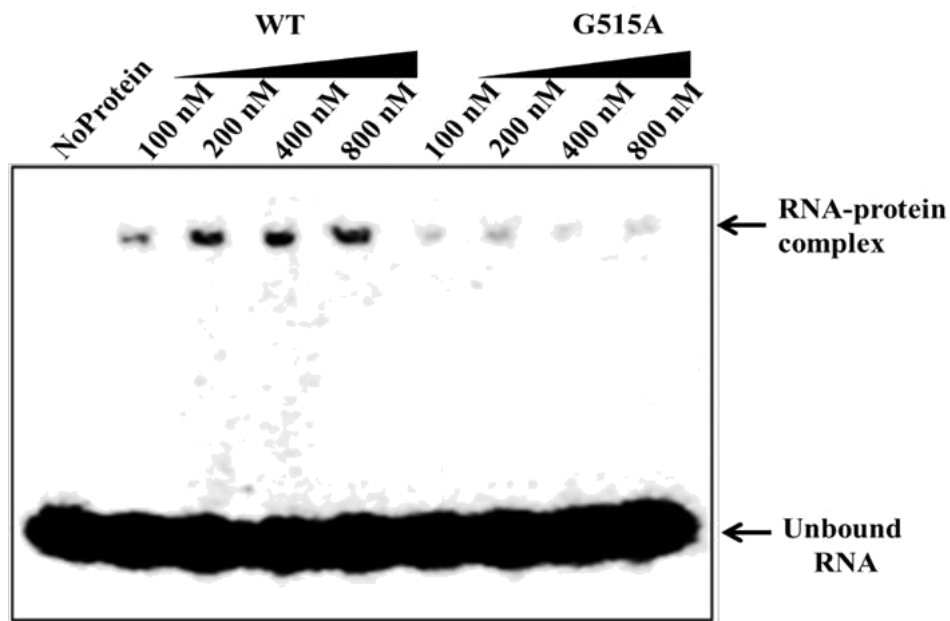


Figure III 5: SpPrp16 shows poor RNA binding ability. EMSA gel illustrating the RNA - protein complex with increasing concentration (100,200,400 and 800 nM) of SpPrp16 WT (lane 2-5) and SpPrp16G515A mutant helicase (lane 6-9) in the presence of 10 nM of 47 nucleotides 5' end labelled RNA incubated for 30 minutes.

III.4 Discussion

Through extensive biochemical studies of budding yeast several splicing complexes have been characterised and their composition and function at specific stages in spliceosomal cycle have been studied. These studies provide extensive information about the RNA-RNA and RNA-protein interactions that are necessary to assemble the various complexes in splicing. Role of budding yeast PRP16 DEAH/D box RNA helicase in second of splicing was revealed by *in vitro* biochemical characterisation of splicing extracts (Schwer and Guthrie, 1991). In this study, the mutant alleles of SpPrp16 - F528S and G515A were used to investigate its catalytic functions.

SpPrpF528S mutant when tested for its ability to unwind dsRNA substrate *in vitro* showed efficient unwinding activity (Vijayakumari et al., 2019). This mutant protein when tested for its ATP hydrolysis also showed efficient ATP hydrolysis indicating its ability to actively translocate along dsRNA substrate to unwind it. The inefficient *in vivo* splicing of *spprp16F528S* mutant but efficient helicase and ATPase activity can be attributed to the probable involvement of a cofactor which might be modulating splicing functions of Prp16 *in vivo*. One example of such co-factor in splicing is Spp2p. In budding yeast SPP2 gene is a high-copy number suppressor of temperature-sensitive mutants of *prp2-1*. Further, Prp2 and Spp2p proteins are shown to physically interact (Silverman et al., 2004; Roy et al., 1995). There are examples from previous studies where single residue mutants of DExD/H family of proteins like Prp22, Prp2 and Prp43 in budding yeast (Schneider et al., 2002; Tanaka et al., 2006) showed efficient *in vitro* ATPase and helicase activities but defective *in vivo* splicing so it possible that SpPrp16F528 residue is critical for coupling the enzymatic activity of the protein with its *in vivo* splicing functions.

SpPrp16 with G515A mutation in its helicase domain when tested for its ability to unwind dsRNA substrate *in vitro* showed inefficient unwinding activity which is in contrast to lack of *in vivo* splicing defect seen for majority of transcripts in cells with *spprp16G515A* mutant allele (Drisya V., IISc thesis). This MBP tagged SpPrp16G515A mutant protein when tested for its ATP hydrolysis in this study also showed defective ATP hydrolysis. This *in vitro* phenotype was also seen for the budding yeast Prp16 mutant with G373S mutation that correspond to G515 residue of fission yeast protein. The RNA binding ability of SpPrp16G515A mutant was compared to wild type Prp16 helicase protein by *in vitro* EMSA assay. The assay revealed the RNA binding of Prp16 is severely impaired with G515A

mutation. The defective helicase and ATPase enzymatic activity of this mutant can be attributed to its impaired RNA binding ability.

Chapter IV

Understanding the role of SpPrp16 in splice-site recognition

IV.1 Introduction

Pre-mRNA splicing occurs by precise recognition and removal of introns which is brought about in two transesterification reactions by dynamic action of several conserved proteins and five snRNPs that associate to form multi mega-dalton spliceosomal complex (Wahl et al., 2009). The recognition of intronic features like the 5' splice-site (5'ss), branch site (BS) and 3' splice-site (3'ss) by spliceosomal factors is very crucial for the alignment of splice-sites in the catalytic center for first step and subsequent transesterification reactions. During splicing, the spliceosome undergoes a cascade of several compositional and structural rearrangement illustrated by formation and disruption of various RNA-protein, RNA-RNA and protein-protein interactions where non-snRNP ATP dependent DExD/H box helicases play a crucial role (Staley et al., 1998). Prp16, a DEAH box RNA helicase mediates conformational change in the spliceosome assembly, triggers the ejection of Cwc25 and Yju2 (early catalysis factors) by their translocation along the RNA or by structural rearrangement which destabilises and displaces these proteins (Tseng et al., 2011, Lardelli et al., 2010). Prp16 is also known to play a role in disrupting U2-U6 helix I (RNA-RNA interaction) to facilitate catalytic second step reaction along with cwc2, a NTC component (Hogg et al., 2014). However, the role of ATP dependent RNA helicases in splice-site selection and the role of snRNA-*cis* elements in pre-mRNA are not explored in *S. pombe* these organisms. Here, we undertook to study the role of SpPrp16 in splice-site recognition using conditional allele previously generated in our lab (Drishya V., IISc Thesis; Vijayakumari et al., 2019) through assays for splicing on cellular and plasmid expressed mini-gene transcripts.

IV.2 Material and Methods

Primer extension

Primer extension on RNA to score for pre-mRNA, lariat intermediate and mRNA was done using radioactive end labelled reverse primer corresponding to 3'exon. A total of 40 microgram RNA per sample was precipitated in 100 percent alcohol in presence of 1x TAE, yeast tRNA, 3M CH₃COONa keeping at -80°C for 3-4 hours. The samples were pelleted down at 13000 rpm for 40 minutes, washed with 70 percent alcohol, pellets were dried for 5

minutes at 65°C and dissolved in 11 µl of DEPC treated H₂O. A 20 µl reaction was setup for reverse transcribed primer extension reaction of each sample using 10 µl of RNA and γ p³² end labelled primer in volume which will contain 4 lakh counts per minute and 1 µl 10 mM dNTP. This was incubated at 56°C, for 5 minutes then snap chilled in ice. Now to each reaction following were added - 1x MMLV buffer (NEB), MMLV RT (NEB 40 units) and incubated for 1.5 hour (extension) at 37°C. Then the reaction was terminated at 75°C for 10 minutes. Following components were added after inactivation - 1x TAE, yeast tRNA, 3M CH₃COONa, 100 percent alcohol and precipitation was allowed by overnight incubation at -20°C. The samples were spun at 13000 rpm for 40 minutes and the radioactive supernatant was discarded. 70 percent alcohol wash was given, and the pellet was dried. Samples for loading were prepared by addition of formamide dye and incubation at 95°C for 5 minutes and snap chilled. Samples were loaded on 40 cm long 4 percent urea page gel (which was pre run for 1 hour approximately with dye only). The gel was exposed to Phosphor imager film and analysed by scanning using phosphor imager.

Semi-quantitative RT-PCR

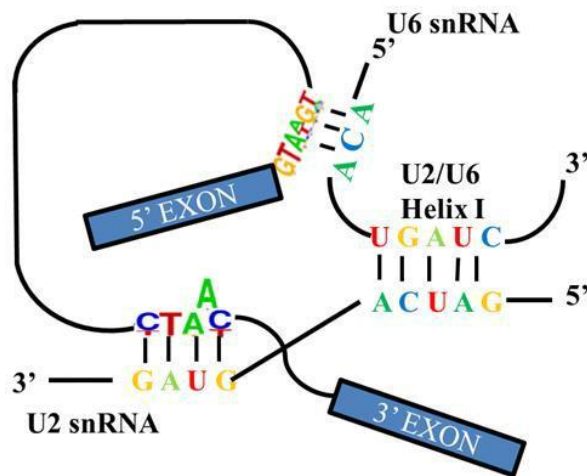
For 10 µl volume of reverse transcription reaction, 2 µg of DNase I treated RNA samples and required volume of water was denatured at 65°C for 5 minutes followed by snap chilling on ice. 200 ng of the gene specific and actin RP and 1µl of 10 mM dNTPs were added. The reaction mix containing primers and dNTPs was denatured at 65°C for 15 minutes and snap chilled on ice. The cocktail of primer and dNTP was added to the snap chilled RNA and to this mix, 10 units of RNase inhibitor (NEB), 2 µl of 5X reverse transcription buffer and 50 units of MMLV (Moloney murine leukemia virus) reverse transcriptase was added. Reverse transcription was carried out at 37°C for 90 minutes and the reaction was terminated by heat inactivation at 70°C for 10 minutes. 200 ng of cDNA was used for PCR and the amplification was done in the presence of α p³² dATP (1 µci per PCR reaction, specific activity 3200 Ci/mMol, BRIT) for labelling the PCR product and the products were run on 8% native PAGE. Signal intensities of RNA and pre-mRNA are obtained by photo-stimulated luminescent counts in a phosphor imager.

IV.3 Results

Exploring the role of base pairing interactions between U6 snRNA and 5' Splice-site

Prior data in the laboratory by collaborator (Drisya V., IISc Thesis) and others has determined the global splicing profile in *spprp16+* and *spprp16F528S* strains by deep sequencing of the transcriptome followed by bio-informatic analysis of splicing events (Vijayakumari et al., 2019). These data confirm a critical and widespread role for SpPrp16 for splicing of intronic transcripts in fission yeast. These prior global intronic signatures could distinguish intron sets that are SpPrp16 dependent and a small set of introns that are independent of SpPrp16 for splicing. These intron sets did not show any significant difference with respect to the sequence consensus of 5'ss, polypyrimidine tract, BS and 3'ss. Also, other general intronic features which may determine the dependence of introns on SpPrp16 like intronic AU content, length of intron, distance between 5'ss and BS, distance between BS and 3'ss distance did not differ between the dependent and independent category introns. From the SpPrp16 and SpPrp16F528S RNA seq data analysis, it was predicted that minor variations in the frequency of occurrence of specific nucleotides at the +4, +5 and +6 positions may discriminate between SpPrp16 dependent and independent introns (Drisya V., IISc Thesis; Vijaykumari et al., 2019). The +4, +5 and +6 nucleotides of the 5'ss in SpPrp16 dependent vs independent introns showed variation in the strength of interaction with the ACA conserved residues of U6 snRNA (ACAGAGA box). A significant percentage of SpPrp16 dependent introns had complete 5'ss-U6 snRNA complementarity at +4, +5 and +6 of 5'ss-U6 snRNA interaction (**Figure IV.1**) (Drisya V., IISc Thesis; collaborator Pushpinder Singh Bawa, IBAB, Bangalore). Based on leads from these in-depth bio-informatic studies in this study, we chose in this study *Seb1+ II* from the SpPrp16 dependent intron category for detailed experimental investigations on the effects of mutation at its 5'ss. For these studies mini-gene plasmids with wild type *seb1+ E1-II-E2* expressed from the fission yeast constitutive *tbp1* promoter were generated. Further, *cis* mutations in this mini-transcript were made, to test their splicing in *spprp16+* and *spprp16F528S* strain (**Figure IV.2C**). For the latter, mutagenic primers were designed to replace +4 T and +6 T residues to +4 A and +6 A residues at the 5'ss of *Seb1 II* using the WT mini-gene pDblet *seb1+ E1-II-E2* plasmid template.

A.



B.

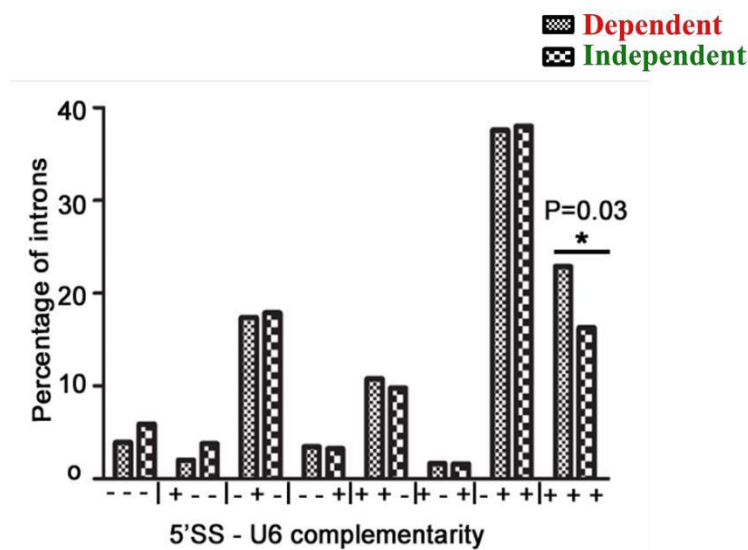


Figure IV.1: A. Diagrammatic representation of 5'ss- U6 snRNA, BS-U2 snRNA and U6-U2 snRNA base pairing. B. Analysis of 5'ss-U6 snRNA base-pairing (Drisy V., IISc Thesis; Pushpinder Singh Bawa IBAB, Bangalore). B. Graphical representation of the number of SpPrp16 dependent and independent category based on the complementarity of 5'ss +4, +5 and +6 nucleotides with the U6 snRNA sequence - ACA. Base pairing at each position is denoted by a '+' sign and no base pairing by '-' sign. The number of introns with complete complementarity indicated as '+++' is significantly different between the dependent and independent intron categories at $p = 0.03$.

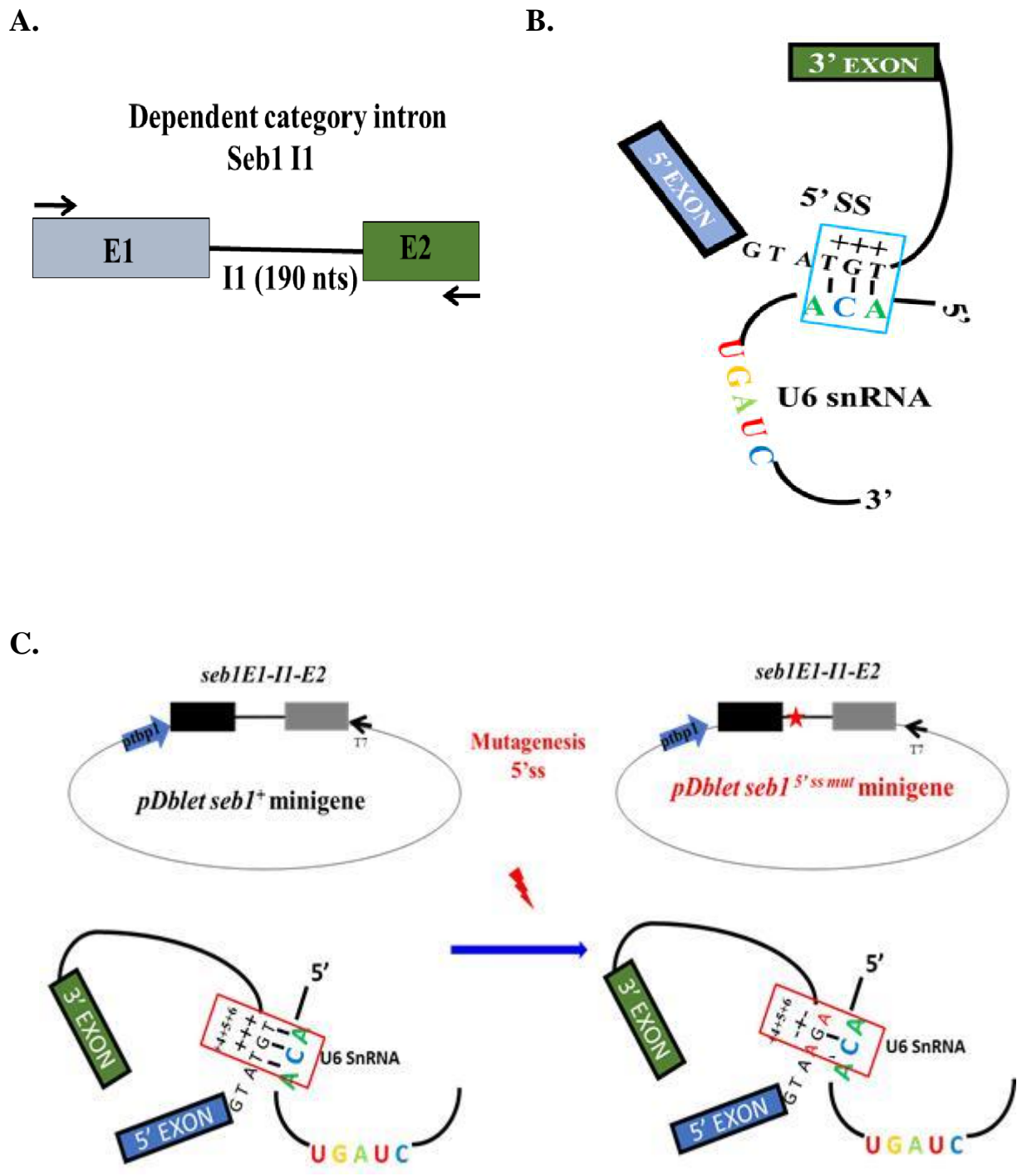


Figure IV.2: Diagrammatic representation of **A.** *seb1* E1-I1-E2 mini-gene segment for cloning in fission yeast shuttle vector pDblet under *tbp1* promoter **B.** Base pairing of +4+5+6 nucleotide in *seb1* I1 (*intron1*) with invariant ACA nucleotides of U6 snRNA. **C.** mutagenesis at +4 and +6 nucleotides of 5'ss of *seb1* I1.

These primers were used in inverse PCR reactions. The PCR product obtained, was treated with DpnI to digest away the template plasmid. As a control the input template DNA pDblet *seb1+ E1-II-E2* used for PCR was also treated with equivalent concentration of DpnI and an equimolar concentration of it was used to transform *E. coli* DH5 alpha. On transforming the inverse PCR reactions that would mutagenize 5'ss in *seb1+ E1-II-E2* we obtained 75 colonies, while from the negative control DpnI treated input template DNA gave no colony as expected. The bacterial colonies from each of these mutagenesis experiments were taken up for screening to confirm the occurrence of mutations. Plasmids were isolated from around 10 transformants and two each were sequenced (pDblet *seb1 II 5'ss mut #1* and pDblet *seb1 II 5'ss mut #2*). Mutations at the desired residues were confirmed by sequencing. The pDblet *seb1 II+* and pDblet *seb1 II 5'ss mut* mini-gene were individually used to transform fission yeast *spprp16+* and *spprp16F528S* strains and transformants selected on EMM L⁻ U⁻ media. Purified transformants were inoculated in liquid cultures and RNA was prepared for analysing splicing status of these mini-gene transcripts. RNA isolated was used in primer extension assays where using end labelled T7 RP would prime cDNA (**Figure IV.3**). The *Seb1 II* transcript with and without mutations at 5'ss were efficiently spliced in the *spprp16+* wild type strain. While the wild type mini-transcript was inefficiently spliced in the *spprp16F528S* mutant strain (**Figure IV.3**), the 5'ss mutant mini transcript showed better splicing in the *spprp16F528S* mutant strain. This data shows rescue of poor splicing of *seb1 II* mini-transcript when the interaction between 5'ss and U6 snRNA is weakened. This data provides experimental evidence for the bio-informatic predictions that strength of 5'ss-U6 snRNA interaction contribute in the dependence or independence of introns on SpPrp16 activity.

In the complementary exercise to experimentally prove relation between SpPrp16 function and 5'ss-U6 snRNA interaction we chose to strengthen the 5'ss-U6 snRNA base pairing interaction in a cellular intron *new13+ II (intron1)* that was predicted to be SpPrp16 independent for splicing as the NGS data showed to have normal levels of spliced mRNA. We created two different fission yeast mini-gene plasmids with wild type *new13+ E1-II-E2* and mini-gene *new13 E1-II-E2* with mutations at 5'ss (**Figure IV.4**). The mutagenic primers were designed to replace +4 A to +4 T at the 5' splice-site of *new13 II* using the WT mini-gene plasmid template. Inverse PCR was carried out using mutagenic primers using pDblet *new13+ E1-II-E2* as template. DpnI treated inverse PCR product obtained was used to transform *E. Coli* DH5 alpha. From the inverse PCR reactions to mutagenize *new13+ E1-II-E2*, we obtained 68 colonies while control reaction with input template DNA used in inverse PCR

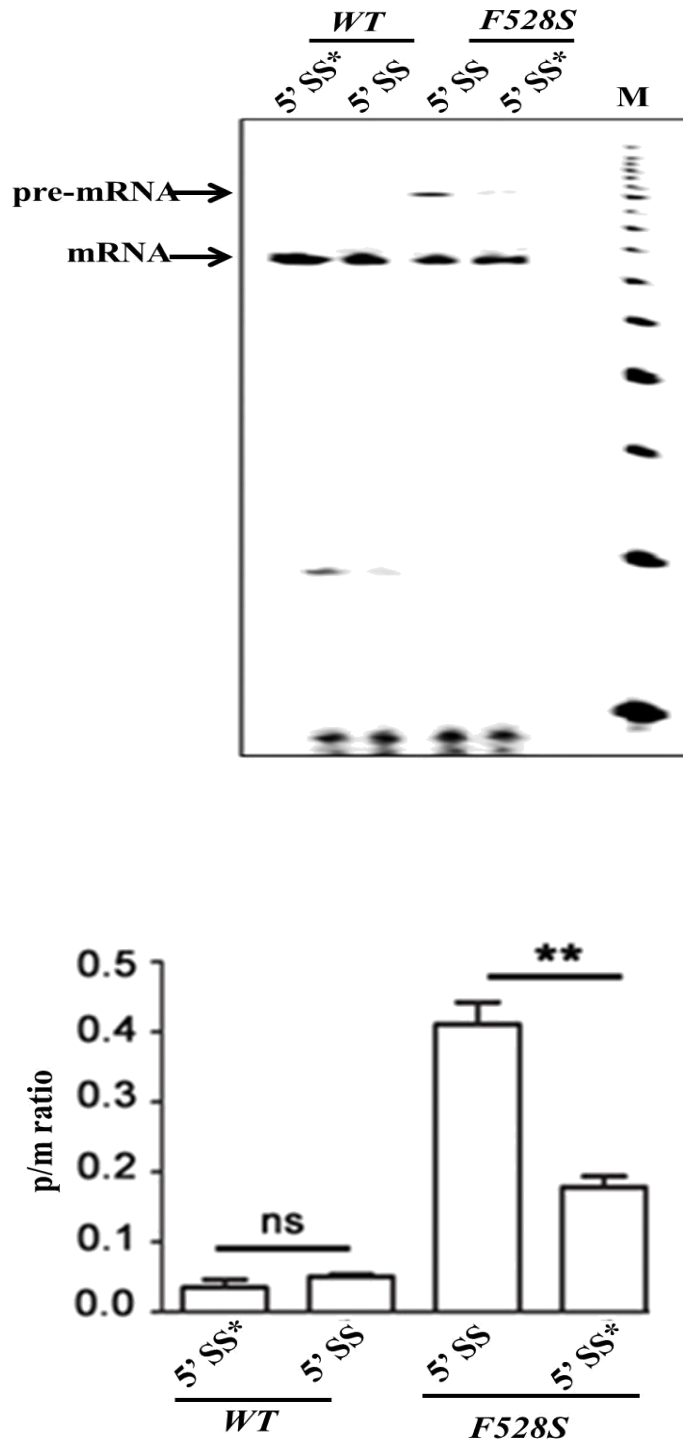


Figure IV.3: SpPrp16 aids the destabilization 5'ss-U6 snRNA. Primer extension assay to assess the splicing of *seb1 E1-II-E2* mini-transcripts having wildtype or mutant 5'ss (depicted as 5'ss and 5'ss* respectively) in the *spprp16+* and *spprp16F528S* mutant cells. Lane M - 100 nts to 1000 nts DNA size marker. Quantification of the data which shows there is significant rescue of splicing defect in *spprp16F528S* mutant cells with mutant 5'ss.

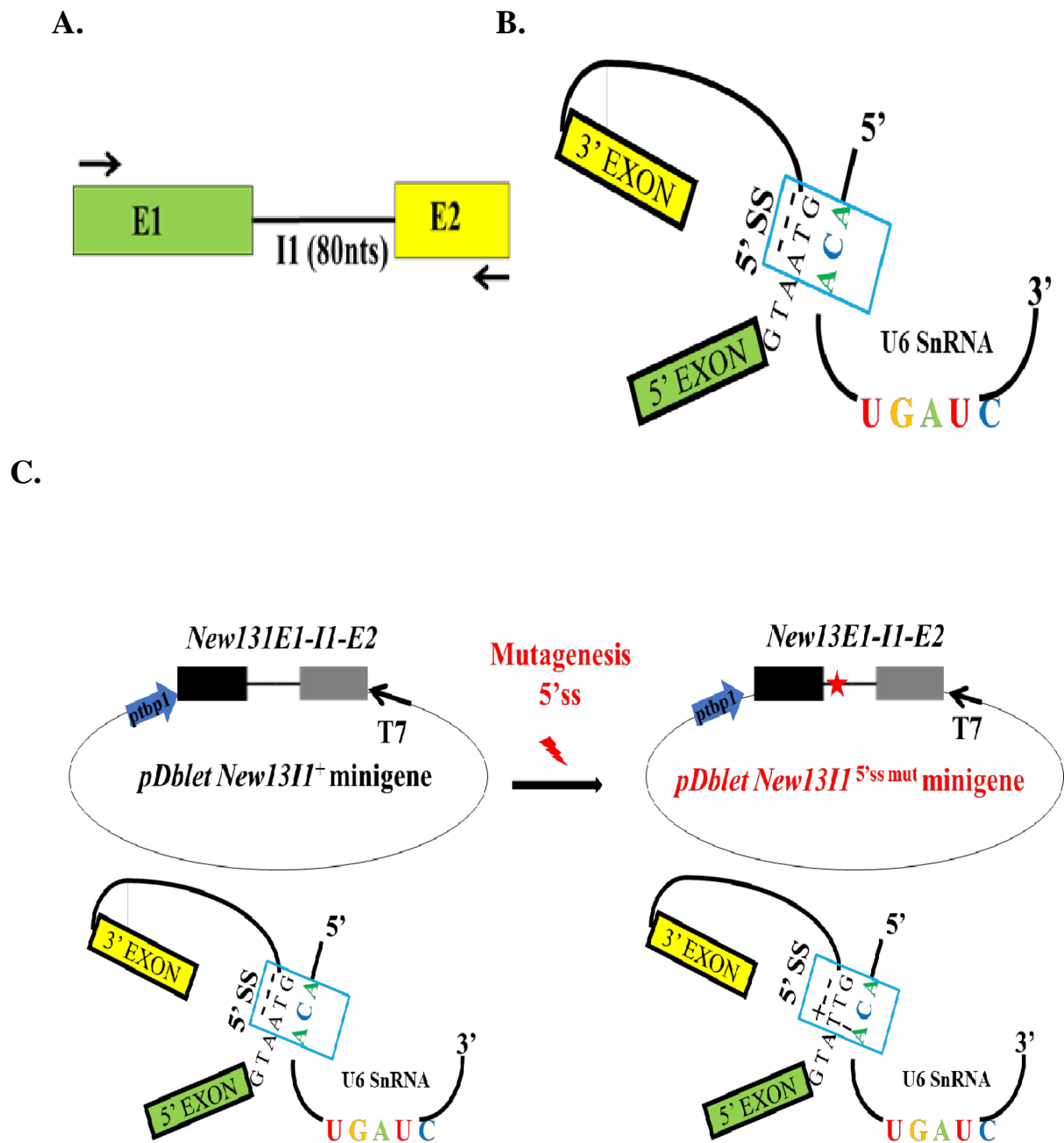


Figure IV.4: **A.** Diagrammatic representation of *new13+* *E1-I1-E2* mini-gene segment for cloning in fission yeast shuttle vector pDblet under *tbp1* promoter **B.** Base pairing potential of +4+5+6 nucleotides in *new13+* *I1* with invariant ACA nucleotides of U6 snRNA. **C.** mutagenesis at +4 position of 5'ss of *new13 I1* to strengthen the base pairing of 5'ss and U6 snRNA.

and Dpn1 treated gave no colony as expected. Plasmids were isolated from around 10 transformants and two were sequenced (pDblet *new13 II+* and pDblet *new13 II 5'ss mut*). Mutations at desired residues were confirmed by sequencing. *spprp16+* and *spprp16F528S* strains were transformed with the pDblet *new13 II+* and pDblet *new13 II 5'ss mut* mini-gene, transformants were selected on EMM L⁻ U⁻ media and colony purified. Splicing status of these mini-gene transcripts was analysed. On DNase I treated RNA we carried out semi-quantitative RT-PCR using T7 RP and *new13 E1* FP (**Figure IV.5**). As predicted by NGS data *new13+ II* a Prp16 independent category intron was spliced as efficiently as wild type in *spprp16F528S* mutant. No significant change in splicing efficiency was observed for the intron with mutation at its 5'ss. Strengthening 5'ss-U6 snRNA complementarity for *new13 II* does not render it to become strongly dependent on SpPrp16, thus it is plausible yet other intronic features in *new13+ II* may be responsible for making it SpPrp16 independent.

We re-examined the NGS data to investigate whether the strength of 5'ss-U6 snRNA interaction affects the splicing of introns wherein co-relations were noted between splicing efficiency and natural sequence variations in cellular introns of other transcripts. From this screening we chose *sec6102+ I3* and *I5* as additional case for experimental validation. *Sec6102+ I3* has complete complementarity at 5'ss-U6 snRNA interaction and is predicted to be dependent category intron based on NGS reads. However, in the same cellular transcript the *Sec6102+ I5* shows loss of complementarity at +4 and +6 position and could represent an SpPrp16 independent category of intron. This observation was taken up for validation by semi-quantitative RT-PCR on cellular RNA from *spprp16+* and *spprp16F528S* mutant strains where we examined their splicing efficiency using the DNase I treated RNA from *spprp16+* and *spprp16F528S* mutant cells. cDNA synthesis was done using a reverse primer corresponding to exon immediately downstream of the intron being tested. We find *intron 3* of *sec6103* with predicted strong 5'ss-U6 snRNA is inefficiently spliced in the *spprp16F528S* mutant cells when compared to *spprp16+* cells. We also confirmed *sec6103+ I5*, with predicted weak 5'ss-U6 snRNA is efficiently spliced (**Figure IV.6**). This data show that for cellular introns SpPrp16 dependence and independence correlates with variations in their 5'ss-U6 snRNA strength.

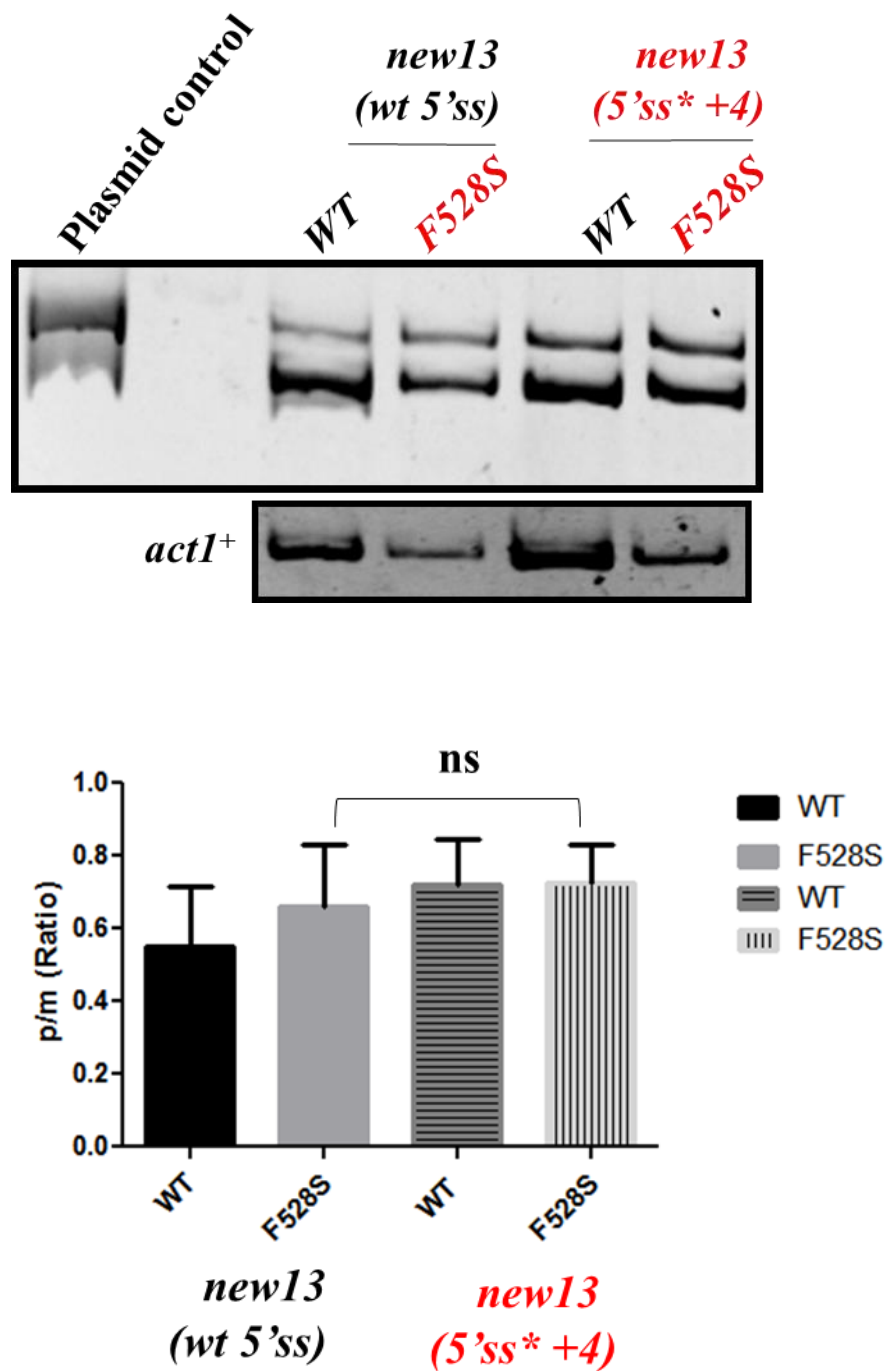


Figure IV.5: Semi-quantitative RT-PCRs to analyse the splicing of *new13 II* in mini-transcripts comprising *E1-II-E2* (exon1-intron1-exon2) with wild-type or mutant 5'ss. Splicing efficiency was tested in WT (*leu1:sprrp16+*) and F528S (*leu1:sprrp16F528S*) mutant strains. The mutations introduced are highlighted in red.

sec6102	Intron 3	<pre> TGT ACA </pre>	Dependent
	Intron 5	<pre> CGG ACA </pre>	Independent

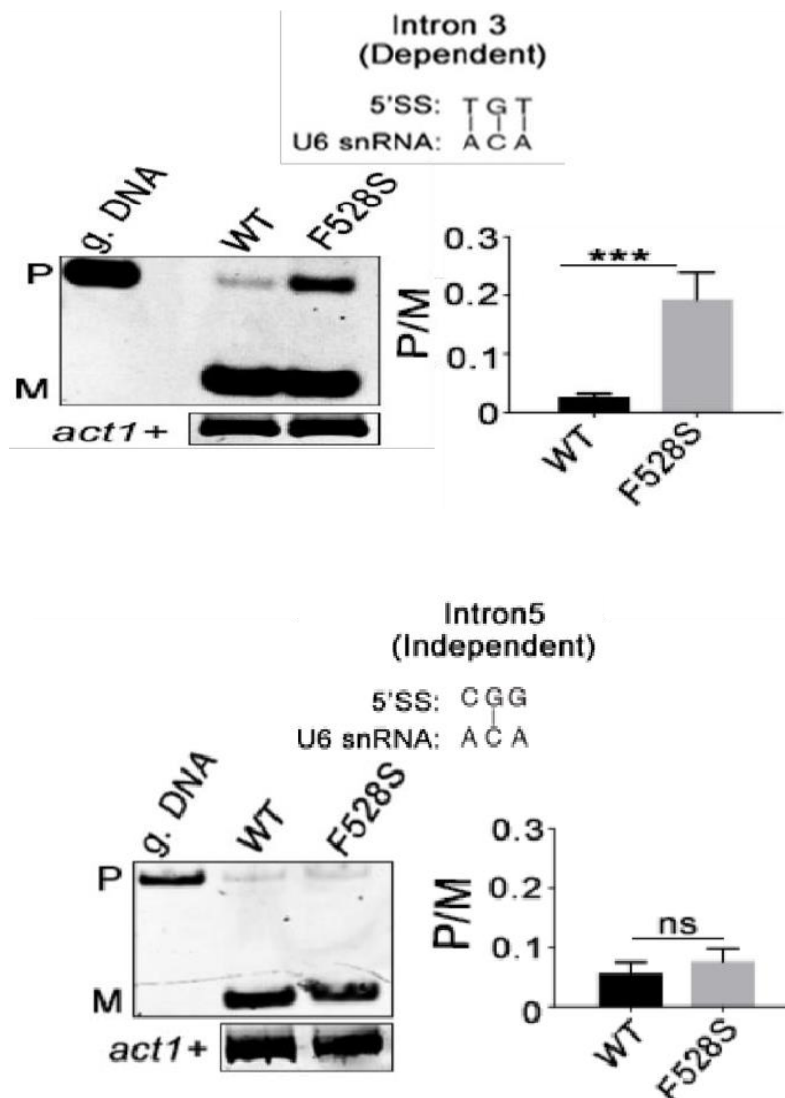
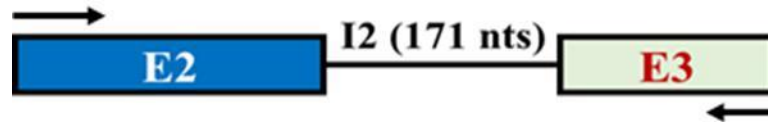


Figure IV.6: Introns within the same transcript display differential dependence on SpPrp16 are correlated to their 5'ss-U6 snRNA interaction. Cellular RNA from *spprp16+* and *spprp16F528S* strain semi-quantitative RT-PCR for SpPrp16 dependent vs SpPrp16 independent splicing. **A.** High p/m ratio shows splicing of *sec6102+ I3 (intron 3)* is strongly dependent on functional SpPrp16. **B** p/m ratio of *sec6102+ I5 (intron 5)* is nearly equal in both the strains.

Cumulative analysis of 5'ss-U6 snRNA interaction with BS-U2 snRNA strength between dependent and independent intron category

The moderately improved splicing for *sebl II 5'ss* mutant in cells with *spprp16F528S* mutation instigated us to examine whether other snRNA complementarity between BS and U2 snRNA could be an additional feature which can also contribute to dependence on SpPrp16 for efficient splicing. Interestingly, prior statistical work by collaborator in the lab have reported that the correlation between the strength of 5'ss-U6 snRNA interaction and BS-U2 snRNA complementarity was observed for SpPrp16 independent introns through Principal Component Analysis (PCA) (Drisy V., IISc Thesis; Pushpinder Singh Bawa, IBAB, Bangalore). The lack of 5'ss-U6 interactions at all three 5'ss positions +4, +5 and +6 was associated with weakened BS-U2 snRNA complementarity at -3 and -1 residues of the BS. Many introns which spliced independently of SpPrp16 showed loss of complementarity at 5'ss at +4 and +5 residues with U6 snRNA showed loss of complementarity at -4 and +1 position of BS-U2 snRNA interaction. In few SpPrp16 independent introns the loss of complementarity at +4 position of 5'ss was correlated with loss of complementarity at -3 residue of BS with U2 snRNA. These prior observations hint at the cumulative role of weakened 5'ss-U6 snRNA and BS-U2 snRNA interactions in determining the intron's ability to splice independently of SpPrp16. In this study, these leads were taken for experimental validation. We chose a candidate intron *tif313+ I2* that belongs to the category of dependent introns as seen from transcriptome data (**Figure IV.7A**). This intron which has very weak 5'ss-U6 snRNA interaction i.e. complete loss of complementarity at +4, +5 and +6 position of 5'ss with U6 snRNA. This intron had complete complementarity of its branch site with U2 snRNA. These features render it to be a suitable candidate to examine the individual contribution of BS-U2 snRNA interaction strength and requirement for SpPrp16 for its splicing. A mini-gene transcript construct was made comprising of *tif313+ E2-I2-E3 (tif313 exon 2- intron 2 - exon 3)* for expression from *tbp1* promoter. Mutagenesis was carried as described earlier by inverse PCR using mutagenic primers to change BS -4 nucleotide from A to T. Another mutation introduced changed the residue at -3 position from C to T (**Figure IV.7B**). These mutations should weaken *tif313 I2* BS complementarity with U2 snRNA. All three plasmids would express mini-transcripts from the *tbp1* promoter and these plasmids were used to transformed *spprp16+* and *spprp16F528S* cells. RNA from these transformants were tested for their splicing by semi-quantitative RT-PCRs.

A.



B.

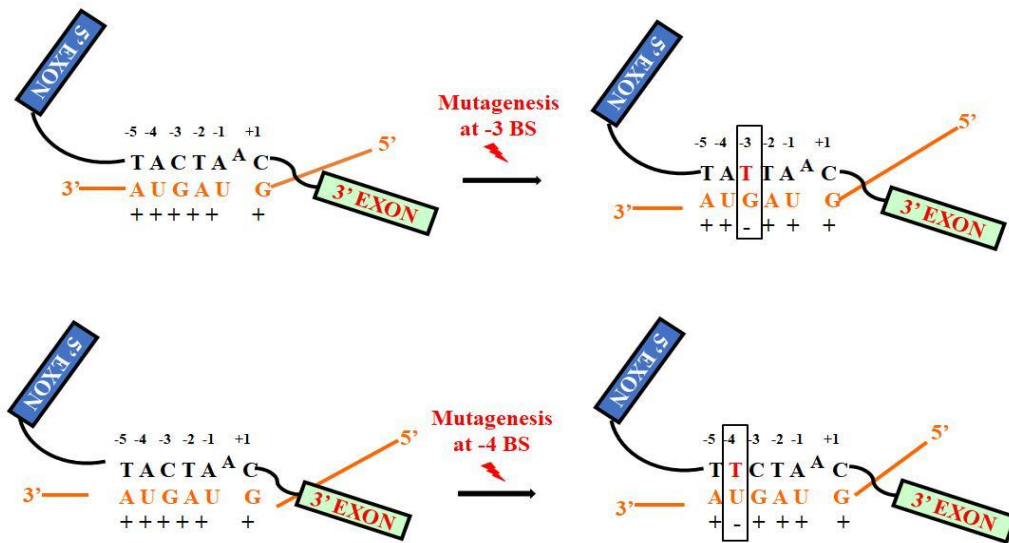
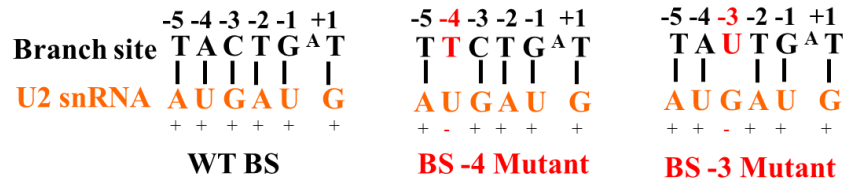
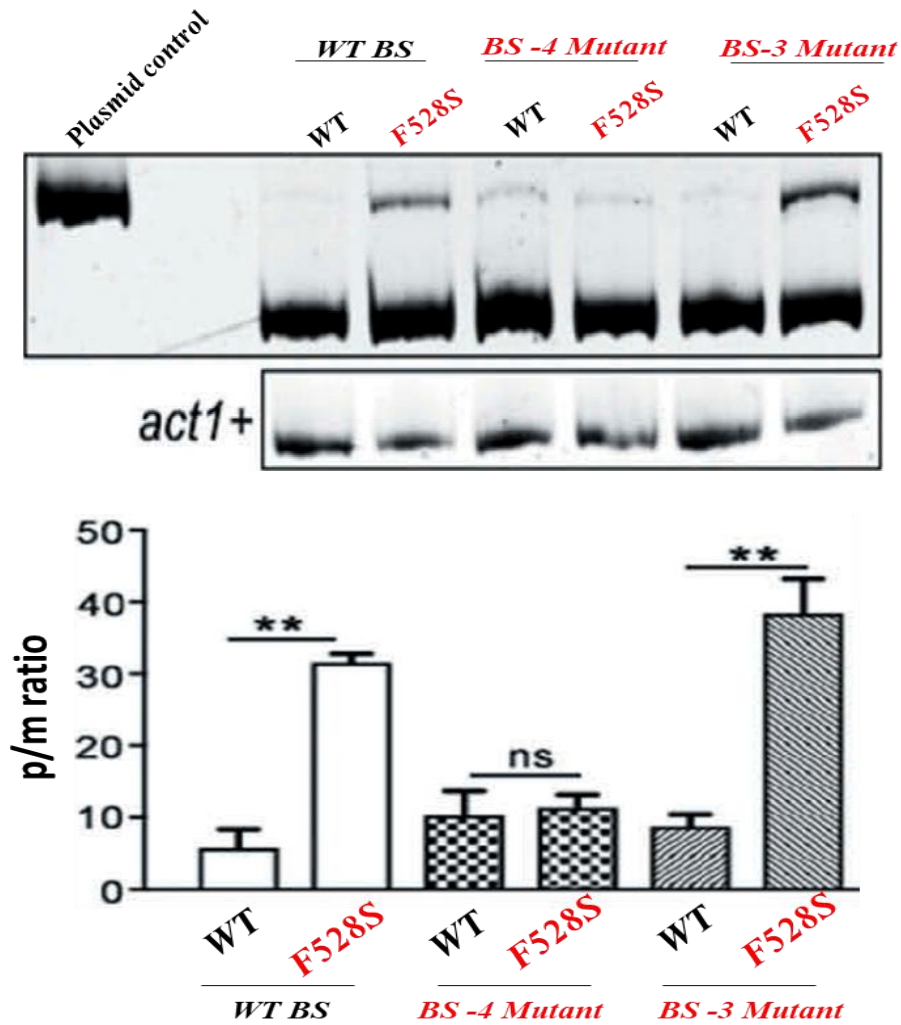


Figure IV.7: Diagrammatic representation of **A.** *tif313*+ E2-I2-E3 gene segment taken for cloning in fission yeast shuttle vector pDblet under *tbp1* promoter mini-gene. **B.** mutagenesis of nucleotides at -3 and -4 position of branch site (A is taken as "0") of *tif313* I2 which weakens the base pairing of *tif313* II BS and U2 snRNA.

A.



B.



The inefficient splicing of the wild type *tif313+ I2* mini-transcript was seen in *spprp16F528S* cells as compared to wild-type cells. Thus, these experiments confirmed that splicing of this intron is dependent on SpPrp16. The inadequate splicing of *tif 313 I2* was exacerbated when the mini-transcript had BS mutation at the -3 residue as we detect increased levels of unspliced pre-mRNA. However, the mini-transcript with BS mutation at -4 position was seen to be spliced efficiently in *spprp16F528S* cells and the splicing efficiency was comparable to *spprp16+* cells (**Figure IV.8B**). These results suggest that the -4 residue of *tif313+ I2* BS plays a pivotal role in its interaction with snRNA and its destabilization requires Prp16 function.

We also looked for cellular transcripts with intronic elements that bear natural sequence variants in the strength of BS-U2 snRNA interaction. *apl5+ I4* and *I2* selected based on this score for experimental validation. *apl5+ I4* had complete complementarity of its BS-U2 to the snRNA and is predicted to be SpPrp16 dependent category intron, whereas in *apl5+ I2* the BS has variations that cause loss of complementarity at -1, -4 and -5 positions to U2 snRNA predicted to be an independent category intron. This observation was taken up for validation by semi-quantitative RT-PCR on cellular transcript where the splicing efficiency of these introns were examined in *spprp16+* and *spprp16F528S* mutant cells. Using the DNase I RNA of both strains, cDNA synthesis was done using a reverse primer corresponding to exon immediately downstream of the intron whose splicing is to be investigated. As predicted intron 4 with strong BS-U2 snRNA complementarity is inefficiently spliced in the *spprp16F528S* mutant compared to wt whereas intron 2, which was predicted to be a dependent category intron with weak 5'ss-U6 snRNA is efficiently spliced (**Figure IV.9**). This data show that the SpPrp16 dependent splicing of *apl5 I4* and SpPrp16 independent splicing of *apl5 I2* correlates with variations in their BS-U2 snRNA strength.

apl5	Intron 4	<pre> A T A C T A C A U G A U G </pre>	Dependent
	Intron 2	<pre> A A G C T G C A U G A U G </pre>	Independent

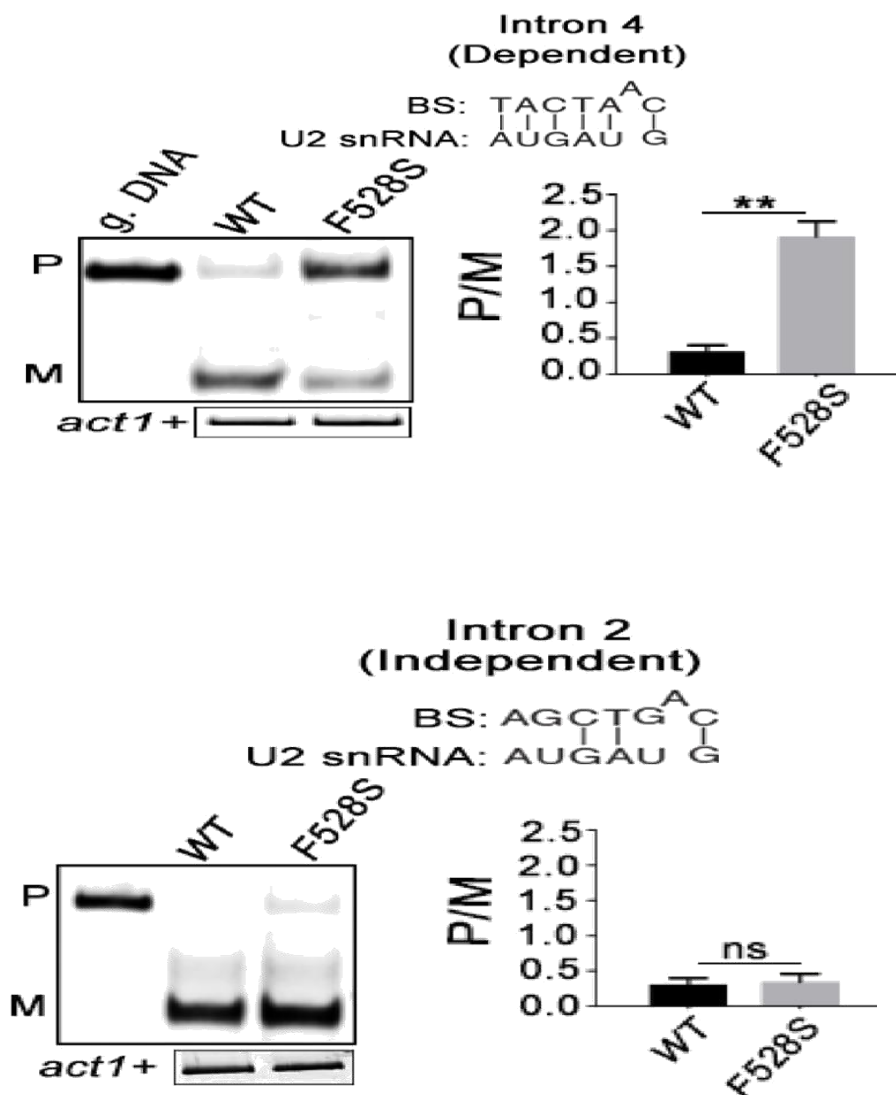


Figure IV.9: Semi-quantitative RT-PCR for two introns in a cellular transcript taken testing splicing status in *spprp16* wt vs *spprp16F528S* mutant strain. The *apl5+ I4* and *I2*, have been chosen for different BS-U2 snRNA interaction strength. The P/M ratio shows I4 is poorly spliced in *spprp16F528S* mutant strain while I2 is efficiently spliced. Bar graphs represent data from three biological replicates. ** p< 0.005 and ns = non-significant.

IV.4 Discussion

Studies on DExH/DExD box containing splicing factors from humans and *S. cerevisiae* have played a pivotal role in our understanding of spliceosomal remodelling that facilitates the formation and disruption of crucial RNA-protein, RNA-RNA and protein-protein interactions. Role of Prp16 helicase is well characterised for interaction with BS, and in second step catalysis by studies in budding yeast. Here, we investigated the role of fission yeast Prp16 in the recognition of splice-sites in *S. pombe* introns that bear degenerate splice-site signals. In depth bioinformatics analysis of whole genome transcriptome sequencing data from *spprp16+* and *spprp16F528S* mutant strain (Drisya V., IISc Thesis) revealed introns with strong U6 snRNA-5'ss (+4, +5, +6) interactions show defective splicing in the *spprp16F528S* mutant. Experimental validation for a candidate intron *seb1 II* which had complementarity at +4+5+6 position was done. Weakening the U6 snRNA-5'ss interaction resulted in adequate splicing of *Seb1 II* in *spprp16F528S* mutant, validating role of SpPrp16 in 5'ss recognition in fission yeast. This role of SpPrp16 in 5'ss recognition was further validated by analysing splicing efficiencies of introns within other cellular transcript with natural sequence variations. The SpPrp16 dependent intron with predicted strong 5'ss-U6 snRNA interaction were spliced inadequately in *spprp16F528S* mutant while in intron with naturally weaker 5'ss-U6 snRNA interaction spliced efficiently.

In the complementary study to strengthen the 5'ss-U6 snRNA interaction, we chose the candidate intron *new13 II* and it was noted to splice independently of SpPrp16. Upon Strengthening 5'ss-U6 snRNA complementarity, does not render it to become strongly dependent on SpPrp16. Thus, it is plausible yet other intronic features in *new13 II* could be responsible for its SpPrp16 independent splicing.

Prior study by collaborator in the lab had noted correlation between the strength of 5'ss-U6 snRNA interaction and BS-U2 snRNA complementarity for SpPrp16 independent introns. The loss of complementarity at 5'ss-U6 interactions was associated with weakened BS-U2 snRNA interactions in this class of introns. This observation was experimentally validated by choosing *tif313+ I2* a candidate dependent category intron with very weak 5'ss-U6 snRNA interaction i.e. complete loss of complementarity at +4, +5 and +6 position of 5'ss with U6 snRNA and shows complete complementarity at BS-U2 snRNA interactions. Upon weakening the BS-U2 snRNA interaction *tif313 I2* could be converted into SpPrp16 independent intron. Here, we observed particularly the -4 residue at branch site consensus sequence plays crucial role in BS-U2 snRNA interaction and its destabilization requires Prp16 function. Therefore, from this study we infer that the global dependence on Prp16 for

splicing in a genome is dictated by the strength of splice-site - snRNA interactions. Prp16 functions are also noted at juncture of 5'ss cleavage in fission yeast. This study identified strong U6 snRNA-5'ss interactions as a factor which individually or combined with the strength of BS-U2 interaction can dictate dependence on SpPrp16.

Chapter V

Summary and Conclusions

Nuclear pre-mRNA splicing plays an important role in gene regulation. Splicing takes place by two concerted transesterification reaction facilitated by a large multi-megadalton RNA-protein complex called Spliceosome. It comprises of five U snRNPs and several non-snRNP factors whose assembly and role in splicing catalysis have been extensively studied in budding yeast and mammalian system. DExD/H box helicases are one of the crucial non-snRNP proteins which comprise spliceosome. They play essential roles in formation of ordered crucial RNA-RNA, RNA-protein and protein-protein interactions, which in turn are important for aligning reactive groups of the pre-mRNA for catalysis. These rearrangements occur during spliceosome assembly, catalysis and dissociation (Moore et al.,1993; Will and Lührmann, 2011). DExD/H box containing helicases also ensure splicing fidelity by kinetic proofreading of intronic elements – 5' splice-site, branch site consensus sequence and the 3' splice-site (Burgess and Guthrie, 1993; Yang et al., 2013). Therefore, DExD/H helicases are indispensable for the generation of a functional transcriptome from any eukaryotic genome.

The splicing reactions and spliceosomal factors are conserved across species but the exon-intron architectures vary across species. The fission yeast genome with multiple short introns, degenerate intronic consensus elements and unconventionally positioned polypyrimidine tract is a useful alternative model to study splicing mechanisms that occur by intron definition (Käufer and Potashkin, 2000; Kuhn and Käufer, 2003). Since, such intronic features are common to most fungal and other higher eukaryotes, fission yeast is a suitable model to understand splicing mechanisms in these short introns. Interestingly, prior studies from our laboratory on the functional orthologues of some predicted second step fission yeast splicing factors (Slu7, Prp18 and Prp16) demonstrated their functions before catalysis which is different from their budding yeast counterparts. The enzymatic activities of DExH box helicases in the spliceosome and their role in splice-site recognition in *S. pombe* is largely unexplored. Prp16 is one such DExH box helicase which is well characterised in *S. cerevisiae* as an essential factor that remodels the spliceosome catalytic center after the first catalytic reaction. Prp16 recognizes the branch nucleotide at the branch consensus intronic element and the intron-exon 3'ss and help in formation of catalytic center for the second step reaction. Prp16 proofreads and rejects aberrant lariat intron-3'exon intermediates from participating in second step reaction.

Here, in this study we carried out functional studies on one such DExH box helicase SpPrp16 using two mis-sense mutants that were previously isolated in the laboratory. Its interaction with intronic *cis* elements were experimentally studied to validate the prior observations from deep transcriptome studies on cells with wild-type SpPrp16 or a slow growing mis-sense mutant. We also investigated the ATPase and RNA binding activity of wild type and these

mutant proteins and have created other mutants in DEAH box motif containing helicase domain.

Functional conservation of Prp16 and its role in splicing Prp16 in fission yeast

Here, we first examined the functional conservation of the fission yeast C-terminal conserved helicase domain in a temperature sensitive budding yeast mutant *scprp16-2*. For these studies we generated clones of chimeric Prp16 proteins for expression in budding yeast where N-terminal region was taken from the budding yeast ScPrp16 and translationally fused to the C-terminal helicase domain region of fission yeast SpPrp16 wild-type protein. Chimeric Prp16 protein, from the two different yeasts, was able to rescue the temperature sensitive growth of budding yeast mutant *scprp16-2* mutant at 37°C, the non-permissive temperature for this budding yeast mutant where its growth was comparable to *scprp16-2* mutant expressing plasmid borne budding yeast full length ScPrp16. The expression of chimeric Prp16 with F528S mutation in the C-terminal failed to rescue the *scprp16-2* mutant at 37°C. Similarly, clones that express only the full-length fission yeast Prp16 were unable to complement *scprp16-2* mutant. These observations show the C-terminal domain of Prp16 is functionally conserved and the budding yeast ScPrp16 N-terminal domain is required for spliceosomal interactions. From this study, we also infer that enzymatic activities SpPrp16 can serve to carry out 3'ss and branch point recognition of budding yeast introns.

To functionally characterise the *S. pombe* essential gene *spprp16+* we resorted to further study the two missense mutants *spprp16G515A* and *spprp16F528S* previously created in lab by next-generation transcriptomics (Drishya V., IISc Thesis; Vijayakumari et al., 2019). These studies showed that the *spprp16G515A* was splicing proficient, whereas in the *spprp16F528S* mutant splicing arrest before the first step of catalysis was observed for many intronic cellular transcripts, as predicted by whole genome transcriptomics (Vijayakumari et al., 2019). As budding yeast ScPRP16 functions largely during the second step of splicing, we took up re-examination of the fission yeast RNA transcriptome in *spprp16F528S* mutant to find cellular introns which may be arrested before second step, indicated by reduced mRNA levels without corresponding increase in pre-mRNA. Two putative candidates were found *alp41+ I5* (42 nucleotide) and *gms2+ I2* (43 nucleotide). Semi-quantitative RT-PCR assay was adopted to analyse the splicing of these introns where characteristic feature of second step defect (reduced mRNA with no precursor accumulation) was not observed. We also resorted to splicing analysis by primer extension assay using a mini-gene expressed *alp41+*

transcript with I5 where we did not observe any lariat intermediate RNAs (an intermediate product of splicing after first catalysis step). Hence, we conclude that low read counts for spliced mRNA and failure to detect pre-mRNA in the NGS dataset for *spprp16F528S* mutant could be an artefact of RNA sequencing or an indirect outcome of splicing that alters the stability of this mRNA in the *spprp16F528S* mutant.

The conserved G373 in *ScPRP16* corresponds to G515 residue in fission yeast *spprp16+*. The budding yeast *prp16G373S* mutant can suppress mutations in the *ACT1* intron branch nucleotide (Burgess and Guthrie, 1993). Hence, we created the analogous mutation in fission yeast protein. Further, to analyse SpPrp16 interactions with branch point nucleotide the branch point mutation was made in *tIID+ E1-II-E2eGFP* mini-gene where invariant branch nucleotide A was substituted to C. These transcripts were studied in *spprp16+ dbr1Δ* and *spprp16G515A dbr1Δ* double mutant (strains generated by Drisya V., IISc). An additive and thus more severe splicing arrest with increased pre-mRNA was noted for mini-transcript with A to C *cis* mutation even in strains wild type for *spprp16+ dbr1Δ*. This was replicated in the *spprp16G515A dbr1* splicing factor mutant as well. This contrasts with the ability of corresponding budding yeast *scprp16-1* mutant to suppress the splicing defects of the Br-C substrates. Thus, we infer that Branch site recognition by SpPrp16 could differ between the two yeasts. Additionally, to expand the repertoire of fission yeast mutants for future functions studies two other mutants *spprp16T643K* and *spprp16D712A* were created in this study. These residues were chosen based on mutants studied in its *S. cerevisiae* homolog ScPRP16 where such conditional alleles have been reported. Both mutants *spprp16T643K* and *spprp16D712R* grew like the wild-type strain at all the temperatures. Preliminary splicing status of a cellular intron 1 in *tif313+ 171* was tested by semi-quantitative RT-PCR indicates poor splicing in the *spprp16T643K* mutant while the intron spliced efficiently in *spprp16D712R* strain. As growth phenotypes are similar to the wild type in both the strains perhaps splicing arrest is adequate to support growth. For future analyses, genetic and transcriptomic studies could be carried out.

Biochemical characterization of SpPrp16 helicase mutants

In prior studies done by collaborator in laboratory (Drisya V., IISc Thesis) *in vitro* dsRNA unwinding activities of bacterially expressed and purified helicase domain of wild type *spprp16+*, *spprp16F528S* and *spprp16G515A* mutants were studied. *spprp16F528S*, slow growing mutant, had a functional helicase domain *in vitro* which was comparable to wild type. *spprp16G515A* was a poor enzyme *in vitro*. Using the same bacterially purified helicase

domain proteins, parallelly, in this study we examined their ATPase activities. Both time-dependent and protein concentration dependent ATPase activity was measured for the MBP tagged SpPrp16+, SpPrp16F528S and SpPrp16G515A helicase domain proteins. SpPrp16F528S helicase showed near normal ATPase activity comparable to wild type. In contrast weak ATP hydrolysis was shown by SpPrp16G515A protein domain. To test if the *in vitro* ATPase and helicase functions of these proteins correspond to its RNA binding ability, we also probed RNA binding by the wild-type and SpPrp16G515A helicase proteins. The wild-type helicase protein formed RNA-protein complexes but the SpPrp16G515A protein exhibited RNA binding over a wide range of protein concentrations. These data suggest that the poor dsRNA unwinding activity by SpPrp16G515A mutant protein could be mainly due to its distinguishably weaker *in vitro* RNA binding. Interestingly, this compromised *in vitro* enzymatic activity does not manifest *in vivo* in *spprp16G515A* cells as splicing efficiency is near normal. Thus, we infer the role of SpPrp16 in pre-mRNA splicing, and its ATP hydrolyzing ability can be modulated by interactions with other components of the spliceosome as is known for other splicing DExH/D box ATP dependent RNA helicases.

SpPrp16 plays role in splice-site recognition

The global splicing profile in *spprp16+* and *spprp16F528S* strains by deep sequencing confirmed a critical and global role for SpPrp16 in fission yeast. Further, these work from lab collaborators (Drisya V., IISc Thesis; Pushpinder Singh Bawa, IBAB, Bangalore; Vijayakumari et al., 2019) showed the intronic 5'ss consensus, particularly minor variations in the frequency of specific nucleotides at its +4 to +6 positions could discriminate SpPrp16 dependent *vs.* independent splicing events. Further, since the U6 snRNA-5'ss and U2 snRNA-BS base pairing interactions play a critical role in the formation of catalytic center for the first transesterification reaction and its conformational change is needed for the second splicing reaction these interactions were re-examined in this study. Based on leads from these in depth bio-informatic studies in the laboratory, here we chose a SpPrp16 dependent intron *seb1+ II* for experimental study of the effects of mutation at its 5'ss. Alterations of 5'ss +4 T and +6 T residues to +4 A and +6 A are predicted to caused feeble 5'ss-U6 snRNA interactions. Primer extension assays analysed the splicing of mini-transcripts *seb1+ E1-II-E2*, with wild type of 5'ss mutations, in strains *spprp16+* and the *spprp16F528S*. We find the splicing defect of *seb1+ II* in *spprp16F528S* mutant was partially rescued when the 5'ss and U6 snRNA was weakened. This observation therefore validated the prediction that the strength of 5'ss-U6 snRNA interaction could be a feature which determine the dependence or

independence of introns on SpPrp16 activity (Vijayakumari et al., 2019). To experimentally prove the relationship between SpPrp16 function and 5'ss-U6 snRNA interaction we chose to strengthen the 5'ss-U6 snRNA base pairing interaction in a cellular predicted intron *new13 II*. +4 A was altered to +4 T at the 5' splice-site of *new13 II*. Semi-quantitative RT-PCR was used to analyse its splicing. No significant change in splicing efficiency was observed for the intron with mutation at 5'ss which improved its interaction with U6 snRNA. Strengthening 5'ss-U6 snRNA complementarity, does not render it to become strongly dependent on SpPrp16, thus there is possibility of other intronic features in *new13* introns to be responsible for its SpPrp16 independent splicing. The strength of 5'ss-U6 snRNA interaction affecting the splicing of introns were supported by the co-relations we observed between the splicing efficiencies of introns within other cellular transcripts with natural sequence variations influence their 5'ss-U6 snRNA interaction. We chose *sec6102+ I3* and *I5* as additional cases for experimental validation. *sec6102+ I3* with complete complementarity at 5'ss-U6 snRNA interaction and predicted to be dependent category intron spliced inefficiently in the *spprp16F528S* mutant cells when compared to *Spprp16+*. However, *sec6102+ I5*, a predicted dependent category intron in the same transcript with weak 5'ss-U6 snRNA interaction was efficiently spliced. This data further reaffirmed 5'ss-U6 snRNA interaction as a feature which determine the dependence or independence of introns on SpPrp16 activity.

Partial improvement in splicing for *seb1 II 5'ss* in F528S mutant instigated us to examine if the cumulative effects of 5'ss-U6 snRNA and BS-U2 snRNA interactions could be contributing to an intron's dependence on SpPrp16 as predicted by bioinformatic analysis of transcriptome datasets (Drisy V., IISc Thesis; Pushpinder Singh Bawa, IBAB, Bangalore). This observation was validated in this study by choosing a candidate intron *tif313+ I2* that is a SpPrp16 dependent intron with very weak 5'ss-U6 snRNA interaction but with complete complementarity between the BS-U2 snRNA. Therefore, we took up alteration of the BS -4 residue from A to T and at BS -3 residue from C to T. Semi-quantitative RT-PCR assays examined the splicing of these mutant mini-transcripts as compared to mini-transcripts with wild-type BS. All analyses were done in both the *spprp16+* and *spprp16F528S* strains. We found that the mini-transcript with BS mutant -4 residue was spliced efficiently in *spprp16F528S* cells at levels nearly equal to that of *spprp16+* cells. However, mutation at -3 position of BS exacerbated the splicing defects of the already inadequately spliced *tif313+ I2*. These results suggest that the U2 snRNA interactions of the -4 residue of *tif313+ I2* BS is pivotal, and its destabilization requires Prp16 function. We also looked for cellular transcripts with intron elements that bear natural sequence variants in the strength of BS-U2 snRNA interaction, *apl5 I4* and *I2* were selected and taken for experimental validation. *apl5 I4* with

complete BS-U2 snRNA complementarity and predicted SpPrp16 dependent category intron, spliced inefficiently in the F528S mutant compared to wt whereas in *apl5 I2* with weak BS-U2 snRNA complementarity and predicted to be independent category intron was efficiently spliced. These analyses together underscore the requirement of SpPrp16 in destabilizing the interaction of these intronic elements with snRNA to bring about splicing. Investigations utilizing these mini-transcripts in other fission yeast Prp16 mutants would throw light on the interplay of splice-site-U snRNA strength and conformational transitions facilitated by splicing helicase Prp16 in the short introns of fission yeast.

Taken together from this study we infer the catalytic C-terminal domain of Prp16 is conserved across species and highlights its early functions in splicing and recognition of splice-sites in the *S. pombe* introns. As future directions we aim to generate additional strong conditional alleles in Prp16 for mutational analysis of enzymatic domain of SpPrp16 and further assay its splicing functions, its role in interplay of splice-site-U snRNA strength and conformational transitions facilitated by helicase Prp16 in fission yeast introns. Complementation of budding yeast *prp16* mutants with other SpPrp16 mutations in the chimeric Prp16 and study the role of fission yeast SpPrp16 in splice-site recognition of budding yeast introns can be examined. Also, to study the interacting partners of Prp16 in the fission yeast spliceosome for further characterisation of Prp16 and precise understanding of its involvement in the molecular processes in fission yeast splicing, through immuno pulldown studies.

References

- Absmeier, E., Wollenhaupt, J., Mozaffari-Jovin, S., Becke, C., Lee, C.T., Preussner, M., Heyd, F., Urlaub, H., Lührmann, R., Santos, K.F., and Wahl, M.C. (2015).** The large N-terminal region of the Brr2 RNA helicase guides productive spliceosome activation. *Genes Dev* **29**, 2576-258
- Agafonov, D.E., Deckert, J., Wolf, E., Odenwalder, P., Bessonov, S., Will, C.L., Urlaub, H., and Luhrmann, R. (2011).** Semiquantitative proteomic analysis of the human spliceosome via a novel two-dimensional gel electrophoresis method. *Mol cell Biol* **31**, 2667-2682.
- Arenas, J.E., and Abelson, J.N. (1997).** Prp43: An RNA helicase-like factor involved in spliceosome disassembly. *Proc Natl Acad Sci U S A* **94**, 11798-11802.
- Ast, G. (2004).** How did alternative splicing evolve? *Nat Rev Genet* **5**, 773-782.
- Banerjee, S., Khandelia, P., Melangath, G., Bashir, S., Nagampalli, V., and Vijayraghavan, U. (2013).** Splicing functions and global dependency on fission yeast *slu7* reveal diversity in spliceosome assembly. *Mol cell Biol* **33**, 3125-3136.
- Ben Yehuda, S., Russell, C.S., Dix, I., Beggs J.D., and Kupiec, M. (2000).** Extensive genetic interactions between PRP8 and PRP17/CDC40, two yeast genes involved in pre-mRNA splicing and cell cycle progression. *Genetics* **154**, 61–71.
- Ben Yehuda, S., Dix, I., Russell, C.S., Levy, S., Beggs, J.D., and Kupiec, M. (1998).** Identification and functional analysis of hPRP17, the human homologue of the PRP17/CDC40 yeast gene involved in splicing and cell cycle control. *RNA* **4**, 1304-1312.
- Bessonov, S., Anokhina, M., Will, C.L., Urlaub, H., and Luhrmann, R. (2008).** Isolation of an active step I spliceosome and composition of its RNP core. *Nature* **452**, 846-850.
- Bleichert, F., and Baserga, S.J. (2007).** The long unwinding road of RNA helicases. *Mol Cell* **27**, 339-352.
- Bottner, C.A., Schmidt, H., Vogel, S., Michele, M., and Kaufer, N.F. (2005).** Multiple genetic and biochemical interactions of Brr2, Prp8, Prp31, Prp1 and Prp4 kinase suggest a function in the control of the activation of spliceosomes in *Schizosaccharomyces pombe*. *Curr Genet* **48**, 151-161.
- Brennwald, P., Liao, X., Holm, K., Porter G., and Wise, J.A. (1988).** Identification of an essential *Schizosaccharomyces pombe* RNA homologous to the 7SL component of signal recognition particle. *Mol Cell Biol* **8**, 1580-1590.
- Burgess, S., Couto, J.R., and Guthrie, C. (1990).** A putative ATP binding protein influences the fidelity of branchpoint recognition in yeast splicing. *Cell* **60**, 705-717.

- Burgess, S.M., and Guthrie, C. (1993).** A mechanism to enhance mRNA splicing fidelity: the RNA-dependent ATPase Prp16 governs usage of a discard pathway for aberrant lariat intermediates. *Cell* **73**, 1377-1391.
- Chan, S.P., Kao, D.I., Tsai, W.Y., and Cheng, S.C. (2003).** The Prp19p-associated complex in spliceosome activation. *Science* **302**, 279-82.
- Chen, W., Shulha, H.P., Ashar-Patel, A., Yan, J., Green, K.M., Query, C.C., Rhind, N., Weng, Z., and Moore, M.J. (2014).** Endogenous U2·U5·U6 snRNA complexes in *S. pombe* are intron lariat spliceosomes. *RNA* **20**, 308-320
- Chen, J.Y., Stands, L., Staley, J.P., Jackups, R.R., Latus, L.J., and Chang, T.H. (2001).** Specific alterations of U1-C protein or U1 small nuclear RNA can eliminate the requirement of Prp28p, an essential DEAD box splicing factor. *Mol Cell* **7**, 227–232.
- Cheng, S.C., and Abelson, J. (1987).** Spliceosome assembly in yeast. *Genes Dev* **1**, 1014-1027.
- Chiu, Y.F., Liu, Y.C., Chiang, T.W., Yeh, T.C., Tseng, C.K., Wu, N.Y., and Cheng, S.C. (2009).** Cwc25 is a novel splicing factor required after Prp2 and Yju2 to facilitate the first catalytic reaction. *Mol cell biol* **29**, 5671-5678.
- Collins, L., and Penny, D. (2006).** Proceedings of the SMBE Tri-National Young Investigators' Workshop 2005. Investigating the intron recognition mechanism in eukaryotes. *Mol Biol Evol* **23**, 901-910.
- Cordin, O., Hahn, D., Alexander, R., Gautam, A., Saveanu, C., Barrass, J.D., and Beggs, J.D. (2014).** Brr2p carboxy-terminal Sec63 domain modulates Prp16 splicing RNA helicase. *Nucleic Acids Res* **42**, 13897-13910.
- Couto, J.R., Tamm, J., Parker, R., and Guthrie, C. (1987).** A trans-acting suppressor restores splicing of a yeast intron with a branch point mutation. *Genes Dev* **1**, 445-455.
- Crotti, L.B., Bacikova, D., and Horowitz, D.S. (2007).** The Prp18 protein stabilizes the interaction of both exons with the U5 snRNA during the second step of pre-mRNA splicing. *Genes Dev* **21**, 1204-1216.
- Dandekar, T., Ribes, V., and Tollervey, D. (1989).** *Schizosaccharomyces pombe* U4 small nuclear RNA closely resembles vertebrates U4 and is required for growth. *J Mol Biol* **208**, 371-379.
- Dix, I., Russell, C.S., O'Keefe, R.T., Newman, A.J., and Beggs, J.D. (1998).** Protein–RNA interactions in the U5 snRNP of *Saccharomyces cerevisiae*. *RNA* **4**, 1675–1686.
- Fabrizio, P., Dannenberg, J., Dube, P., Kastner, B., Stark, H., Urlaub, H., and Luhrmann, R. (2009).** The evolutionarily conserved core design of the catalytic activation step of the yeast spliceosome. *Mol Cell* **36**, 593-608.

Fleckner, J., Zhang, M., Valcarcel, J., and Green, M.R. (1997). U2AF65 recruits a novel human DEAD box protein required for the U2 snRNP-branchpoint interaction. *Genes Dev* **11**, 1864-1872.

Fox-Walsh, K.L, Dou, Y., Lam, B.J., Hung, S.P, Baldi, P.F, and Hertel, K.J. (2005). The architecture of pre-mRNAs affects mechanisms of splice-site pairing. *Proc Natl Acad Sci U S A* **102**, 16176-81.

Frank, D., and Guthrie, C. (1992). An essential splicing factor, SLU7, mediates 3' splice site choice in yeast. *Genes Dev* **6**, 2112-2124.

Frank, D.N., Roiha, H., and Guthrie, C. (1994). Architecture of the U5 small nuclear RNA. *Mol Cell Biol* **14**, 2180-2190.

Goguel, V., and Rosbash, M. (1993). Splice site choice and splicing efficiency are positively influenced by pre-mRNA intramolecular base pairing in yeast. *Cell* **72**, 893-901.

Goodall, G. J., and Filipowicz, W. (1989). The AU-rich sequences present in the introns of plant nuclear pre-mRNAs are required for splicing. *Cell* **3**, 473-483

Gottschalk, A., Kastner, B., Luhrmann, R., and Fabrizio, P. (2001). The yeast U5 snRNP coisolated with the U1 snRNP has an unexpected protein composition and includes the splicing factor Aar2p. *RNA* **7**, 1554–1565.

Gottschalk, A., Neubauer, G., Banroques, J., Mann, M., Lührmann, R., and Fabrizio, P. (1999). Identification by mass spectrometry and functional analysis of novel proteins of the yeast [U4/U6.U5] tri-snRNP. *EMBO J* **18**, 4535–4548.

Gozani, O., Feld, R., and Reed, R. (1996). Evidence that sequence-independent binding of highly conserved U2 snRNP proteins upstream of the branch site is required for assembly of spliceosomal complex A. *Genes Dev* **10**, 233-243.

Guo, M., Lo, P.C., and Mount, S.M. (1993). Species-specific signals for the splicing of a short Drosophila intron in vitro. *Mol Cell Biol* **13**, 1104-18.

Hamann, F., Enders, M., and Ficner, R. (2019). Structural basis for RNA translocation by DEAH-box ATPases. *Nucleic Acids Res* **47**,4349–4362,

Hawkins, J.D. (1988). A survey on intron and exon lengths. *Nucleic Acids Res* **16**, 9893–9905

Hogg, R., de Almeida, R.A., Ruckshanthi, J.P., and O'Keefe, R.T. (2014). Remodeling of U2-U6 snRNA helix I during pre-mRNA splicing by Prp16 and the NineTeen Complex protein Cwc2. *Nucleic Acids Res* **42**, 8008-8023

Horowitz, D.S., and Krainer, A.R. (1997). A human protein required for the second step of pre-mRNA splicing is functionally related to a yeast splicing factor. *Genes Dev* **11**, 139-151.

Horowitz, D.S., and Abelson, J. (1993). Stages in the second reaction of pre-mRNA splicing: the final step is ATP independent. *Genes Dev* **7**, 320-329.

Hotz, H. R., and Schwer, B. (1998). Mutational analysis of the yeast DEAH-box splicing factor Prp16. *Genetics* **149**, 807–815.

Ismaili, N., Sha, M., Gustafson, E.H., and Konarska, M.M. (2001). The 100-kDa U5 snRNP protein (hPrp28p) contacts the 5' splice site through its ATPase site. *RNA* **7**, 182–193.

Jeffares, D.C., Rallis, C., Rieux, A., Speed, D., Převedorovský, M., Mourier, T., Marsellach, F.X., Iqbal, Z., Lau, W., Cheng, T.M., Pracana, R., Müllender, M., Lawson, J.L., Chessel, A., Bala, S., Hellenthal, G., O'Fallon, B., Keane, T., Simpson, J.T., Bischof, L., Tomiczek, B., Bitton, D.A., Sideri, T., Codlin, S., Hellberg, J.E., van Trigt, L., Jeffery, L., Li, J.J., Atkinson, S., Thodberg, M., Febrer, M., McLay, K., Drou, N., Brown, W., Hayles, J., Carazo Salas, R.E., Ralser, M., Maniatis, N., Balding, D.J., Balloux, F., Durbin R., and Bähler, J. (2015). The genomic and phenotypic diversity of *Schizosaccharomyces pombe*. *Nat Genet* **47**, 235–241.

Jiang, J., Horowitz, D.S., and Xu, R.M. (2000). Crystal structure of the functional domain of the splicing factor Prp18. *Proc Natl Acad Sci U S A* **97**, 3022–3027.

Jones, M.H., Frank, D.N., and Guthrie, C. (1995). Characterization and functional ordering of Slu7p and Prp17p during the second step of pre-mRNA splicing in yeast. *Proc Natl Acad Sci U S A* **92**, 9687–9691.

Jurica, M.S., and Moore, M.J. (2003). Pre-mRNA splicing: awash in a sea of proteins. *Mol cell* **12**, 5–14.

Käufer, N.F., and Potashkin, J. (2000). Analysis of the splicing machinery in fission yeast: a comparison with budding yeast and mammals. *Nucleic Acids Res* **28**, 3003–3010.

Kim, D.U., Hayles, J., Kim, D., Wood, V., Park, H.O., Won, M., Yoo, H.S., Duhig, T., Nam, M., Palmer, G., Han, S., Jeffery, L., Baek, S.T., Lee, H., Shim, Y.S., Lee, M., Kim, L., Heo, K.S., Noh, E.J., Lee, A.R., Jang, Y.J., Chung, K.S., Choi, S.J., Park, J.Y., Park, Y., Kim, H.M., Park, S.K., Park, H.J., Kang, E.J., Kim, H.B., Kang, H.S., Park, H.M., Kim, K., Song, K., Song, K.B., Nurse, P., and Hoe, K.L. (2010). Analysis of a genome-wide set of gene deletions in the fission yeast *Schizosaccharomyces pombe*. *Nature Biotech* **28**, 617–623.

Kim D.H., and Rossi J.J. (1999). The first ATPase domain of the yeast 246-kDa protein is required for in vivo unwinding of the U4/U6 duplex. *RNA* **5**, 959–971.

Kim, S.H., and Lin, R.J. (1993). Pre-mRNA splicing within an assembled yeast spliceosome requires an RNA-dependent ATPase and ATP hydrolysis. *Proc Nat Acad Sci U S A* **90**, 888–892.

Kim, S.H., Smith, J., Claude, A., and Lin, R.J. (1992). The purified yeast pre-mRNA splicing factor PRP2 is an RNA-dependent NTPase. *EMBO J* **11**, 2319–2326.

Kistler, A.L., and Guthrie, C. (2001). Deletion of MUD2, the yeast homolog of U2AF65, can bypass the requirement for sub2, an essential spliceosomal ATPase. *Genes Dev* **15**, 42–49.

- Koodathingal, P., and Staley, J.P. (2013).** Splicing fidelity: DEAD/H-box ATPases as molecular clocks. *RNA biol* **10**, 1073-1079.
- Koodathingal, P., Novak, T., Piccirilli, J.A., and Staley, J.P. (2010).** The DEAH box ATPases Prp16 and Prp43 cooperate to proofread 5' splice site cleavage during pre-mRNA splicing. *Mol Cell* **39**, 385-395.
- Krämer, A., Keller, W., Appel, B., and Lührmann, R. (1984).** The 5' terminus of the RNA moiety of U1 small nuclear ribonucleoprotein particles is required for the splicing of messenger RNA precursors. *Cell* **38**, 299-307.
- Kuhn, A.N., and Kaufer, N.F. (2003).** Pre-mRNA splicing in *Schizosaccharomyces pombe*: regulatory role of a kinase conserved from fission yeast to mammals. *Curr Genet* **42**, 241-251.
- Kupfer, D.M., Drabenstot, S.D., Buchanan, K.L., Lai, H., Zhu, H., Dyer, D.W., Roe, B.A., and Murphy, J.W. (2004).** Introns and splicing elements of five diverse fungi. *Eukaryotic Cell* **3**, 1088-1100.
- Laggerbauer, B., Achsel, T., and Luhrmann, R. (1998).** The human U5-200kD DEXH-box protein unwinds U4/U6 RNA duplexes in vitro. *Proc Natl Acad Sci U S A* **95**, 4188-4192.
- Lamond, A.I., Konarska, M.M., Grabowski, P.J., and Sharp, P.A. (1988).** Spliceosome assembly involves the binding and release of U4 small nuclear ribonucleoprotein. *Proc Natl Acad Sci U S A* **85**, 411-415.
- Lardelli, R.M., Thompson, J.X., Yates, J.R., and Stevens, S.W. (2010).** Release of SF3 from the intron branchpoint activates the first step of pre-mRNA splicing. *RNA* **16**, 516-528.
- Lim, L.P., and Burge, C.B. (2001).** A computational analysis of sequence features involved in recognition of short introns. *Proc Natl Acad Sci U S A* **98**, 11193-11198.
- Lindsey, L.A., and Garcia-Blanco, M.A. (1998).** Functional conservation of the human homolog of the yeast pre-mRNA splicing factor Prp17p. *J Biol Chem* **273**, 32771-32775.
- Liu, Y.C., Chen, H.C., Wu, N.Y., and Cheng, S.C. (2007).** A novel splicing factor, Yju2, is associated with NTC and acts after Prp2 in promoting the first catalytic reaction of pre-mRNA splicing. *Mol Cell Biol* **27**, 5403-5413.
- Lossky, M., Anderson, G.J., Jackson, S.P., and Beggs, J. (1987).** Identification of a yeast snRNP protein and detection of snRNP-snRNP interactions. *Cell* **51**, 1019-1026.
- Lützelberger, M., Groß, T., and Käufer, N. F. (1999).** Srp2, an SR protein family member of fission yeast: In vivo characterization of its modular domains. *Nucleic Acids Res* **27**, 2618-2626.
- Madhani, H.D., and Guthrie, C. (1994).** Genetic interactions between the yeast RNA helicase homolog Prp16 and spliceosomal snRNAs identify candidate ligands for the Prp16 RNA-dependent ATPase. *Genetics* **137**, 677-687.

- Martin, A., Schneider, S., and Schwer, B. (2002).** Prp43 is an essential RNA-dependent ATPase required for release of lariat-intron from the spliceosome. *J Biol Chem* **277**, 17743-17750.
- McPheeters, D.S., and Muhlenkamp, P. (2003).** Spatial Organization of Protein-RNA Interactions in the Branch Site-3' Splice Site Region during pre-mRNA Splicing in Yeast. *Mol Cell Biol* **23**, 4174-4186.
- Mefford, M.A., and Staley, J.P. (2009).** Evidence that U2/U6 helix I promote both catalytic steps of pre-mRNA splicing and rearranges in between these steps. *RNA* **15**, 1386-1397.
- Melangath, G., Sen, T., Kumar, R., Bawa, P., Srinivasan, S., and Vijayraghavan, U. (2017)** Functions for fission yeast splicing factors SpSlu7 and SpPrp18 in alternative splice-site choice and stress-specific regulated splicing. *PloS One*, **12**, e0188159.
- Moore, M.J., Query, C.C., and Sharp, P.A. (1993).** Splicing of precursors to messenger RNAs by the spliceosome. *The RNA World* pp. 303-357.
- Mount, S.M., Pettersson, I., Hinterberger, M., Karmas, A., and Steitz, J.A. (1983).** The U1 small nuclear RNA-protein complex selectively binds a 5' splice site in vitro. *Cell* **33**, 509-518.
- Noble, S.M., and Guthrie, C. (1996).** Identification of novel genes required for yeast pre-mRNA splicing by means of cold-sensitive mutations. *Genetics* **143**, 67-80.
- O'Day, C.L., Dalbadie-McFarland, G., and Abelson, J. (1996).** The *Saccharomyces cerevisiae* Prp5 protein has RNA-dependent ATPase activity with specificity for U2 small nuclear RNA. *J Biol Chem* **271**, 33261-33267.
- Ohrt, T., Prior, M., Dannenberg, J., Odenwalder, P., Dybkov, O., Rasche, N., Schmitzova, J., Gregor, I., Fabrizio, P., Enderlein, J., and Lührmann R. (2012).** Prp2-mediated protein rearrangements at the catalytic core of the spliceosome as revealed by dcFCCS. *RNA* **18**, 1244-1256.
- Perriman, R., Barta, I., Voeltz, G.K., Abelson, J., and Ares, M. Jr. (2003).** ATP requirement for Prp5p function is determined by Cus2p and the structure of U2 small nuclear RNA. *Proc Natl Acad Sci U S A* **100**, 13857-13862.
- Porter, G., Brennwald, P., and Wise, J.A. (1990).** UI small nuclear RNA from *Schizosaccharomyces pombe* has unique and conserved features and is encoded by an essential single copy gene. *Mol Cell Biol* **10**, 2874-2881.
- Potashkin, J., Naik, K., and Wentz-Hunter, K. (1993).** U2AF homolog required for splicing in vivo. *Science* **262**, 573-575.
- Potashkin, J., and Frendewey, D. (1989).** Splicing of the U6 RNA precursor is impaired in fission yeast pre-mRNA splicing mutants. *Nucleic Acids Res* **17**, 7821-7831.
- Query, C.C., and Konarska, M.M. (2004).** Suppression of Multiple Substrate Mutations by Spliceosomal *prp8* Alleles Suggests Functional Correlations with Ribosomal Ambiguity

Mutants. *Mol Cell* **14**, 343-354.

Query, C.C., and Konarska, M.M. (2005). Insights into the mechanisms of splicing: More lessons from the ribosome. *Genes and Development* **19**, 2255-2260.

Raghunathan, P.L., and Guthrie, C. (1998). RNA unwinding in U4/U6 snRNPs requires ATP hydrolysis and the DEIH-box splicing factor Brr2. *Curr Biol* **8**, 847–855.

Reed, R. (2000). Mechanisms of fidelity in pre-mRNA splicing. *Curr Opin Cell Biol* **12**, 340-345.

Reed, R., and Maniatis, T. (1985). Intron sequences involved in lariat formation during pre mRNA splicing, *Cell* **41**, 95-105.

Reyes, J.L., Gustafson, E.H., Luo, H.R., Moore, M.J., and Konarska, M.M. (1999). The C-terminal region of hPrp8 interacts with the conserved GU dinucleotide at the 5' splice site. *RNA* **5**, 167–179.

Reyes, J.L., Kois, P., Konforti, B.B., and Konarska, M.M. (1996). The canonical GU dinucleotide at the 5' splice site is recognized by p220 of the U5 snRNP within the spliceosome. *RNA* **2**, 213–225.

Robberson, B.L., Cote, G.J., and Berget, S.M. (1990). Exon definition may facilitate splice site selection in RNAs with multiple exons. *Mol Cell Biol* **10**, 84–94.

Romfo, C.M., Alvarez, C.J., van Heeckeren, W.J., Webb, C.J., and Wise, J.A. (2000). Evidence for splice site pairing via intron definition in *Schizosaccharomyces pombe*. *Mol Cell Biol* **20**, 7955-7970.

Roy, J., Kim, K., Maddock, J.R., Anthony, J.G., and Woolford, J.L. (1995). The final stages of spliceosome maturation require Spp2p that can interact with the DEAH box protein Prp2p and promote step 1 of splicing. *RNA* **1**, 375-390

Ruby, S.W., Chang, T.H., and Abelson, J. (1993). Four yeast spliceosomal proteins (PRP5, PRP9, PRP11, and PRP21) interact to promote U2 snRNP binding to pre-mRNA. *Genes Dev* **7**, 1909–1925.

Ruskin, B., and Green, M.R. (1985). An RNA processing activity that debranches RNA lariats. *Science* **229**, 135-140.

Sakharkar, M.K., Chow, V.T., Chaturvedi, I., Mathura, V.S., Shapshak, P., and Kanguane, P. (2004). A report on single exon genes (SEG) in eukaryotes. *Frontiers in Bioscience* **9**, 3262-3267.

Sakharkar, M.K., Perumal, B.S., Lim, Y.P., Chern, L.P., Yu, Y., and Kanguane, P. (2005). Alternatively spliced human genes by exon skipping--a database (ASHESdb). *In Silico Biol* **5**, 221-225.

- Santos, K.F., Jovin, S.M., Weber, G., Pena, V., Lührmann, R., and Wahla, M.C. (2012).** Structural basis for functional cooperation between tandem helicase cassettes in Brr2 mediated remodelling of the spliceosome. *Proc Natl Acad Sci U S A* **109**, 17418-17423.
- Sapra, A.K., Arava, Y., Khandelia, P., and Vijayraghavan, U. (2004).** Genome-wide analysis of pre-mRNA splicing: intron features govern the requirement for the second-step factor, Prp17 in *Saccharomyces cerevisiae* and *Schizosaccharomyces pombe*. *J Biol Chem* **279**, 52437-52446.
- Schwartz, S.H., Silva, J., Burstein, D., Pupko, T., Eyraes, E., and Ast, G. (2008).** Large-scale comparative analysis of splicing signals and their corresponding splicing factors in eukaryotes. *Genome Res* **18**, 88-103.
- Schneider, S., Hotz, H.R., and Schwer, B. (2002).** Characterization of dominant-negative mutants of the DEAH-box splicing factors Prp22 and Prp16. *J Biol Chem* **277**, 15452-15458.
- Schneider, M., Will, C.L., Anokhina, M., Tazi, J., Urlaub, H., and Lührmann, R. (2010).** Exon Definition Complexes Contain the Tri-snRNP and Can Be Directly Converted into B-like Precatalytic Splicing Complexes. *Mol Cell* **38**, 223-235.
- Schwer, B. (2001).** A new twist on RNA helicases: DExH/D box proteins as RNPsases. *Nature Struct Biol* **8**, 113–116.
- Schwer, B., and Gross, C.H. (1998).** Prp22, a DExH-box RNA helicase, plays two distinct roles in yeast pre-mRNA splicing. *EMBO J* **17**, 2086-2094.
- Schwer, B., and Guthrie, C. (1991).** PRP16 is an RNA-dependent ATPase that interacts transiently with the spliceosome. *Nature* **349**, 494-499.
- Schwer, B., and Guthrie, C. (1992).** A conformational rearrangement in the spliceosome is dependent on PRP16 and ATP hydrolysis. *EMBO J* **11**, 5033-5039.
- Semlow, D.R., and Staley, J.P. (2012).** Staying on message: ensuring fidelity in pre-mRNA splicing. *Trends Biochem Sci* **37**, 263–273.
- Seshadri V, Vaidya VC, and Vijayraghavan U. (1996).** Genetic studies of the PRP17 gene of *Saccharomyces cerevisiae*: A domain essential for function maps to a nonconserved region of the protein. *Genetics* **143**, 45–55.
- Sharp, P.A. (1985).** Splicing of messenger RNA precursors. *Harvey Lect* **81**, 1-31.
- Sharp, P.A., Konarksa, M.M., Grabowski, P.J., Lamond, A.I., Marciniak, R., and Seiler, S.R. (1987).** Splicing of messenger RNA precursors. *Cold Spring Harb. symposia on quantitative biology* **52**, 277-285.
- Silverman, J., Takai, H., Buonomo, S.B.C., Eisenhaber, F., and De Lange, T. (2004).** Human Rif1, ortholog of a yeast telomeric protein, is regulated by ATM and 53BP1 and functions in the S-phase checkpoint. *Genes Dev* **18**, 2108-2119.

- Sipiczki, M. (2000).** Where does fission yeast sit on the tree of life? *Genome Biol* **1**, Reviews 1011.
- Small, E.C., Leggett, S.R., Winans, A.A., and Staley, J.P. (2006).** The EF-G-like GTPase Snu114p Regulates Spliceosome Dynamics Mediated by Brr2p, a DExD/H Box ATPase. *Mol Cell* **23**, 389–399.
- Smith, C.W., and Valcárcel, J. (2000).** Alternative pre-mRNA splicing: the logic of combinatorial control. *Trends Biochem Sci* **25**, 381-338.
- Staley, J.P., and Guthrie, C. (1998).** Mechanical devices of the spliceosome: motors, clocks, springs, and things. *Cell* **92**, 315-326.
- Steitz, J.A., Dreyfuss, G., Krainer, A.R., Lamond, A.I., Matera, A.G., and Padgett, R.A. (2008).** Where in the cell is the minor spliceosome? *Proc Natl Acad Sci U S A* **105**, 8485-8486.
- Stevens, S.W. and Abelson, J. (1999).** Purification of the yeast U4/U6.U5 small nuclear ribonucleoprotein particle and identification of its proteins. *Proc Natl Acad Sci U S A* **96**, 7226–7231.
- Stevens, S.W., Ryan, D.E., Ge, H.Y., Moore, R.E., Young, M.K., Lee, T.D., and Abelson, J. (2002).** Composition and functional characterization of the yeast spliceosomal pentasnrNP. *Mol Cell* **9**, 31–44.
- Sun, J.S., and Manley, J.L. (1995).** A novel U2-U6 snRNA structure is necessary for mammalian mRNA splicing. *Genes Dev* **9**, 843-854.
- Talerico, M., and Berget, S.M. (1994).** Intron definition in splicing of small Drosophila introns. *Mol Cell Biol* **14**, 3434-3445.
- Tanaka, N., Aronova A., and Schwer, B. (2007).** Ntr1 activates the Prp43 helicase to trigger release of lariat-intron from the spliceosome. *Genes Dev* **21**, 2312-2325.
- Tanaka, N., and Schwer, B. (2006).** Mutations in PRP43 that uncouple RNA-dependent NTPase activity and pre-mRNA splicing function. *Biochemistry* **45**, 6510-6521.
- Tang, J., Abovich, N., Fleming, M. L., Seraphin, B., and Rosbash, M. (1997).** Identification and characterization of a yeast homolog of U1 snRNP-specific protein C. *EMBO J* **16**, 4082-4091.
- Tani, T., and Ohshima, Y. (1989)** The gene for the U6 small nuclear RNA in fission yeast has an intron. *Nature* **337**, 87–90.
- Teigelkamp, S., McGarvey, M., Plumpton, M., and Beggs, J.D. (1994).** The splicing factor PRP2, a putative RNA helicase, interacts directly with pre-mRNA. *EMBO J* **13**, 888-897.
- Teigelkamp, S., Mundt, C., Achsel, T., Will, C.L., and Luhrmann, R. (1997).** The human U5 snRNP-specific 100-kD protein is an RS domain-containing, putative RNA helicase with significant homology to the yeast splicing factor Prp28p. *RNA* **3**, 1313-1326.

- Teigelkamp, S., Newman, A.J., and Beggs, J.D. (1995).** Extensive interactions of PRP8 protein with the 5' and 3' splice sites during splicing suggest a role in stabilization of exon alignment by U5 snRNA. *EMBO J* **14**, 2602–2612.
- Tsai, R.T., Fu, R.H., Yeh, F.L., Tseng, C.K., Lin, Y.C., Huang, Y.H., and Cheng, S.C. (2005).** Spliceosome disassembly catalyzed by Prp43 and its associated components Ntr1 and Ntr2. *Genes Dev* **19**, 2991-3003.
- Tseng, C.K., Liu, H.L., and Cheng, S.C. (2011).** DEAH-box ATPase Prp16 has dual roles in remodeling of the spliceosome in catalytic steps. *RNA* **17**, 145-154.
- Umen, J.G., and Guthrie, C. (1995).** Mutagenesis of the yeast gene PRP8 reveals domains governing the specificity and fidelity of 3' splice site selection. *Genetics* **143**, 723-739.
- Valadkhan, S. (2005).** snRNAs as the catalysts of pre-mRNA splicing. *Current Opin Chem Bio* **9**, 603-608.
- Van Nues, R.W., and Beggs, J.D. (2001).** Functional contacts with a range of splicing proteins suggest a central role for Brr2p in the dynamic control of the order of events in spliceosomes of *Saccharomyces cerevisiae*. *Genetics* **157**, 1451-1467.
- Vidal, V.P., Verdone, L., Mayes, A.E., and Beggs, J.D. (1999).** Characterization of U6 snRNA–protein interactions. *RNA* **5**, 1470–1481.
- Vijayakumari, D., Sharma, A.K., Bawa, P.S., Kumar, R., Srinivasan, S., and Vijayraghavan, U. (2019).** Early splicing functions of fission yeast Prp16 and its unexpected requirement for gene Silencing is governed by intronic features. *RNA Biol* **16**, 754-769
- Vijaykrishna, N., Melangath, G., Kumar, R., Khandelia, P., Bawa, P., Varadarajan, R., and Vijayraghavan, U. (2016)** The fission yeast pre-mRNA processing factor 18 (prp18+) has intron-specific splicing functions with links to G1-S cell cycle progression. *J Biol Chem* **291**, 27387-27402.
- Vijayraghavan, U., Company, M., and Abelson, J. (1989).** Isolation and characterization of pre-mRNA splicing mutants of *Saccharomyces cerevisiae*. *Genes Dev* **3**, 1206-1216.
- Villa, T., and Guthrie, C. (2005).** The Isy1p component of the NineTeen complex interacts with the ATPase Prp16p to regulate the fidelity of pre-mRNA splicing. *Genes Dev* **19**, 1894-1904.
- Wagner, J.D., Jankowsky, E., Company, M., Pyle, A.M., and Abelson, J.N. (1998).** The DEAH-box protein PRP22 is an ATPase that mediates ATP-dependent mRNA release from the spliceosome and unwinds RNA duplexes. *EMBO J* **17**, 2926–2937.
- Wahl, M.C., Will, C.L., and Luhrmann, R. (2009).** The spliceosome: design principles of a dynamic RNP machine. *Cell* **136**, 701-718.
- Wang, Y., Wagner, J.D., and Guthrie, C. (1998).** The DEAH-box splicing factor Prp16 unwinds RNA duplexes *in vitro*. *Curr Biol* **8**, 441-451.

Warkocki, Z., Odenwalder, P., Schmitzova, J., Platzmann, F., Stark, H., Urlaub, H., Ficner, R., Fabrizio, P., and Luhrmann, R. (2009). Reconstitution of both steps of *Saccharomyces cerevisiae* splicing with purified spliceosomal components. *Nature Struct Biol* **16**, 1237-1243.

Webb, C. J., Romfo, C. M., Van Heeckeren, W. J., and Wise, J. A. (2005). Exonic splicing enhancers in fission yeast: Functional conservation demonstrates an early evolutionary origin. *Genes Dev* **19**, 242-254.

Wiest, D.K., O'Day, C.L., and Abelson, J. (1996) In vitro studies of the Prp9.Prp11.Prp21 complex indicate a pathway for U2 small nuclear ribonucleoprotein activation. *J Biol Chem* **271**, 33268–33276

Will, C.L., and Lührmann, R. (2006). Spliceosome structure and function. *The RNA World* pp. 369–400

Will, C.L., Rümpler, S., Klein Gunnewiek, J., van Venrooij, W.J., and Lührmann, R. (1996). In vitro reconstitution of mammalian U1 snRNPs active in splicing: the U1-C protein enhances the formation of early (E) spliceosomal complexes. *Nucleic Acids Res* **24**, 4614–4623.

Wlodaver, A.M., and Staley, J.P. (2014). The DExD/H-box ATPase Prp2p destabilizes and proofreads the catalytic RNA core of the spliceosome. *RNA* **20**, 282–294.

Wood, V., Gwilliam, R., Rajandream, M. A., Lyne, M., Lyne, R., and Stewart, A., Sgouros, J., Peat, N., Hayles, J., Baker, S., Basham, D., Bowman, S., Brooks, K., Brown, D., Brown, S., Chillingworth, T., Churcher, C., Collins, M., Connor, R., Cronin, A., Davis, P., Feltwell, T., Fraser, A., Gentles, S., Goble, A., Hamlin, N., Harris, D., Hidalgo, J., Hodgson, G., Holroyd, S., Hornsby, T., Howarth, S., Huckle, E.J., Hunt, S., Jagels, K., James, K., Jones, L., Jones, M., Leather, S., McDonald, S., McLean, J., Mooney, P., Moule, S., Mungall, K., Murphy, L., Niblett, D., Odell, C., Oliver, K., O'Neil, S., Pearson, D., Quail, M.A., Rabinowitsch, E., Rutherford, K., Rutter, S., Saunders, D., Seeger, K., Sharp, S., Skelton, J., Simmonds, M., Squares, R., Squares, S., Stevens, K., Taylor, K., Taylor, R.G., Tivey, A., Walsh, S., Warren, T., Whitehead, S., Woodward, J., Volckaert, G., Aert, R., Robben, J., Grymonprez, B., Weltjens, I., Vanstreels, E., Rieger, M., Schäfer, M., Müller-Auer, S., Gabel, C., Fuchs, M., Düsterhöft, A., Fritzc, C., Holzer, E., Moestl, D., Hilbert, H., Borzym, K., Langer, I., Beck, A., Lehrach, H., Reinhardt, R., Pohl, T.M., Eger, P., Zimmermann, W., Wedler, H., Wambutt, R., Purnelle, B., Goffeau, A., Cadieu, E., Dréano, S., Gloux, S., Lelaure, V., Mottier, S., Galibert, F., Aves, S.J., Xiang, Z., Hunt, C., Moore, K., Hurst, S.M., Lucas, M., Rochet, M., Gaillardin, C., Tallada, V.A., Garzon, A., Thode, G., Daga, R.R., Cruzado, L., Jimenez, J., Sánchez, M., del Rey, F., Benito, J., Domínguez, A., Revuelta, J.L., Moreno, S., Armstrong, J., Forsburg, S.L., Cerutti, L., Lowe, T., McCombie, W.R., Paulsen, I., Potashkin, J., Shpakovski, G.V., Ussery, D., Barrell, B.G and Nurse, P. (2002). The genome sequence of *Schizosaccharomyces pombe*. *Nature* **415**, 871-80.

Xu, Y.Z., and Query, C.C. (2007). Competition between the ATPase Prp5 and branch region-U2 snRNA pairing modulates the fidelity of spliceosome assembly. *Mol Cell* **28**, 838-849.

Yang, F., Wang, X.Y., Zhang, Z.M., Pu, J., Fan, Y.J., Zhou, J., Query, C.C., and Xu, Y.Z. (2013). Splicing proofreading at 5' splice sites by ATPase Prp28p. *Nucleic Acids Res* **41**, 4660-4670.

Yeh, T.C., Liu, H.L., Chung, C.S., Wu, N.Y., Liu, Y.C., and Cheng, S.C. (2011). Splicing factor Cwc22 is required for the function of Prp2 and for the spliceosome to escape from a futile pathway. *Mol Cell Biol* **31**, 43-53.

Zamore, P.D., Patton, J.G., and Green, M.R. (1992). Cloning and domain structure of the mammalian splicing factor U2AF. *Nature* **355**, 609-614

Zhang, M. Q. (1998). Statistical features of human exons and their flanking regions. *Human Mol Genetics* **7**, 919–932,

Zhang, X., and Schwer, B. (1997). Functional and physical interaction between the yeast splicing factors Slu7 and Prp18. *Nucleic Acids Res* **25**, 2146–2152

Zhou, Z., and Reed, R. (1998). Human homologs of yeast prp16 and prp17 reveal conservation of the mechanism for catalytic step II of pre-mRNA splicing. *EMBO J* **17**, 2095-2106.

Theses Referred:

Drisya, V. (2016). Functional insights into the canonical and non-canonical roles of the fission yeast splicing factor SpPrp16. *Thesis IISc*, Bangalore.

Piyush Khandelia. (2008). Molecular Genetics studies on pre-mRNA splicing factors of fission and budding yeasts. *Thesis IISc*, Bangalore.

APPENDIX A

Isolation of genomic DNA from *S. pombe*

1. The desired strain was grown to saturation in 5ml of YES or selective EMM broth as required.
2. Cells were harvested by centrifugation at 3000 rpm for 3 min and the pellet resuspended in 200 μ l breaking buffer
3. Composition of breaking buffer 2% triton-X 100
1% SDS 100mM NaCl
10mM Tris
HCl, pH 8
1mM EDTA
4. 200 μ l phenol: chloroform (1:1) and 200 μ l of 0.5mm acid washed glass beads was added to the cell suspension containing breaking buffer.
5. This was continuously vortexed for 20 minutes at room temperature
6. Subsequently 200 μ l of 1X TE was added and vigorously vortexed for 10 minutes more at room temperature
7. The mixture was then spun at 12,000 rpm for 10 minutes to collect the supernatant.
8. To the supernatant collected on a fresh tube, 1 ml of 100% ethanol was added and spun at 12,000 rpm.
9. The pellet formed was washed with 70% ethanol, dried, resuspended in 400 μ l sterile milli Q water containing 5 μ l of RNaseI (10mg/ml) and incubated at 37°C for 1 hour
10. Equal volume of phenol: chloroform (1:1) was added, vigorously mixed and spun at 12,000 rpm for 5 minutes.
11. The aqueous phase containing DNA was transferred to a new tube and precipitated in 100% ethanol at -20°C for 12 hours.
12. The DNA in ethanol was spun down at 12,000 rpm for 10 minutes, pellet washed with 70% ethanol and the air-dried pellet was resuspended in 30-40 μ l sterile milli Q water.

Total RNA isolation from *S. pombe* by TRI-reagent

1. 10 OD (595 nm) of *S. pombe* cells after the required time of incubation was harvested by centrifugation at 3000 rpm for 3 minutes. The cell pellet obtained was washed once with water and frozen in liquid nitrogen. The frozen pellets can be stored at -80°C until further use.
2. The cell pellet containing tube was transferred to a liquid nitrogen bath with slots.
3. The pellet was ground to fine powder using a micropestle and care was taken not to thaw the cells in the process. Each sample required around 5 minutes of continuous grinding.
4. 1 ml of prechilled TRI-reagent was added to the thoroughly ground cell powder and mixed by vigorous vortexing.
5. The samples were allowed to stand at room temperature for 10 minutes followed by the addition of 200 µl of chloroform which required 2 minutes of vortexing.
6. The mixture was further allowed to stand for 15 minutes after which it was spun at 13,000 rpm for 15 minutes to separate the mixture into 3 distinct phases. The upper aqueous phase containing RNA, the middle interphase of DNA and the lower phase with lipids and proteins.
7. The aqueous phase was transferred to a fresh tube and mixed with 500 µl of isopropanol. The mixture was gently mixed and incubated at room temperature for 10 minutes.
8. The RNA was pelleted by spinning at 13,000 rpm for 15 minutes.
9. The pellet was washed with 70% ethanol. After discarding ethanol, the pellet was air dried and dissolved in 50-70 µl DEPC treated sterile milli-Q water (65°C for 5 to 10 minutes).
10. The RNA obtained was quantified using a spectrophotometer or nanodrop. The typical yield of RNA ranged from 1- 4.5 µg/µl.

DNase Treatment

25µg of RNA sample extracted using Tri-reagent (Sigma) was treated with 4 units of RNase free DNaseI (NEB) in the presence of 100 mM MgCl₂ in a reaction volume of 50 µl at 37°C for 30 minutes. The reaction was stopped by addition of 2µl of 0.5M EDTA. The DNase I treated RNA samples were heat inactivated at 65°C for 7-8 minutes and precipitated using 3M sodium acetate and incubated at -20°C in ethanol overnight.

End labelling of oligonucleotide for Primer extension assays

5 μ M Primer – 1 λ

γ P³² ATP – 2.5 λ (25 μ Ci)

PNK- 1 λ

10x PNK - 1 λ

The reaction mix was incubated at 37°C for 1 hour and 75 μ l of 1X TE was added to stop the reaction followed by heat inactivated at 72°C for 20 minutes. The radiolabeled probe was purified by passage through G-25 sephadex column.

Purification of wild type and mutant helicase proteins

Single colony of C41 *E. coli* transformants from each of the pMALC2X *spprp16* plasmids bearing the fragment which encodes the wild type and both helicase mutant proteins was inoculated in a 500 ml LB broth initially to an O.D595 of 0.4. 20 μ M of IPTG was added to these log phase cultures and further grown for 3 hours at 37°C. The pellet collected from each of these cultures was dissolved in lysis buffer (volume of lysis buffer is 10 times the wet weight of the pellet) and sonicated at 2 pulse per cycle - 60 times, 50% duty cycle (Branson Sonifier). The lysate was cleared from the cell debris by centrifuging at 15,000 rpm for 20 minutes. To the cleared lysate collected in a 50 ml falcon tube, 600 μ l of amylose resin slurry, NEB (pre-equilibrated with lysis buffer) was added and incubated in a low speed moving rotator at 4°C for 6 hours to allow binding. The bead bound lysate was then transferred to a 10 ml column which allowed packing of the column with the amylose resin and subsequent to this, the flow through was collected. The column was then washed 3 times with wash buffer containing 0.1 mM maltose (Sigma Aldrich) to avoid non-specific protein association with the resin. Then the resin bound protein was eluted using elution buffer containing 10mM maltose. 600 μ l of the elution buffer was used for each elution and 8 such eluates were collected. The aliquot of the eluate containing protein was identified using Bradford test and protein containing fractions were pooled. The sample was transferred to a dialysis bag and dialyzed against 500 ml of dialysis buffer containing 50% glycerol for 6 hours (replaced with fresh dialysis buffer after 3 hours). The concentration of the protein was estimated using Bradford assay and an average concentration of 300 ng/ μ l was obtained for all the three proteins. Composition of the buffers used for this purification protocol is described below:

Lysis Buffer

20 mM HEPES-KOH (pH-7.9)

200 mM KCl

1 mM EDTA

1 mM PMSF

2 mM β -mercaptoethanol

Wash Buffer

20 mM HEPES-KOH (pH-7.9)

200 mM KCl

1 mM EDTA

1 mM PMSF

2 mM β -mercaptoethanol

0.1 mM Maltose

Elution Buffer

20 mM HEPES-KOH (pH-7.9)

200 mM KCl

1 mM EDTA

1 mM PMSF

2 mM β -mercaptoethanol

0.1 mM Maltose

Dialysis Buffer

20 mM HEPES-KOH (pH-7.9)

100 mM KCl

0.1 mM PMSF

50% glycerol

APPENDIX B

YES (Rich media)

Amount per litre	Final concentration
5g yeast extract	0.5% yeast extract
30 g glucose	3% glucose
225 mg adenine sulphate	1.31 mM adenine
225 mg L-histidine	1.45 mM L-histidine
225 mg L-leucine	1.71 mM L-leucine
225 mg uracil	2.01 mM uracil
225 mg L-lysine hydrochloride	1.23 mM L-lysine
20g Bactoagar	2% agar (for solid media)

EDINBURGH MINIMAL MEDIA (EMM)

Amount per litre	Final concentration
20g glucose	2% glucose
3g potassium hydrogen phthalate	14.7 mM potassium hydrogen phthalate
2.2 g dibasic sodium phosphate	15.5 mM dibasic sodium phosphate
5g ammonium chloride	93.5 mM ammonium chloride
20 ml 50X salt stock	1X salt stock
1ml 1000X vitamin stock	1X vitamin stock
0.1 ml 10,000X mineral stock	1X mineral stock
20g bacto agar	2% agar (for solid media)

50X Salt stock

Amount per liter	Final concentration
52.5 g MgCl ₂ .6H ₂ O	0.26 M MgCl ₂ .6 H ₂ O
0.735 g CaCl ₂ .2H ₂ O	5 mM CaCl ₂ .2H ₂ O
50 g KCl	0.67 M KCl
2 g Na ₂ SO ₄	4.1 mM Na ₂ SO ₄

1000X Vitamin stock

Amount per liter	Final concentration
1 g Pantothenic acid	81.2 mM Pantothenic acid
10 g nicotinic acid	81.2 mM nicotinic acid
10 g inositol	4.20 mM inositol
10 mg biotin	40.9 µM biotin

10,000 X Mineral Stock

Amount per liter	Final concentration
5 g Boric acid	80.9mM Boric acid
4 g Magnesium sulphate	33.2 mM MnSO ₄
4 g Zinc sulphate heptahydrate	13.9 mM ZnSO ₄ .7H ₂ O
2g Ferric chloride hexahydrate	7.40 mM FeCl ₂ .6H ₂ O
0.4 g Molybdenic acid	0.32 mM Molybdenic acid
1g Potassium iodide	6.02 mM KI
0.4 g Cupric sulphate pentahydrate	1.60 mM CuSO ₄ .5H ₂ O
10 g Citric acid	47.6 mM citric acid

Amino acids for EMM

Component	Amount per liter
Adenine sulphate	225mg/liter
L-leucine	225mg/liter
L-histidine	225mg/liter
Uracil	225 mg/liter
Lysine hydrochloride	225mg/liter

EMM with 5-FOA

Prepare 50 ml of EMM agar with the following components:

2 g glucose

0.3 g potassium hydrogen phthalate

0.22 g dibasic sodium phosphate

0.5 g ammonium chloride

2 ml 50X salt stock

0.1 ml 1000X vitamin stock

0.001 ml 10,000X mineral stock

22.5 mg Adenine sulphate

22.5 mg L- leucine

4.5 mg Uracil

2 g Bacto agar

All these components were added to make 50 ml of EMM agar

Preparation of 5-FOA solution:

0.1g-0.2 g of 5-FOA was added to 50 ml of sterile milli Q water pre-warmed to 55°C and continuously mixed on a magnetic stirrer until completely dissolved. Filter sterilize the 5-FOA solution using a 0.02-micron Millipore filter and add the filtered solution to the previously prepared molten 50 ml EMM agar. Store the plates in dark at 4°C until further use.

APPENDIX C

List of primers used in the study

ScPRP16 chiFP: 5' CCGCTCGAGGTCGACTCTGGTTATGGGTCATT 3'
ScPRP16 chiRP: 5' CCATCGATAGATTGTTGAATATGTTCC 3'
SpPrp16 chiFP: 5' CCATCGATAGTGCTGCTACATCCCTTGCT 3'
SpPrp16 chiRP: 5' CCATCGATGTCGACATTTTGAGATGGGAACC 3'
SpPrp16 helicase BamHI FP: 5' CGGGATCCCTTTCTGTTATACGTGATAACC 3'
SpPrp16 helicase SalI RP: 5' CGACGTCGACACCAAGGGATTTTAAA 3'
SpPrp16 G515XFP: 5' CTTATTGTAGTTNKGAGACTGGTTCTGGT 3'
SpPrp16 T643XFP: 5' CAAGTTGCTCGTTNKTCCGCTACTATGAA 3'
SpPrp16 T643XRP: 5' TTCATAGTAGCGGAMNNAACGAGCAACTTG 3'
SpPrp16 D712XFP: 5' GACAGGGCAGGAANNKATTGAAGCTACATG 3'
SpPrp16 D712XRP: 5' CATGTAGCTTCAATMNNTTCCTGCCCTGTC 3'
SpPrp16F528X FP: 5' ACCCAATTAGCTCAANNKTTATATGAGGAT 3'
SpPrp16F528X RP: 5' ATCCTCATATAAMNNTTGAGCTAATTGGGT 3'
SpPrp16G515X FP: 5' CTTATTGTAGTTNKGAGACTGGTTCTGGT 3'
SpPrp16G515X RP: 5' ACCAGAACCAGTCTCMNNAACTACAATAAG 3'
Helicase BamH1 FP: 5'CGGGATCCCTTTCTGTTATACGTGATAACC 3'
Helicase SalI RP: 5'CGACGTCGACACCAAGGGATTTTAAA 3'
SpPrp16 chi FP: 5' CCATCGATAGTGCTGCTACATCCCTTGCT 3'
seb1 E1 FP: 5' ATGCTATACAGCATGCGCCATCTG 3'
seb1 E2 RP: 5' GGAGGAAATGTTGAAGCCTTCTCC 3'
tif313BS -4 FP: 5' CTTCCATGCTATTTCTAACACGAAACAGA 3'
tif313BS-4 RP: 5' TCTGTTTCGTGTTAGAAATAGCATGGAAG 3'
tif313BS -3 FP: 5' CTTCCATGCTATTATTAACACGAAACAGA 3'
tif313BS -3 RP: 5' TCTGTTTCGTGTTAATAATAGCATGGAAG 3'
gms 2 ATG FP: 5' ATGCTTTTGCCAATTATTATGCTTAC 3'
gms 2 E2 FP: 5'GCAATGGCTCTCACTGAGTTTCG 3'
gms 2 E3 RP: 5' TTACGATTCGGCGAGAGGAA 3'
apl5 E4 FP: 5' CAAAATCGCCAATTCGCGTTGAA 3'
apl5 E5 RP: 5' TTA CTCTTTCCCGGATGTTTTTTC 3'
apl5 E2 FP: 5' CAGATACAGACGTTTTAATGTTAACG 3'
apl5 E3 RP: 5' TAGAGAAGTGTGAGAGACCGT 3'

sec6102 E3 FP: 5' TCATTCCAGTTTACGGTGCAG 3'
sec6102 E4 RP: 5' AGATGATCCATCTAAAACGCG 3'
sec6102 E5 FP: 5' GATCGAGTTTTATTTCAGAATGCT 3'
sec6102 E6 RP: 5' CCAGACGAAACATAGGTTACAG 3'
act1 FP: 5' GCTGCTCAATCTTCCTCCCTTG 3'
act1 RP: 5' GGTCCGCTCTCTCATCATACTCTT 3'
tFIID FP: 5' GTATCTGGCATTGTTCCAACCCTTC 3'
tFIID RP: 5' GGGTTGTATTCTGCATTACG 3'
tFIID E2 RP: 5' TGCATTACGTGCATGTAGCGCAATAGT 3'
Snu2 RP: 5' GAACAGATACTACACTTGATC 3'
GFP-RP: 5' GAACAGATACTACACTTGATC 3'

APPENDIX D

Strain	Genotype	Source
FY527	<i>h⁻ ura4-D18 leu1-32 his3-D1 ade6-M216</i>	Prof. S. Forsburg
FY528	<i>h⁺ ura4-D18 leu1-32 his3-D1 ade6-M210</i>	Prof. S. Forsburg
<i>sprrp16Δ / sprrp16⁺</i>	<i>h⁺ / h⁻ sprrp16::kanMX6/sprrp16⁺ ade6M210/ade6M216 his3-D1/his3-D1 ura4D18/ura4D18</i>	Drisya V
<i>sprrp16 pREP4Xsprrp16⁺</i>	<i>h⁺ sprrp16::kanMX6 ura4-D18 leu1-32 his3- D1 ade6 M210 pREP4Xsprrp16⁺</i>	Drisya V
WT (<i>sprrp16⁺</i>)	<i>h⁺ sprrp16::kanMX6 ura4-D18 leu1-32 his3- D1 ade6-M210 leu1:Pnmt81sprrp16⁺</i>	Drisya V
F528S (<i>sprrp16F528S</i>)	<i>h⁺ sprrp16::kanMX6 ura4-D18 leu1-32 his3- D1 ade6-M210 leu1:Pnmt81sprrp16F528S</i>	Drisya V
G515A (<i>sprrp16G515A</i>)	<i>h⁺ sprrp16::kanMX6 ura4-D18 leu1-32 his3- D1 ade6-M210 leu1:Pnmt81sprrp16G515A</i>	Drisya V
<i>sprrp16⁺ dbr1 (WT dbr1Δ)</i>	<i>h⁺ sprrp16::kanMX6 spdbr1::KanMX6 ura4- D18 his3-D1 ade6-M210 leu1:Pnmt81sprrp16⁺</i>	Drisya V
<i>sprrp16G515A dbr1 (G515A dbr1Δ)</i>	<i>h⁺ sprrp16::kanMX6 spdbr1::KanMX6 ura4- D18 his3-D1 ade6-M210 leu1:Pnmt81sprrp16G515A</i>	Drisya V
T643K (<i>sprrp16T643K</i>)	<i>h⁺ sprrp16::kanMX6 ura4-D18 leu1-32 his3- D1 ade6-M210 leu1:Pnmt81sprrp16T643K</i>	This study
D712R (<i>sprrp16D712R</i>)	<i>h⁺ sprrp16::kanMX6 ura4-D18 leu1-32 his3- D1 ade6-M210 leu1:Pnmt81sprrp16D712R</i>	This study

LIST OF ABBREVIATIONS

g.DNA	genomic DNA
μl	Microliter
μg	Microgram
5-FOA	5-Fluororotic acid
bp	base pairs
BrP	branch point
cDNA	complementary DNA
cpm	counts per minute
DEPC	diethyl pyrocarbonate
dNTP	deoxyribonucleotide phosphate
E	exon designation
I	intron designation
EE	Exon-Exon
EI	Exon-Intron
EDTA	Ethylene diamine tetra acetic acid
Kb	kilo base pairs
kDa	kilo Dalton
mg	Milligram
MQ	milli-Q
mRNA	messenger RNA
Mya	million years ago
ng	Nanogram
NMD	non-sense mediated decay
nmt	no message in thiamine
NTC	<u>n</u> ineteen <u>c</u> omplex
nts	Nucleotides

O.D.	optical density
ORF	open reading frame
PAGE	polyacrylamide gel electrophoresis
PCR	polymerase chain reaction
PEG	polyethylene glycol
pre-mRNA	precursor messenger RNA
Prp	pre-RNA processing
Py(n)	Polypyrimidine
rpm	revolutions per minute
RT	reverse transcription
Sc	<i>Saccharomyces cerevisiae</i>
SDS	sodium dodecyl sulphate
Slu	synthetic lethal U snRNA
snRNA	small nuclear ribonucleic acid
snRNP	small nuclear ribonucleoprotein
Sp	<i>Schizosaccharomyces pombe</i>
ss	splice-site (5' or 3')
TAE	Tris-acetate EDTA buffer
TE	Tris-EDTA
ts	temperature-sensitive
cs	cold sensitive
U2AF	U2-auxiliary factor

PUBLICATION

Vijayakumari, D., **Sharma, A. K.**, Bawa, P. S., Kumar, R., Srinivasan, S., & Vijayraghavan, U. (2019). Early splicing functions of fission yeast Prp16 and its unexpected requirement for gene Silencing is governed by intronic features. *RNA Biol* 16, 754-769